

GENCORP
AEROJET

AD-A235 644



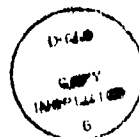
Y O S 1991

1

Hydrocarbon-Fuel/Combustion- Chamber-Liner Materials Compatibility

Contract NAS 3-25070
Final Report
NASA CR-187104
April 1991

Prepared For:
National Aeronautics and Space Administration
Lewis Research Center
Cleveland, Ohio 44135



UNCLASSIFIED
EXCEPT WHERE SHOWN
OTHERWISE
Limitation Unlimited

Acquisition For	
DTIC STUDY	<input checked="" type="checkbox"/>
DTIC TAB	<input type="checkbox"/>
Unannounced	<input type="checkbox"/>
Justification	
By	
GAT/PL/...	
Analyst's name	
Date	
A1	

Propulsion Division

DTIC COPY

91 5 08 008

GENCORP
AEROJET

Propulsion Division

P O Box 13222
Sacramento CA 95813-6000
Tel: 916-355-1000

26 April 1991

5173:DM4051
SJR:il

National Aeronautics and Space Administration
Lewis Research Center
21000 Brookpark Road
Cleveland, Ohio 44135

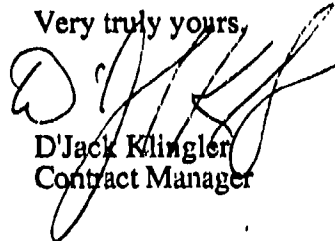
Attention: Elizabeth A. Roncace, Project Manager
MS 500-219

Subject: Contract NAS 3-25070, Hydrocarbon -Fuel /Combustion-
Chamber-Liner Materials Compatibility
Final Report

Dear Ms. Roncace:

In accordance with subject contract, one (1) copy of Enclosure (1) is submitted.

Very truly yours,



D'Jack Klingler
Contract Manager

Enclosure:

- (1) Hydrocarbon -Fuel /Combustion-Chamber-Liner Materials Compatibility
Final Report

cc: See Attached Distribution List

SJR:3339

91 5 08 003

DISTRIBUTION LIST FOR FINAL REPORT

Hydrocarbon-Fuel/Combustion-Chamber--
Liner Materials Compatibility

No. of Copies

National Aeronautics & Space Administration
Lewis Research Center
21000 Brookpark Road
Cleveland, Ohio 44135

Attn: Contracting Officer, MS 500-305
S. B. Foust, MS 500-200
Technical Utilization Office, MS 7-3
Report Control Office, MS 60-1
AFSC Liaison Office, MS 501-3
Library, MS 60-3
R. J. Quentmeyer, MS 500-219
E. A. Roncace, M.S. 500-219

1
2
1
1
2
2
6
1

National Aeronautics & Space Administration
Headquarters
Washington, D. C. 20546

Attn: Director, Advanced Program Development/MD
Director, Propulsion Power & Energy Div./RP
Deputy Director, Propulsion, Power & Energy Div./RP
W. J. D. Escher/RP

1
1
1
1

National Aeronautics & Space Administration
Ames Research Center
Moffett Field, CA 94035
Attn: Library

1

National Aeronautics & Space Administration
Flight Research Center
P. O. Box 273
Edwards, CA 93523
Attn: Library

1

National Aeronautics & Space Administration
George C. Marshall Space Flight Center
Huntsville, Alabama 35812

Attn: Library 1
R. Richmond/ER21 1
J. L. Moses/ER21 1
J. S. Richards/HA31 1
C. S. Cornelius/EP61 1

National Aeronautics & Space Administration
Goddard Space Flight Center
Greenbelt, Maryland 20771
Attn: Library 1

National Aeronautics & Space Administration
John F. Kennedy Space Center
Kennedy Space Center, Florida 32899
Attn: Library 1

National Aeronautics & Space Administration
Lyndon B. Johnson Space Center
Houston, Texas 77001
Attn: Library 1

National Aeronautics & Space Administration
Langley Research Center
Langley Station
Hampton, Virginia 23365
Attn: Library 1

NASA Scientific & Technical Information Facility
P. O. Box 8757
Baltimore-Washington International Airport
Baltimore, Maryland 21240
Attn: Accessing Department 10

Jet Propulsion Laboratory
4800 Oak Grove Drive
Pasadena, CA 91103
Attn: Library 1

Defense Documentation Center
Cameron Station
Building 5
5010 Duke Street
Alexandria, Virginia 22314
Attn: TISIA 1

Defense Advanced Research Projects Agency
1400 Wilson Blvd.
Washington, D. C. 22209
Attn: Library

1

Aeronautical System Division
Air Force Systems Command
Wright-Patterson Air Force Base
Dayton, Ohio
Attn: Library

1

Air Force Phillips Laboratory
Edwards, CA 93523
Attn: Library
PL/RKSS L. M. Singler
PL/RKSS D. Penn

1

1

1

Space Division
Los Angeles Air Force Station, CA 90009
Attn: Library

1

Bureau of Naval Weapons
Department of the Navy
Washington, D. C.
Attn: Library

1

Picatinny Arsenal
Dover, New Jersey 07801
Attn: Library

1

U. S. Naval Research Laboratory
Washington, D. C. 20390
Attn: Library

1

Marquardt Corporation
16555 Saticoy Street
Box 2013 South Annex
Van Nuys, CA 91409
Attn: Library

1

Martin-Marietta Corporation
P. O. Box 179
Denver, Colorado 80201
Attn: Library

1

McDonnell Douglas Space Systems
5301 Bolsa Avenue
Huntington Beach, CA 92647
Attn: Library

1

Pratt & Whitney Aircraft Group
United Technologies Corporation
P. O. Box 2691
West Palm Beach, FL 33402
Attn: Library
J. Joyce
D. R. Connell

1
1
1

Rocketdyne Division
Rockwell International
6633 Canoga Avenue
Canoga Park, CA 91304
Attn: Library
R. P. Pauckert
H. C. Dodson
S. C. Fisher/M.S. 1A06
J. Fang
D. Fulton
J. Volkman

1
1
1
1
1
1
1

Space Division
A Division of Rockwell International
12214 Lakewood Blvd.
Downey, CA 90241
Attn: Library

1

Rocket Research Corporation
Willow Road at 116th Street
Redmond, Washington 98052
Attn: Library

1

Boeing Aerospace Company
P. O. Box 3999
Seattle, Washington 98124
Attn: Library

1

John Hopkins University
Applied Physics Laboratory
John Hopkins Road
Laurel, Maryland 20810

1

Curtiss-Wright Corporation
One Passaic St.
Woodridge, New Jersey 07075
Attn: Library

1

General Dynamics/Convair
P. O. Box 80847
San Diego, CA 92138
Attn: Library

1

General Electric Company
Valley Forge Space Center
P. O. Box 8555
Philadelphia, PA 19101
Attn: Library

1

Grumman Aerospace Corporation
Bethpage, NY 11714
Attn: Library

1

Hughes Aircraft Company
Space & Communications Group
P. O. Box 92919
Los Angeles, CA 90009
Attn: Library

1

Walter Kidde & Company
675 Main St.
Belleville, New Jersey 07109
Attn: Library

1

Lockheed Missiles & Space Company
P. O. Box 504
Sunnyvale, CA 94087
Attn: Library

1

U. S. Army Missile Command
Redstone Scientific Information Center
Redstone Arsenal, Alabama 35808
Attn: Document Section

1

U. S. Naval Air Station
Point Mugu, CA 93041
Attn: Technical Library

1

U. S. Naval Weapons Center
China Lake, CA 93557
Attn: Library

1

Aerospace Corporation
2350 E. El Segundo Blvd.
Los Angeles, CA 90045
Attn: Library
A. Zachary

1

1

Garrett Turbine Engine Co.
402 South 36th Street
Phoenix, Arizona 85034
Attn: Library

1

Aerojet Propulsion Division

P. O. Box 13222

Sacramento, CA 95813

Attn: Library

C. Lacefield

S. D. Rosenberg

R. LaBotz

G. D. Homer

1
1
1
1
1

Avco Systems Division

201 Lowell St.

Wilmington, MA 01887

Attn: Library

1

Bell Aerospace Textron

Box 1

Buffalo, New York 14240

Attn: Library

1

Sundstrand Aviation Mechanical

2421 Eleventh Street

Rockford, Illinois 61101

Attn: Library

1

TRW Systems Group

1 Space Park

Redondo Beach, CA 90278

Attn: Library

1

Vought Corporation

3811 Van Dyke Avenue

Sterling Heights, MI 48077

Attn: Library

1

W. J. Schafer Associates, Inc.

20501 Ventura Blvd.

Woodland Hills, CA 91364

Attn: F. Kirby

1

Report No. KBQ-FR-2
NASA CR-187104

April 1991

HYDROCARBON-FUEL/COMBUSTION-CHAMBER-LINER
MATERIALS COMPATIBILITY

Contract NAS 3-25070

Final Report

31 October 1989 – 31 March 1991

Prepared For

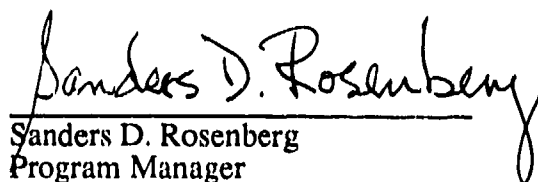
National Aeronautics and Space Administration
Lewis Research Center
21000 Brookpark Road
Cleveland, Ohio 44135

Prepared By:



G. David Homer
Project Engineer

Approved By:



Sanders D. Rosenberg
Program Manager

Aerojet Propulsion Division
P.O. Box 13222
Sacramento, California

ACKNOWLEDGEMENTS

The increased scope phase of the Hydrocarbon-Fuel/Combustion-Chamber-Liner Materials Compatibility Program was carried out by the Aerojet Propulsion Division, Sacramento, California for NASA Lewis Research Center, Cleveland, Ohio. The Program Manager and Project Engineer were Dr. Sanders D. Rosenberg and Dr. G. David Homer, respectively. The Test Engineer responsible for the Carbothermal Test Facility was Mr. Tracy V. Petersen. The NASA-LeRC Program Managers were Mr. Richard Quentmeyer and Ms. Elizabeth A. Roncace. The following individuals also contributed to the success of this program.

R. Beegle
P. Brosseau
J. Cabeal
J. Franklin
M. Gage
R. LaBotz
M. Murphy

R. Pruett
S. Reed
M. Ripley
K. Schaplowsky
L. Schoenman
W. Sobieralski
E. VanderWall

TABLE OF CONTENTS

	Page
1.0 Introduction	1
2.0 Summary	5
3.0 Task 1A – Statistical Data Base	15
3.1 Test Methods	15
3.1.1 Dynamic Test Method	15
3.1.2 Methane Fuel Analysis	20
3.1.3 Post Test Analysis	22
3.2 Dynamic Tests	22
3.2.1 Expanded Operating Conditions	22
3.2.2 Determination of Acceptable Sulfur Levels	44
3.2.3 High Purity Bulk Liquid Methane Survey	57
4.0 Task 2A – Channel Refurbishment	68
4.1 Test Methods	68
4.1.1 Static Test Methods	68
4.1.2 Dynamic Test Methods	68
4.2 Static Tests	70
4.2.1 “Fire Off” Solution	72
4.2.2 Bright Dip Solution	72
4.2.3 Sulfuric Acid Pickle	72
4.2.4 Ferric Chloride Etch Solution	73
4.2.5 Inorganic and Organic Amines	73
4.2.6 Ethylenediamine Tetraacetic Acid (EDTA)	73
4.2.7 Sodium Cyanide Solution	73
4.3 Dynamic Tests	82
5.0 Conclusions	103
Appendix A – Dynamic Test Laboratory Procedures	A-1

LIST OF TABLES

<u>Table No.</u>		<u>Page</u>
1	A Summary of Experimental Results	2
2	Recommended Specification for Sulfur Content In Methane Fuel	10
3	Realistic Cooling Channel Conditions Are Produced in the Aerojet Carbothermal Materials Test Facility	19
4	Vendor Certified Analysis of Technical Grade Methane	21
5	Core Laboratory Analysis of Technical Grade Methane	23
6	Core Laboratory Trace Sulfur Analysis of Technical Grade Methane	24
7	Expanded Data Base for Cooling Channel Operating Conditions	26
8	Dynamic Test Results With Methane Deliberately Contaminated With H ₂ S or CH ₃ SH	45
9	Relative Reactivity of H ₂ S and CH ₃ SH Toward Copper Cooling Channels	56
10	Proposed Sulfur Specification for Propellant Grade Methane	56
11	Department of Defense Requirements (PDSFTT-2) for Liquid Methane	57
12	Typical Specification for Liquid Natural Gas	59
13	Average Field and City Gate Prices for Natural Gas	62
14	Composition of Various Natural Gas Fields	63
15	Assay Results of Quadren Cryogenic Processing Liquid Methane As Compared With PDSFTT-2 Requirements	66
16	Preparation of NASA-Z Coupons for Static Testing	71
17	Screening Tests for Candidate Refurbishment Methods	74
18	Detailed Evaluation of the Aqueous NaCN Refurbishment Method	75
19	Summary of Dynamic Test Data for the Sulfur Corrosion/NaCN Refurbishment Study	84

LIST OF FIGURES

<u>Figure No.</u>		<u>Page</u>
1	Actual Operating Boundaries Achieved for Task 1A	6
2	As Received Cooling Channel of NASA-Z Copper Alloy Test Specimen	7
3	Cooling Channel Showing Minor Sulfur Corrosion After Exposure to Methane Containing 0.5 ppm Isobutylmercaptan	8
4	Cooling Channel Showing Moderate Sulfur Corrosion After Exposure to Methane Containing 0.5 ppm Isobutylmercaptan	9
5	Cooling Channel Showing Heavy Deposits of a Fibrous Form of Cu_2S on All Channel Surfaces After Exposure to 6 ppm CH_3SH	11
6	Pictorial Presentation of Overall Sulfur Corrosion and Cuprous Sulfide Removal Process	13
7	Cooling Channel Surface Features Resulting From the Overall Sulfur Corrosion/NaCN Refurbishment Process	14
8	Schematic of Aerojet Carbothermal Test Facility Setup for Handling Methane Fuel	16
9	Conceptual Design of Aerojet Carbothermal Materials Tester	17
10	Copper Test Specimen Details	18
11	Actual and Proposed Operating Boundaries for Task 1A	25
12	Heat Transfer Efficiency, $\text{Nu}_{(\text{exp})}/\text{Nu}_{(\text{pred})}$, vs Time for Test M307b	28
13	Mass Flow vs Time for Test M307b	29
14	Pressure Drop Across the Cooling Channel vs Time for Test M307b	30
15	Heat Flux vs Time for Test M307b	31
16	Methane Bulk Temperature vs Time for Test M307b	32
17	Cooling Channel Wall Temperature vs Time for Test M307b	33
18	EDS Spectrum of As Received NASA-Z Copper	35
19	EDS Spectrum of Cooling Channel Surface for Test Specimen Used in Test M304	35
20	As Received Cooling Channel of NASA-Z Copper Alloy Test Specimen	36
21	Cooling Channel of Test Specimen After Test M301	37
22	Cooling Channel of Test Specimen After Test M302	38
23	Cooling Channel of Test Specimen After Test M303	39
24	Cooling Channel of Test Specimen After Test M304	40

LIST OF FIGURES (cont.)

<u>Figure No.</u>		<u>Page</u>
25	Cooling Channel of M301 Test Specimen After Removal of the Cu ₂ S Deposits With Aqueous NaCN	41
26	EDS Spectrum of Cooling Channel Surface of M301 Test Specimen After Removal of Sulfur With Aqueous NaCN	42
27	Expanded View of EDS Spectrum Showing Surface Particles Are Grains Enriched in Zirconium and Silver and That Sulfur is Completely Absent	42
28	Cooling Channel of M302 Test Specimen After Removal of the Cu ₂ S Deposits With Aqueous NaCN	43
29	Heat Transfer Efficiency, $Nu_{(exp)}/Nu_{(pred)}$, vs Time for Test M308 (1 ppm H ₂ S)	46
30	Mass Flow vs Time for Test M308 (1 ppm H ₂ S)	47
31	Pressure Drop Across the Cooling Channel vs Time for Test M308 (1 ppm H ₂ S)	48
32	Heat Flux vs Time for Test M308 (1 ppm H ₂ S)	49
33	Methane Bulk Temperature vs Time for Test M308 (1 ppm H ₂ S)	50
34	Cooling Channel Wall Temperature vs Time for Test M308 (1 ppm H ₂ S)	51
35	Cooling Channel of Test M312a Test Specimen After Exposure to 6 ppm CH ₃ SH	53
36	Close-Up of the Fibrous Form of Cu ₂ S on the Test M312a Test Specimen Walls and an EDS Spectrum Showing the Presence of Sulfur	54
37	Comparison of the Average Rate of Decrease in Mass Flow Rate for the Tests With Sulfur Contaminated Methane	55
38	Estimated Requirements for High Purity Liquid Methane Propellant	61
39	Forecasted Cost of Bulk High Purity Liquid Methane	64
40	Static Gas Pressure Refurbishment Apparatus	69
41	EDS Spectrum of Test Coupon ZA1 Before NaCN Refurbishment	77
42	EDS Spectrum of Test Coupon ZA1 After NaCN Refurbishment	77
43	SEM Photomicrograph of a Freshly Electropolished NASA-Z Copper Coupon	78
44	SEM Photomicrographs of Test Coupon ZA1 After Sulfur Corrosion and NaCN Refurbishment	79
45	SEM Photomicrographs of Test Coupon ZA28 After Exposure to 5% (w/w) NaCN	80
46	Pictorial Presentation of Overall Sulfur Corrosion and Cuprous Sulfide Removal Process	81

LIST OF FIGURES (cont.)

<u>Figure No.</u>		<u>Page</u>
47	Heat Transfer Efficiency, $Nu_{(exp)}/Nu_{(pred)}$, vs Time for Test M316. Test Specimen ZA3 After Sulfur Corrosion/NaCN Refurbishment	85
48	Mass Flow vs Time for Test M316. Test Specimen ZA3 After Sulfur Corrosion/NaCN Refurbishment	86
49	Pressure Drop Across the Cooling Channel vs Time for Test M316. Test Specimen ZA3 After Sulfur Corrosion/NaCN Refurbishment	87
50	Heat Flux vs Time for Test 316. Test Specimen ZA3 After Sulfur Corrosion/NaCN Refurbishment	88
51	Methane Inlet Temperature vs Time for Test M316. Test Specimen ZA3 After Sulfur Corrosion/NaCN Refurbishment	89
52	Cooling Channel Wall Temperature vs Time for Test M316. Test Specimen ZA3 After Sulfur Corrosion/NaCN Refurbishment	90
53	Mass Flow Performance for Specimen ZA3 Before Sulfur Corrosion (M307b) and After Sulfur Corrosion/NaCN Refurbishment (M316)	91
54	Heat Transfer Performance of Specimen ZA3 Before Sulfur Corrosion (M307b) and After Sulfur Corrosion/NaCN Refurbishment (M316)	92
55	Mass Flow Performance for Specimen ZA13 Before Sulfur Corrosion (M307a) and After Sulfur Corrosion/NaCN Refurbishment (M315)	93
56	Heat Transfer Performance for Specimen ZA13 Before Sulfur Corrosion (M307a) and After Sulfur Corrosion/NaCN Refurbishment (M315)	94
57	Mass Flow Performance for Specimen ZA18 Before Sulfur Corrosion (M306) and After Sulfur Corrosion/NaCN Refurbishment (M314)	95
58	Heat Transfer Performance for Specimen ZA18 Before Sulfur Corrosion (M306) and After Sulfur Corrosion/NaCN Refurbishment (M314)	96
59	Mass Flow Performance for Specimen ZA23 Before Sulfur Corrosion (M305) and After Sulfur Corrosion/NaCN Refurbishment (M313)	97
60	Heat Transfer Performance for Specimen ZA23 Before Sulfur Corrosion (M305) and After Sulfur Corrosion/NaCN Refurbishment (M313)	98
61	Cooling Channel Surface Features Resulting From the Overall Sulfur Corrosion/NaCN Refurbishment Process	100
62	SEM Photomicrographs of "Copper Wool"	101
63	EDS Spectrum of "Copper Wool" From Close-Up in Figure 62d	102

1.0 INTRODUCTION

This is the final report for the Hydrocarbon Fuel/Combustion-Chamber-Liner Materials Compatibility Program, Contract NAS 3-25070. The total period of performance for this program was 7 November 1986 through 31 March 1991. The initial objectives of the program are detailed in an Interim Final Report that covers the period of performance from 7 November 1986 through 31 October 1989. These results are briefly summarized below. The scope of the program was increased based on the experimental results obtained in achieving the initial objectives. This final report details the results of the work carried out on the increased scope phase of the program which had a period of performance from 31 October 1989 through 31 March 1991.

The original scope of the program had three major objectives. They were (1) to define the corrosive interaction process that occurs between hydrocarbon fuels and candidate combustion chamber liner materials, (2) to develop and evaluate protective measures to remedy the defined corrosive interaction process, and (3) to recommend a test program which will verify the validity of the measures under actual service conditions. A four-task program was conducted to achieve these program objectives, i.e., Task 1 — Corrosive Interaction and Rates Determination, Task 2 — Protective Measures Development and Evaluation, Task 3 — Protective measures Verification Program, and Task 4 — Reporting Requirements. The following is a brief summary of the results of this work. A detailed discussion is provided in the Interim Final Report, Report No. KFQ-FR-1, NASA CR-185203.

Material compatibility studies were conducted between hydrocarbon fuels and copper chamber liner materials. The hydrocarbon fuels tested were MIL-SPEC RP-1, n-dodecane, propane, and methane. The copper chamber liner materials tested were OFHC, NASA-Z, and Zirconium Copper. Two distinct methods were employed. Static tests, in which copper coupons were exposed to fuel for long durations at constant temperature and pressure, were used to provide compatibility data in precisely controlled environments. Dynamic tests, using the Aerojet Carbothermal Test Facility, were conducted to provide fuel and copper compatibility data under realistic booster engine service conditions. Dynamic test conditions simulated the heat flux, coolant channel wall temperature, fuel velocity, temperature, and pressure expected in the cooling channels of a regeneratively cooled LOX/hydrocarbon booster engine operating at chamber pressures up to 3000 psia. Tests were conducted using (1) very pure grades of each fuel and (2) fuels to which a contaminant, e.g., ethylene, methyl mercaptan, hydrogen sulfide, etc., was added to define the role played by fuel impurities.

1.0, Introduction (cont.)

This material compatibility research was motivated, in part, by prior work conducted by United Technologies Research Center and Rockwell International Rocketdyne Division. In these programs, severe copper corrosion and carbon deposition were encountered during the conduct of electrically heated tube tests. These results have very important implications for the development of long-life oxygen/hydrocarbon booster engines. Thus, the first two objectives of the program were (1) to define the corrosive interaction process that occurs between hydrocarbon fuels and copper combustion chamber liner materials, and (2) to develop and demonstrate protective measures against this corrosive process.

In Task 1 of this program, compatibility tests were conducted between hydrocarbon fuels and copper chamber liner materials. It was found that each of the copper materials exhibited similar compatibility behavior. However, there were significant differences among the various hydrocarbon fuels tested. Table 1 summarizes the test results obtained in Task 1 of this program.

TABLE 1

A SUMMARY OF EXPERIMENTAL RESULTS

	RP-1	Methane	Propane
Carbon	Yes	No	No
Containing	Above T_{wall}	Up to T_{wall}	Up to T_{wall}
Deposits	580 F	934 F	865 F
Copper	Yes*	Yes*	Yes*
Corrosion	With 50 ppm S	Down to 1 ppm S	In All Tests

*Copper corrosion occurs only when sulfur is present in these fuels.
Cuprous sulfide is the corrosion product

Task 1 tests with RP-1 and *n*-dodecane demonstrated a deposition reaction occurs when the surface temperature of the copper exceeded 580 F. The result of this deposition process was the formation of a chemically complex, thin, but very tenacious, tar on all exposed copper surfaces. This tar inhibited heat transfer, but had little effect on the flowrate or pressure drop through the cooling channel. It did not have a major impact on the heat transfer characteristics of the channel.

1.0, Introduction (cont.)

In contrast, Task 1 tests with methane did not show any deposition reactions, even at copper surface temperatures up to 934 F. However, severe corrosion of copper was observed when very small amounts of sulfur impurities (e.g., 1 ppm of methyl mercaptan) were added to the methane. In two tests conducted with a relatively high concentration of methyl mercaptan in the methane (200 and 10 ppm, respectively) the formation of corrosion product (Cu_2S) became so massive as to block entirely the flow of fuel through the channel.

Task 1 tests with propane did not show any carbon deposition, even at copper surface temperatures up to 865 F. However, corrosion of copper by sulfur compounds was observed in every test with propane, and resulted in the formation of powdery black deposits of Cu_2S on the channel surfaces. Samples of the propane used in testing were analyzed by industrial and university laboratories in an attempt to characterize the impurities causing the corrosion. No sulfur compounds could be detected in the gas phase of the propane, even when using very sensitive analytical methods reportedly accurate to levels as low as 50 parts per billion. The inability of the analytical method to identify the source of contamination observed in the propane tests indicates representative samples of the propane could not be delivered to the analytical device. Parametric testing with the propane confirmed earlier results reported by UTRC, i.e., the velocity and inlet temperature of the propane were significant factors in the amount of corrosion product formed in the channel.

Task 2 tests demonstrated the efficacy of metallic coatings as a means of corrosion protection for the cooling channels. Static tests established the nobility of six metals in a high pressure, high temperature environment of methane plus relatively high concentrations of sulfur compounds. Two of the six metals, gold and platinum, were selected for further study. Dynamic test specimen were fabricated and the test channels were protected by a thin layer of electro-deposited gold or platinum. The specimen were subjected to dynamic tests at realistic booster engine conditions while operating with methane coolant containing 5 ppm (by vol) methyl mercaptan. Additional tests were conducted with 5 ppm (by vol) hydrogen sulfide. Corrosion of the cooling channels was effectively reduced by the gold and platinum coatings.

In Task 3, a program plan was developed which called for the fabrication and testing of a 40,000 lbF thrust chamber with copper cooling channels protected from corrosion with a metallic coating, e.g., gold. Tests were described in which the chamber is to be cooled with (1) sulfur-

1.0, Introduction (cont.)

free methane and (2) methane containing a measured amount of sulfur contaminant to demonstrate the effectiveness of the coatings in extending the useable chamber life in booster engines to be used in recoverable, reusable vehicles.

The increased scope phase of the program added two major tasks to the original objectives: Task 1A — Statistical Data Base and Task 2A — Channel Refurbishment.

Task 1A — Statistical Data Base, is to develop a more extensive experimental data base for the compatibility of methane and NASA-Z copper alloy over a wide range of coolant channel operating conditions. To extend and better define the data base established in Task 1, a series of tests were conducted with methane deliberately contaminated with sulfur compounds to determine the corrosion rate of the channels as a function of sulfur content of the fuel, and to determine if there is an acceptable limit for sulfur compounds in the fuel. The objectives of Task 1A were achieved with a five-subtask program, i.e., Task 1A.1 — Fuel Acquisition, Task 1A.2 — Specimen Fabrication, Task 1A.3 — Test Facility Preparation, Task 1A.4 — Thermal Sciences Laboratory Tests, and Task 1A.5 — Thermal Sciences Data Analysis and Interpretation.

Task 2A — Channel Refurbishment, is to develop and demonstrate a method of protecting the chamber liner by refurbishment of corroded cooling channels. The objectives of Task 2A were achieved with a five-subtask program, i.e., Task 2A.1 — Selection of Candidate Methods, Task 2A.2 — Static Laboratory Tests, Task 2A.3 — Post Static Test Analysis, Task 2A.4 — Dynamic Laboratory Tests, and Task 2A.5 — Post Dynamic Test Analysis. The results of the research conducted in Tasks 1A and 2A were reported in Task 4A — Reporting Requirements.

2.0 SUMMARY

The statistical data base, generated under Task 1A for the compatibility of methane with NASA-Z copper alloy, was expanded to cover a wide range of coolant channel operating conditions with and without added sulfur contaminants in the methane fuel. Dynamic tests, using the Aerojet Carbothermal Test Facility, were carried out under conditions simulating heat flux, coolant channel wall temperature, fuel velocity, temperature, and pressure expected in the cooling channels of a regeneratively cooled LOX/hydrocarbon booster engine operating at chamber pressures up to 3000 psi. All dynamic test specimen were analyzed for carbon deposition and sulfur corrosion by scanning electron microscopy (SEM), optical microscopy, and electron dispersion spectroscopy (EDS).

The dynamic test results with low sulfur content methane fuel, i.e., 0.5 ppm isobutyl mercaptan which is approximately equivalent to 0.1 ppm hydrogen sulfide (H_2S), showed that neither carbon deposition nor sulfur corrosion were serious enough to lead to measurable losses in cooling channel heat transfer, mass flow rate, and pressure drop across the channel, during the course of 15-25 minute test runs. The Task 1A experimental test matrix actually achieved for low sulfur content methane had the operating boundaries shown in Figure 1. Thus, even at coolant channel wall temperatures as high as 1094 F, cooling channel performance did not deteriorate. However, post dynamic test analysis of the test specimen by optical microscopy, SEM, and EDS did show minor amounts of carbon deposition and moderate amounts of sulfur corrosion under the most severe operating conditions, i.e., 1094 F wall temperature and a low heat flux of 20 BTU/in.²-sec. Virtually no carbon deposition was detectable under less severe test conditions, but minor amounts of the sulfur corrosion product cuprous sulfide (Cu_2S) were found in all the test specimen. These results clearly show that carbon deposition is never a significant problem and that sulfur corrosion is present even with low sulfur content methane, although the extent of sulfur corrosion was not severe enough to degrade cooling channel performance. Figures 2, 3, and 4 are SEM photomicrographs showing as received cooling channels, minor corrosion, and the moderate corrosion found for $T_{wall} = 1094$ F at a heat flux of 20 BTU/in.²-sec, respectively.

Dynamic test results using methane deliberately contaminated with small amounts of either methylmercaptan (CH_3SH) or H_2S clearly showed that sulfur corrosion was severe enough to seriously degrade cooling channel performance even at levels as low as 1 ppm H_2S . For example, all dynamic tests with added sulfur contaminants showed substantial declines in heat transfer, mass flow rate, and heat flux, and corresponding increases in the pressure drop

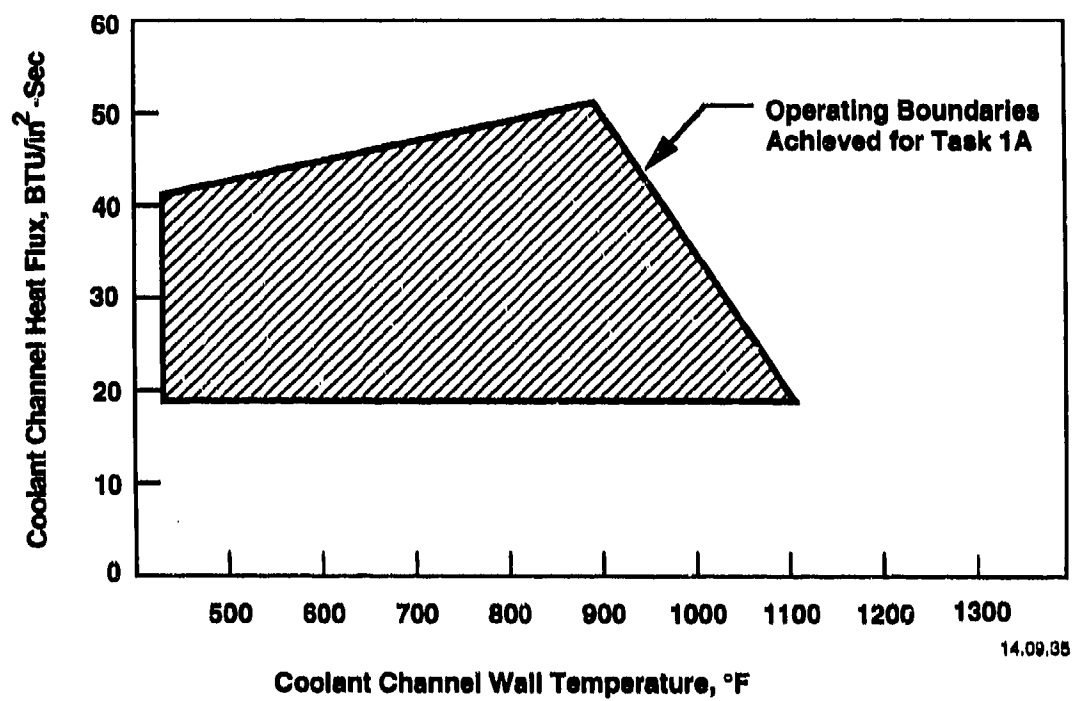


Figure 1. Actual Operating Boundaries Achieved for Task 1A

AR

AR



15-10-32

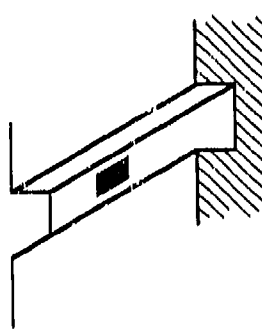


**Figure 2. As Received Cooling Channel of NASA-Z Copper Alloy Test Specimen.
Machine Marks Are the Only Distinctive Features**

M301



000098 20KV X200 150um

M301



000099 20KV X500 60um

15-18-33

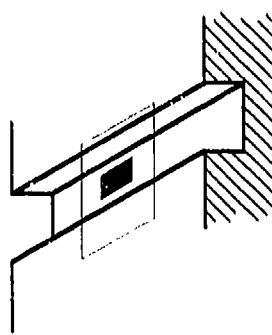
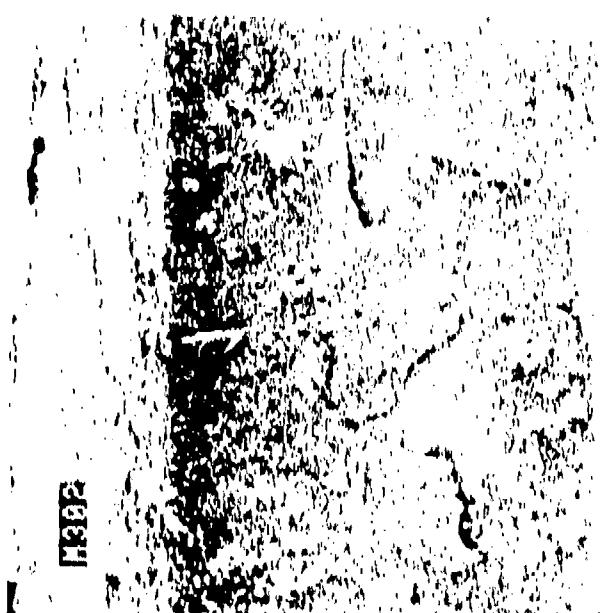


Figure 3. Cooling Channel Showing Minor Sulfur Corrosion After Exposure to Methane Containing 0.5 ppm Isobutylmercaptan at a Wall Temperature of 425°F and Heat Flux of 19 Btu/in.² -sec. Note, Cu₂S Deposits Do Not Cover Channel Surface and Machine Marks Are Still Visible



000007 20KV X500 60um 15-10-96



000006 20KV X200 150um

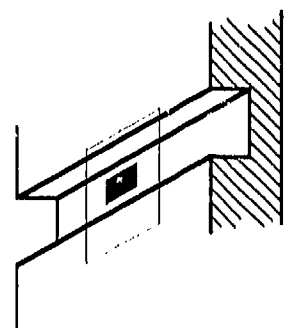


Figure 4. Cooling Channel Showing Moderate Sulfur Corrosion After Exposure to Methane Containing 0.5 ppm Isobutylmercaptan at a Wall Temperature of 1094°F and Heat Flux of 20 Btu/in.² -sec. Note, Cu₂S Deposits Cover Most of Channel Surface

2.0, Summary (cont.)

across the channel. In a test with 10 ppm CH_3SH the build up of Cu_2S corrosion products nearly blocked all flow through the channel by the end of a 28 minute run. Figure 5 are SEM photomicrographs showing heavy deposits of a fibrous form of Cu_2S on all cooling channel surfaces.

A careful comparison of the performance data for the tests with sulfur contaminated methane suggested that H_2S is more aggressive than CH_3SH or other mercaptans. This is expected on the basis of sound chemistry principles. Furthermore, the data with and without added sulfur suggests that a specification for methane fuel capable of protecting a reusable copper alloy booster engine from significant corrosion must have very low limits for sulfur. The recommended specification is shown in Table 2. It should be noted that the Department of Defense purchase description for propellant grade bulk liquid methane, PDSFTT-2, allows 1 ppm total sulfur with no differentiation between types of sulfur compounds. Such a specification would be completely inadequate for protecting a reusable copper alloy booster engine.

TABLE 2

**RECOMMENDED SPECIFICATION FOR SULFUR CONTENT IN
METHANE FUEL**

<u>Sulfur Contaminant</u>	<u>Specification</u>
H_2S	0.1 ppm (max)
Mercaptans	0.2 ppm (max)
Total Sulfur	0.5 ppm (max)

High purity bulk liquid methane, LCH_4 , that meets the requirements shown in Table 1 has very limited availability at this time. There are no major suppliers and only one small supplier, Quadren Cryogenic Processing, Ltd., located 40 miles north of Sacramento, California. QCP has capacity to meet projected aerospace needs up to the year 2004. The technology to produce high purity LCH_4 is well in hand, but the economic incentives to do so are not there for potential major suppliers such as Air Products, because the aerospace market is extremely small in comparison to other markets with less demanding purity requirements. Thus, high purity bulk LCH_4 is likely to remain in limited supply for the foreseeable future and NASA might be well advised to consider producing their own fuel on-site by purifying readily available pipeline natural gas using licensed technology, should a large aerospace demand for high purity LCH_4 materialize.

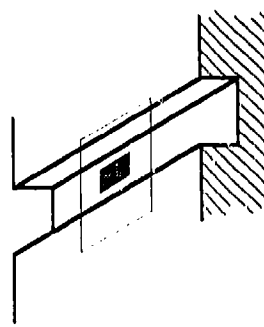
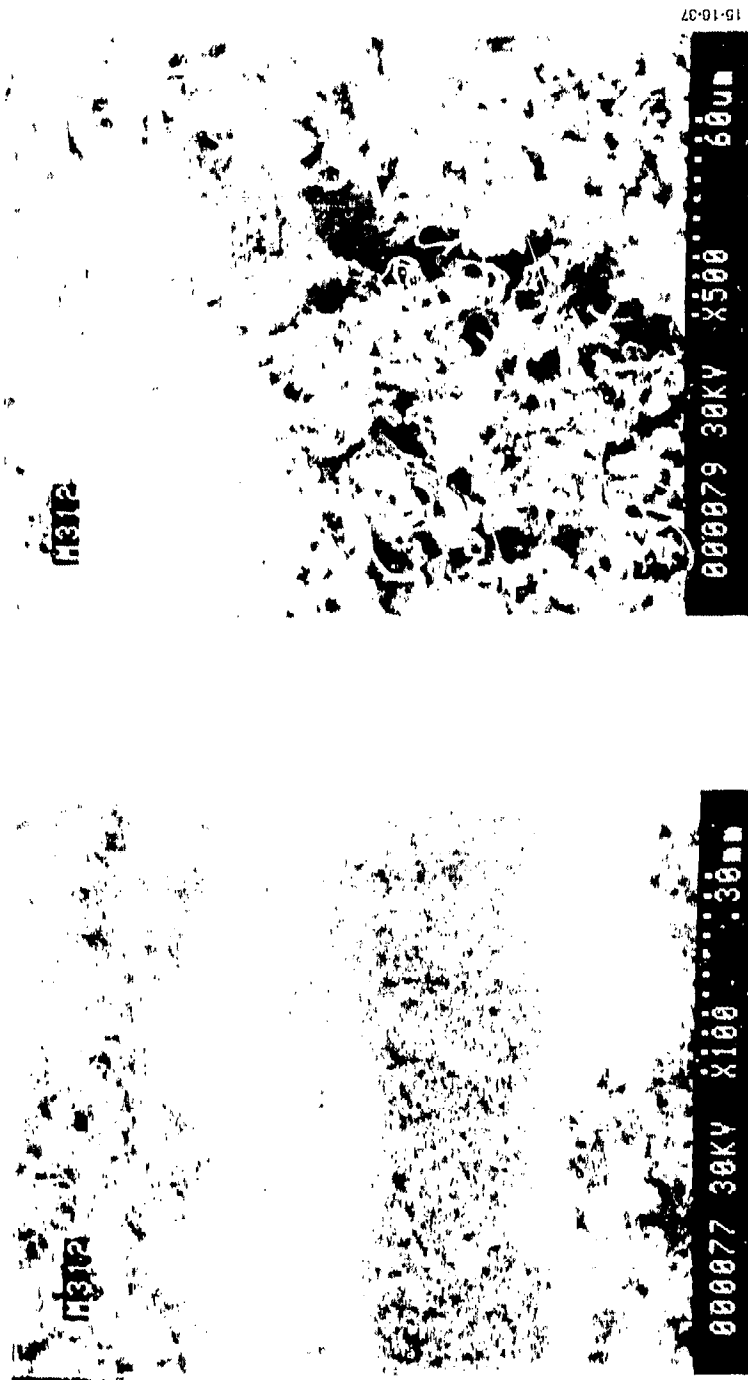


Figure 5. Cooling Channel Showing Heavy Deposits of a Fibrous Form of Cu_2S on All Channel Surfaces After Exposure to 6 ppm CH_3SH .

2.0, Summary (cont.)

A cooling channel refurbishment technique was developed under Task 2A for the purpose of removing Cu_2S corrosion products from the cooling channels of a copper alloy booster engine inadvertently exposed to fuel containing excessive amounts of sulfur contaminants. Static tests with sulfur corroded NASA-Z coupons were used to identify and fully characterize a feasible process. SEM and EDS were used to characterize the coupon surfaces before corrosion and after refurbishment. The efficacy of the process was demonstrated using the sulfur corroded dynamic test specimen from Task 1A. After refurbishment, the dynamic test specimen were re-tested with low sulfur methane and the overall performance was compared with the performance of the same specimen prior to corrosion. SEM and EDS were used to determine the condition of the cooling channels after the sulfur corrosion/refurbishment process.

The static test results identified only one process capable of efficiently removing Cu_2S without attacking the bare copper alloy. This process involves a brief, i.e., less than 5 minutes, treatment with 5% (w/w) aqueous sodium cyanide (NaCN) which dissolves the Cu_2S . The resulting copper surface is highly pitted and rough. This roughening is primarily due to the nature of the initial corrosion process which involves preferential grain boundary attack by the sulfur corrosive. The overall process is graphically illustrated in Figure 6.

The dynamic test results showed that the sulfur corrosion/NaCN refurbishment process consistently leads to moderate increases in heat transfer performance at the expense of a moderate decrease in mass flow rate relative to the performance of the same test specimen under identical test conditions prior to corrosion. This change in performance is due to the increase in surface roughness which retards mass flow, thus improving heat transfer efficiency. SEM and EDS analysis of the dynamic test specimen after final re-testing showed all exposed surfaces to be roughened as expected. Figure 7 shows the typical cooling channel surface features resulting from the overall sulfur corrosion/NaCN refurbishment process. The most interesting feature is the "copper wool" that was found in small to moderate amounts in all the specimen. It is tightly bound to the channel surfaces and closely resembles the fibrous form of Cu_2S (see Figure 5). Thus, it is likely that the "copper wool" derives from the fibrous form of Cu_2S . In any case, such a surface feature would certainly impede mass flow. Thus, the NaCN refurbishment technique does efficiently remove all the sulfur corrosion products, but it also leaves a highly roughened surface that can be expected to lead to performance changes.

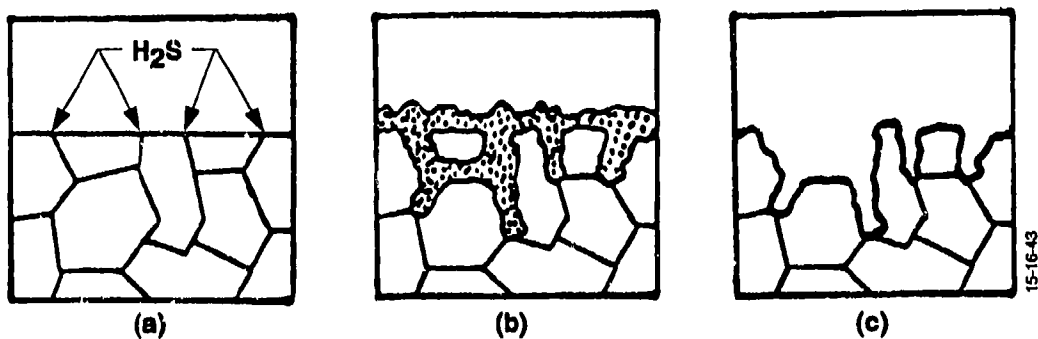
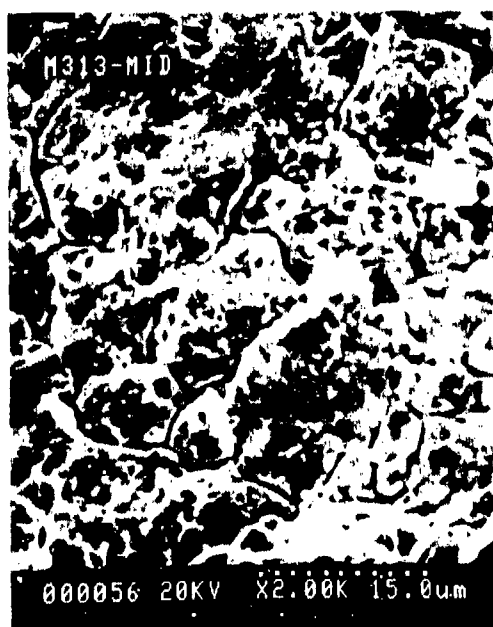


Figure 6. Pictorial Presentation of Overall Sulfur Corrosion and Cuprous Sulfide Removal Process

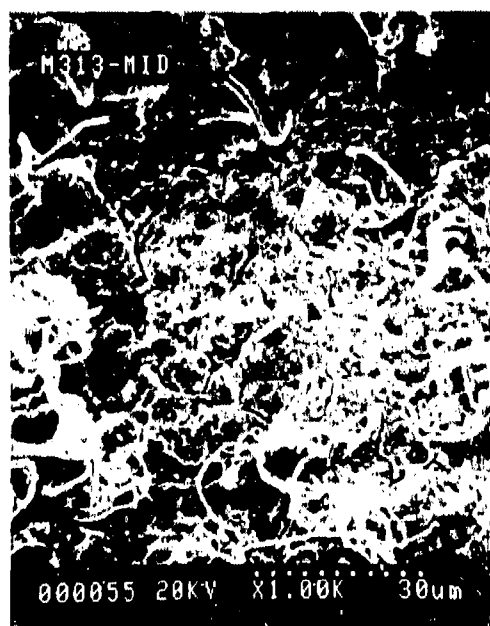
- (a) Preferential Grain Boundary Attack By H_2S on Cu Alloy**
- (b) Resulting Cu_2S Corrosion Product, Has Penetrated the Grain Boundaries, Completely Undermining and Isolating Some Surface Grains**
- (c) Removal of the Cu_2S With Aqueous NaCN Also Leads to the Loss of the Isolated Grains, Leaving a Rough, Highly Pitted Surface**



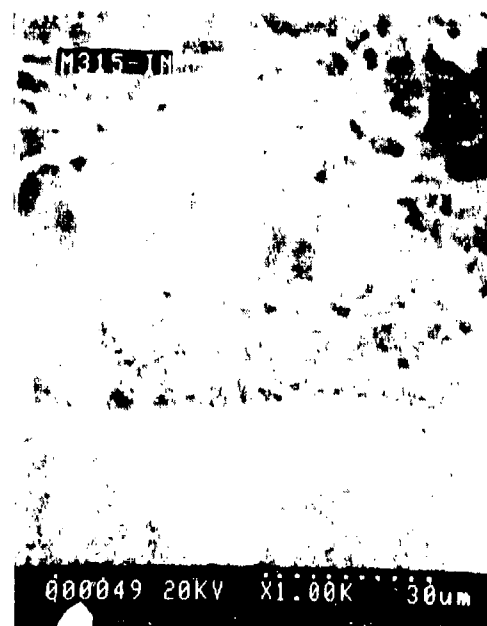
(a)



(b)



(c)



(d)

15-1625

Figure 7. Cooling Channel Surface Features Resulting From the Overall Sulfur Corrosion/NaCN Refurbishment Process

- (a) Well Defined Grain Boundaries and Pitting (Very Common)
- (b) Pitting (Very Common)
- (c) "Copper Wool" (Moderately Common)
- (d) Close-up of "Copper Wool". Note Similarity to Fibrous Form of Cu_2S Shown in Figure 5

3.0 TASK 1A — STATISTICAL DATA BASE

3.1 TEST METHODS

This section describes the test apparatus, test specimen, test procedures, and analytical methods used for the dynamic testing carried out in Task 1A.

3.1.1 Dynamic Test Method

All dynamic testing was carried out in the Aerojet Carbothermal Test Facility. Figure 8 is a schematic diagram of the dynamic test apparatus setup for handling methane fuel.

The apparatus actually incorporates two fuel delivery subsystems, one for high-pressure methane as was used on this program and another for liquid fuels, which was not used. The liquid delivery subsystem is not shown in Figure 8 for the sake of clarity. The methane is precooled to between -200 and -100 F in an LN₂ cooled heat exchanger enroute to the heated copper specimen. The test specimen is heated within the Aerojet Carbothermal Materials Tester without the use of direct ohmic heating. The apparatus incorporates appropriate filters, thermocouples, pressure transducers, heat exchangers, and mass flowmeters to control and monitor the test conditions and record the test data on-line.

Figure 9 is a conceptual diagram of the Aerojet Carbothermal Material Tester. It consists of a large copper block which is heated by ten electrically insulated cartridge heaters embedded in the block. The heat input into the block is transferred by conduction through a test specimen made of the copper material to be tested. The heat is then withdrawn through a 0.020-in. square cooling channel milled in the bottom of each specimen by fuel flowing through the channel. Figure 10 shows photographs of a typical test specimen used in the Aerojet Carbothermal Materials Tester.

Realistic simulations of cooling channel conditions were produced in this facility without the use of direct ohmic heating of the specimen. Table 3 compares channel conditions produced in earlier methane tests, Task 1, with design conditions for the STBE methane engine. Note that each of the relevant design parameters were reproduced, including wall temperature, fuel temperature and pressure, fuel velocity, and heat flux through the channel wall.

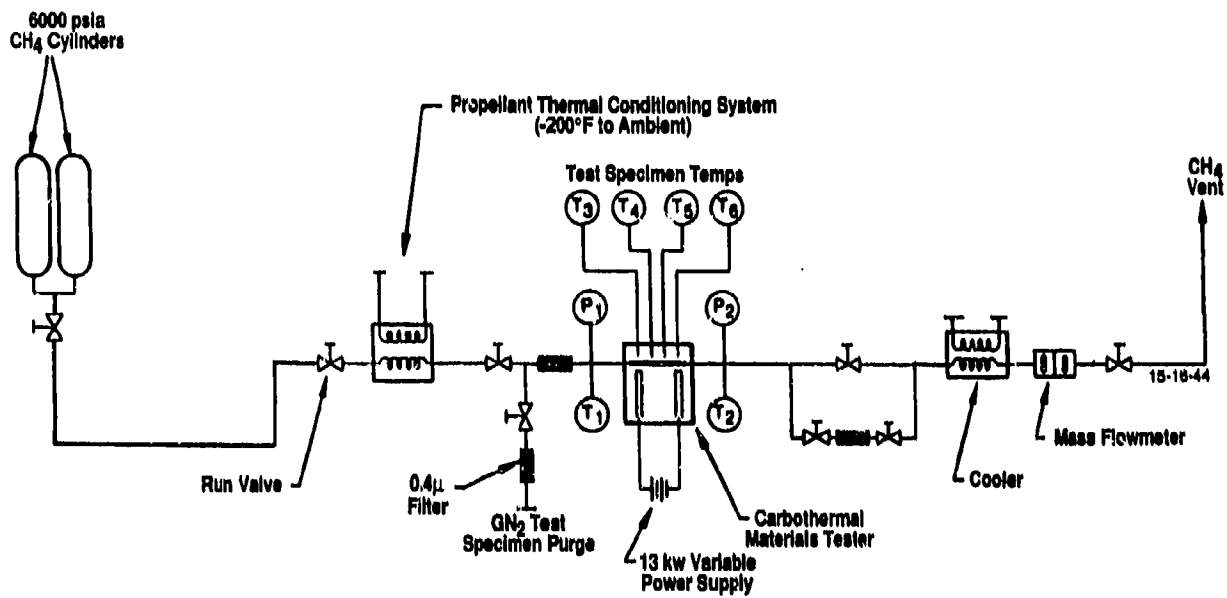
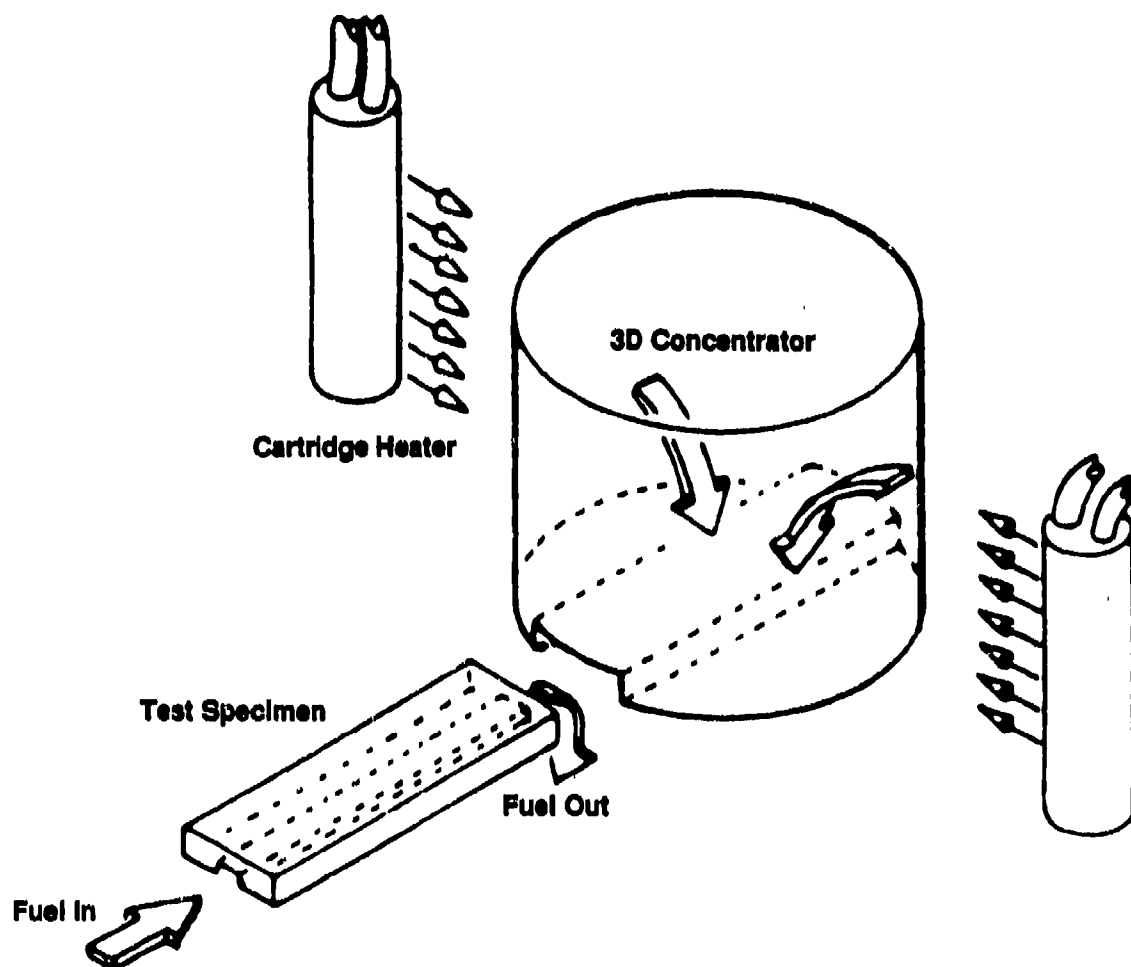


Figure 8. Schematic of Aerojet Carbothermal Test Facility Set-up for Handling Methane Fuel



**The Geometric Concentration of Energy is an
Alternative to Ohmically Heated Test Specimens**

Figure 9. Conceptual Design of Aerojet Carbothermal Materials Tester

0.020 in. Square Channel

Fuel Inlet Tube



15-16-23

OFHC Cover Sheet

Completed CH₄/Cu Test Specimen

As Machined NASA-Z Test Specimen

Figure 10. Copper Test Specimen Details

TABLE 3

REALISTIC COOLING CHANNEL CONDITIONS ARE PRODUCED IN
THE AEROJET CARBOTHERMAL MATERIALS TEST FACILITY

	<u>Methane Test Conditions</u>	<u>STBE Design</u>
Wall Temperature, °F	650-930	800
Max Coolant-Side q/A , Btu/in. ² -s	52	51
Coolant Pressure, psia	4200	4400
Coolant Velocity, ft/s	100 → 1000	300 → 500
Bulk Temperature, °F	-150 → +380	-200 → +70
Test Duration, sec	1000 - 1800	160/mission

3.1, Test Methods (cont.)

Another advantage provided by the Aerojet Carbothermal Materials Tester is that examination of the test specimen can be accomplished without disturbing the surfaces which were in contact with the fuel. The high thermal strains encountered with methane required that the channel be closed out with a thin sheet (0.020 in.) of OFHC copper welded around the channel. After testing, a simple end mill operation opened the channel for examination without disturbing the specimen channel which had been exposed to the flowing fuel.

All dynamic test specimen were machined from the billets of NASA-Z copper alloy supplied by NASA-LeRC. All dynamic specimens were cleaned, prior to testing. SEM photomicrographs of the channel surfaces before testing were taken on three specimens selected at random. No discernible difference was found among these specimen, and it was assumed they were representative of all specimen channels before testing.

Appendix A presents the Test Area checklist which was used in the conduct of the dynamic tests. This checklist describes the sequence of operation that was typically used to conduct a dynamic test.

Each dynamic test was run at a constant wall temperature, as measured by four thermocouples along the channel wall. To achieve this, the power going to the heaters in the Aerojet Carbothermal Materials Tester was manually adjusted during the test with a potentiometer.

Data were collected from the on-line instrumentation of the system through a Daytronic data acquisition system, and stored every 5 seconds on an IBM-AT. A data reduction program was written to calculate test conditions and to analyze the hydraulic and heat transfer performance of the specimen during the test. A listing of the data reduction program, along with a typical page of output from a test, is included in Appendix C of the Interim Final Report.

3.1.2 Methane Fuel Analysis

The methane fuel used in this program was supplied with a vendor certified analysis. In addition, samples were taken and submitted to an outside analytical laboratory for a detailed trace sulfur analysis. The outside analytical laboratory was selected on the basis of a survey concerning the capability to routinely and accurately carry out the required trace sulfur analysis. The survey included recommendations from technical personnel in the oil, natural gas,

3.1, Test Methods (cont.)

and specialty gas industries and professional associations, such as, American Petroleum Institute, Natural Gas Supply Association, American Gas Association, etc. This survey clearly identified gas chromatography with flame photometric detection (FPD) as the method of choice for trace sulfur analysis in petroleum-based products. Numerous independent analytical laboratories service the oil and natural gas industries. However, Core Laboratory based in Dallas, Texas appears to have the best overall capability. They have the capability to detect and quantify all nineteen of the most common sulfur impurities found in petroleum-based products using FPD gas chromatography. Therefore, Core Laboratory was selected as the outside analytical laboratory for trace sulfur analysis.

The methane used in this program was Technical Grade Methane supplied by Linde Speciality Gases. Table 4 shows the vendor certified analysis. The analysis given in Table 4 does not adequately identify the sulfur content for the purpose of this program. The detection limit of 1 ppm is too insensitive since we know from the earlier results reported in the Interim Final Report that 1 ppm sulfur in methane can cause severe corrosion. Secondly, the analysis does not identify the individual sulfur compounds present. This is important since well known chemical principles tell us that some sulfur compounds will be more aggressive corrosives than others. For example, the most likely sulfur impurities in methane are H₂S, CH₃SH, other mercaptans, and sulfides. The expected order as copper corrosives is shown below in equation 1, with H₂S being most corrosive to copper.

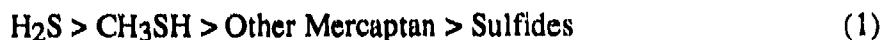


TABLE 4
VENDOR CERTIFIED ANALYSIS OF TECHNICAL GRADE METHANE

<u>Component</u>	<u>Analysis</u>
Methane	99.87%
Air	<1270 ppm
H ₂ O	<1 ppm
CO ₂	<1 ppm
Ethane	<23 ppm
Other Hydrocarbons	<1 ppm
Total Sulfur	N.D. ^a

^aNone detected. Detection limit reported to be 1 ppm.

3.1, Test Methods (cont.)

Duplicate samples of the Technical Grade Methane were submitted to Core Laboratory for both compositional analysis and detailed trace sulfur analysis. Tables 5 and 6 show the results of these analyses. The compositional analysis shown in Table 5 is in good agreement with the vendor supplied certified analysis for methane content and gross sulfur, i.e., both agree that the sulfur content is less than 1 ppm. The minor differences in regards to other components do not impact this program. Table 6 shows that the methane contains 0.5 ppm (vol) of isobutyl mercaptan and no other sulfur compounds. Taking molecular weight and reactivity differences into consideration, 0.5 ppm isobutyl mercaptan should be roughly equivalent to 0.1 ppm H₂S. Thus, the methane used in this program can certainly be considered low sulfur-containing material.

The H₂S and CH₃SH used to deliberately contaminate the methane in some runs was supplied in lecture bottles from Matheson Gas Products and was used as received.

3.1.3 Post Test Analysis

Post test analysis of the dynamic test specimen was carried out using a combination of optical microscopy, SEM, and EDS. The methods were used to determine the presence and severity of coking and/or corrosion.

3.2 DYNAMIC TESTS

3.2.1 Expanded Operating Conditions

One of the primary goals of Task 1A was to expand the data base for the compatibility of methane with NASA-Z copper to cover a wider range of coolant channel operating conditions. The originally proposed operating boundaries are shown as dotted lines in Figure 11 and the operating boundaries actually achieved are shown as solid lines. The difference between the proposed boundaries and those actually achieved reflect the practical limitations of the Aerojet Carbothermal Test Apparatus.

In addition to monitoring cooling channel performance during a test, i.e., heat transfer, mass flow rate, and pressure drop across the channel, the dynamic test specimen were inspected for carbon deposition (coking) and corrosion after each test to allow a correlation to be made between channel performance and the chemical processes taking place in the channels. Table 7 summarizes the results of this phase of the program.

TABLE 5
CORE LABORATORY ANALYSIS OF TECHNICAL
GRADE METHANE COMPOSITION

Component	Analysis (% by vol)	
	With Air	Air Free
Methane	99.92%	99.92%
H ₂	0.000	0.000
CO	0.02	0.02
CO ₂	0.01	0.01
O ₂	Trace	Trace
N ₂	0.00	0.00
SO ₂	0.00	0.00
H ₂ S	0.00	0.00
Ethane	0.02	0.02
Other Hydrocarbons	0.03	0.03

TABLE 6**CORE LABORATORY TRACE SULFUR ANALYSIS OF
TECHNICAL GRADE METHANE**

Sulfur Component	Analysis (ppm by vol)	Detection Limit
H ₂ S	ND	0.1 ppm
CH ₃ SH	ND	0.1 ppm
Ethyl Mercaptan	ND	0.1 ppm
Carbonyl Sulfide	ND	0.1 ppm
Dimethyl Sulfide	ND	0.1 ppm
Carbon Disulfide	ND	0.1 ppm
Isopropyl Mercaptan	ND	0.1 ppm
n-Propyl Mercaptan	ND	0.1 ppm
Methyl Ethyl Sulfide	ND	0.5 ppm
t-Butyl Mercaptan	ND	0.5 ppm
s-Butyl Mercaptan	ND	0.5 ppm
Isobutyl Mercaptan	0.5 ppm	0.5 ppm
Diethyl Sulfide	ND	0.5 ppm
n-Butyl Mercaptan	ND	0.5 ppm
3-Pentanethiol	ND	0.5 ppm
Dimethyl Disulfide	ND	0.5 ppm
Tetrahydrothiophene	ND	0.5 ppm
Ethyl Methyl Disulfide	ND	0.5 ppm
Diethyl Disulfide	ND	0.5 ppm

ND = None detected

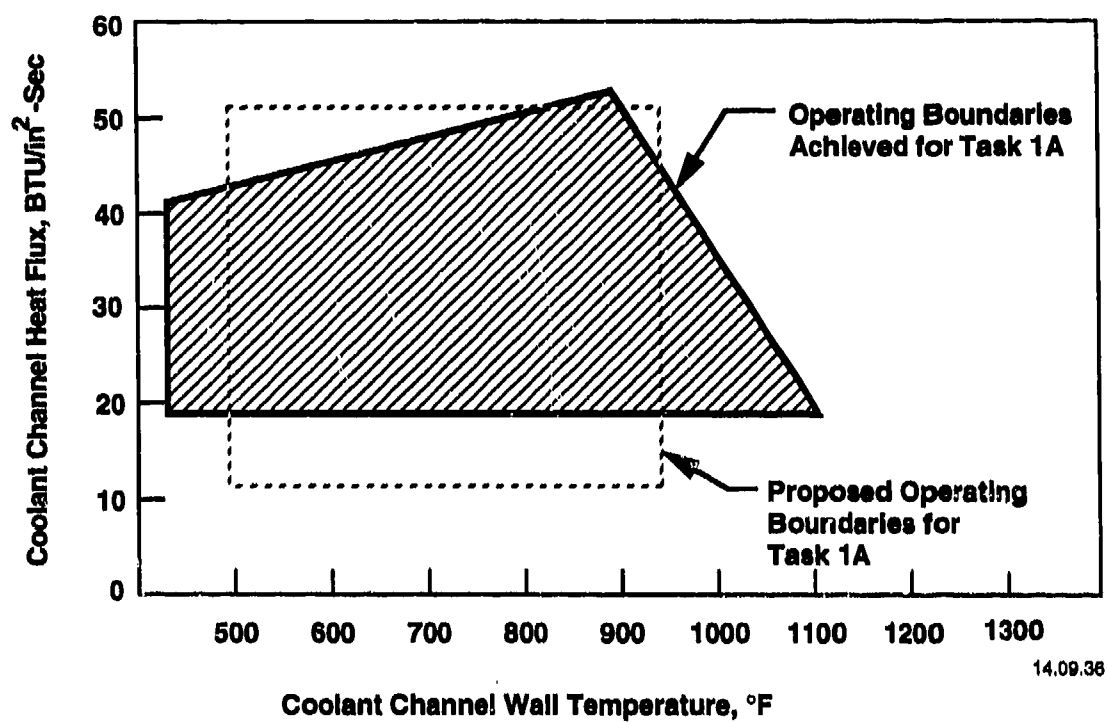


Figure 11. Actual and Proposed Operating Boundaries for Task 1A

TABLE 7

EXPANDED DATA BASE FOR COOLING CHANNEL OPERATING CONDITIONS

Test No.	Test Duration (sec)	Wall Temperature (F)	Heat Flux (BTU/in ² -sec)	Mass Flow Rate (lbs/min)	Pressure Drop Across Channel (psia)	Nu (exp) Nu (pred)	Overall Channel Performance During Test	Post Test Analysis	
								Coking	Sulfur Corrosion
M301	252	425	19.0	0.68	544	1.25	Steady ^a	None	Minor ^b
M302a	237	709	38.7	2.06	1969	0.63	Steady ^a	Minor ^b	Moderate ^c
M302b	447	671	40.0	1.97	1565	0.63	Steady ^a		
M302c	353	948	26.3	0.51	1029	1.17	Steady ^a		
M302d	194	1094	20.1	0.41	978	0.99	Steady ^a		
M303	838	429	43.5	1.76	2440	1.47	Steady ^a	None	Minor ^b
M304	1710	900	54.5	0.69	2493	0.78	Steady ^a	None	Minor ^b
M305	1329	647	28.1	1.06	2349	0.78	Steady ^a	—d	—d
M306	1567	676	31.5	0.93	2536	0.90	Steady ^a	—d	—d
M037a	1352	667	34.6	1.15	2323	0.87	Steady ^a	—d	—d
M307b	1324	638	37.5	1.23	2471	0.91	Steady ^a	—d	—d

a) No significant changes over the duration of the test.

b) Detectable by SEM and EDS.

c) Corrosion may be severe enough to eventually effect channel performance if repeatedly used under these conditions.

d) The test specimen were saved for the refurbishment study.

3.2, Dynamic Tests (cont.)

The data in Table 7 shows that the overall channel performance for all the tests was steady over the duration of the tests. This means that parameters such as heat transfer efficiency, $Nu_{(exp)}/Nu_{(pred)}$, mass flow rate, pressure drop across the channel, heat flux, average bulk methane temperature, and wall temperature all remain constant within experimental error during the run. Figures 12-17 are plots that illustrate this point for a well behaved test, i.e., Test M307b. The slight fluctuations seen in some of the plots are due to fluctuations in the methane inlet temperature brought on by the difficulty in maintaining a uniform flow of LN_2 to the Propellant Thermal Conditioning System. Thus, the fluctuations are characteristic of test apparatus limitations and do not reflect changes in the actual performance of the cooling channels. Performance profiles such as those shown in Figures 12-17 imply that no significant coking or sulfur corrosion is taking place in the cooling channels.

Tests M301 through M304 represent the extreme conditions as defined by the corners of the operating boundaries shown in Figure 11. As previously stated, the practical limitations of our test apparatus did not allow achievement of the originally proposed operating boundaries. Thus, the run times of Tests M301-M303 were relatively short in comparison to the other tests because it was difficult to maintain constant operating conditions. For example, the low mass flow rate tests were difficult to control because the methane tended to freeze in the Propellant Thermal Conditioning System, thus making long duration runs impossible.

Finally, tests M302a through M302d were all carried out with a single test specimen. This was done as an approach to avoiding, as much as possible, the methane freezing problem. In essence, we approached the low mass flow conditions of M302c and M302d in a stepwise manner starting at higher flow rates and lower wall temperatures. This technique did allow data to be collected under steady conditions for approximately 200 sec runs.

Inspection of the test specimen after testing showed that carbon deposition, (coking) was detectable only under the most severe operating conditions, i.e., $T_{wall} = 1094$ F with a low mass flow rate, and that even then the amount of carbon deposit was minor. Thus, coking should never be a significant problem for methane fuel and NASA-Z copper. On the other hand, some sulfur corrosion was detectable in all the specimen, demonstrating that even very low concentrations of sulfur compounds can have a corrosive effect. The methane used for this work had only 0.5 ppm isobutyl mercaptan which is roughly equivalent to only 0.1 ppm

Heat Transfer vs Time Test M307b

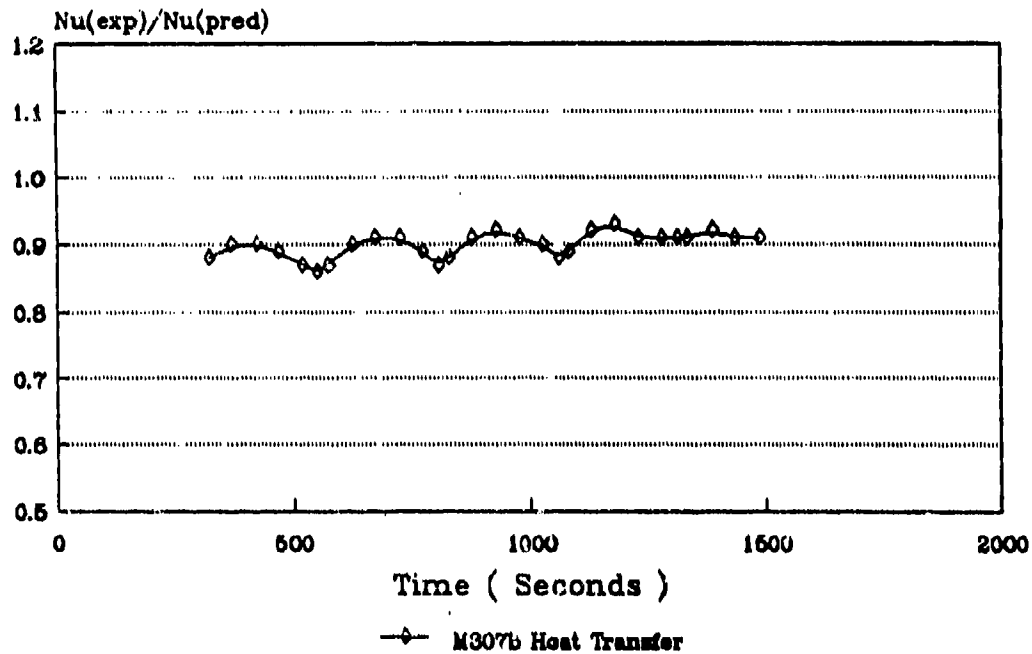


Figure 12. Heat Transfer Efficiency, $Nu(exp)/Nu(pred)$, vs Time for Test M307b
Operating Conditions: $T_{wall} = 638^{\circ}F$, Mass Flow = 1.23 lbs/min

Mass Flow vs Time Test M307b

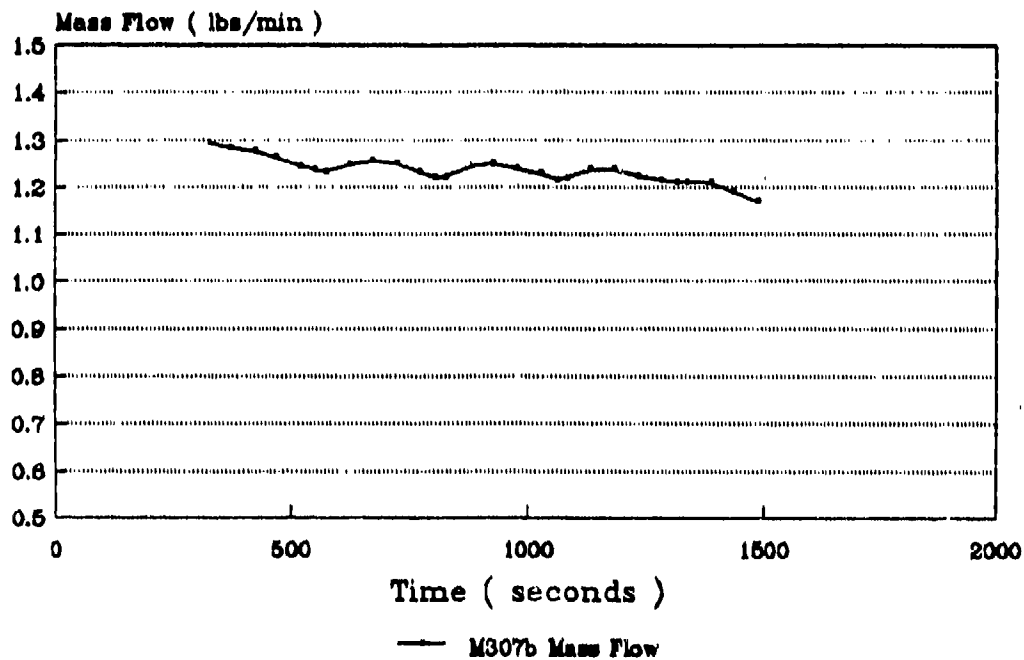


Figure 13. Mass Flow vs Time for Test M307b
Operating Conditions: $T_{\text{wall}} = 638^{\circ}\text{F}$, Mass Flow = 1.23 lbs/min

Pressure Drop vs Time Test M307b

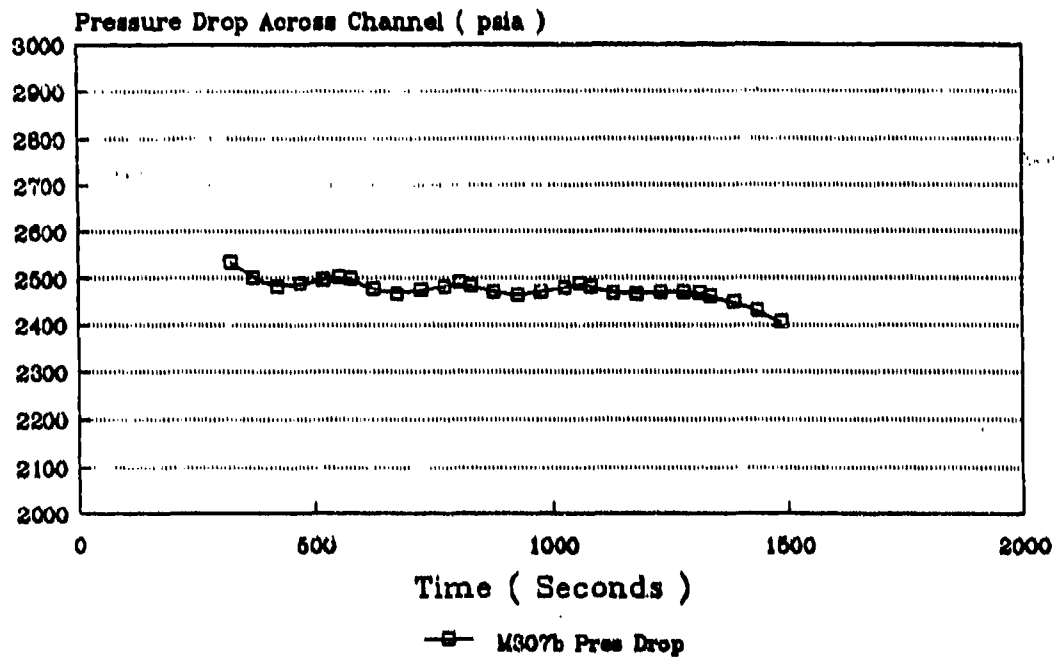


Figure 14. Pressure Drop Across the Cooling Channel vs Time for Test M307b
Operating Conditions: $T_{wall} = 638^{\circ}\text{F}$, Mass Flow = 1.23 lbs/min

Heat Flux vs Time

Test M307b

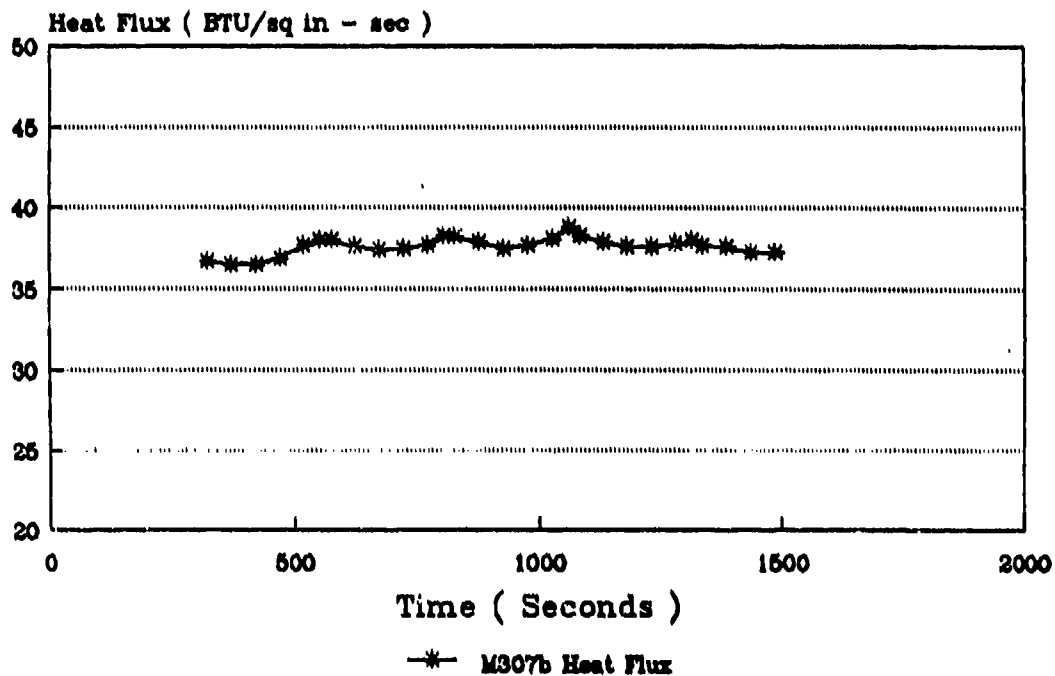


Figure 15. Heat Flux vs Time for Test M307b
Operating Conditions: $T_{wall} = 638^{\circ}\text{F}$, Mass Flow = 1.23 lbs/min

Bulk Temperature vs Time Test M307b

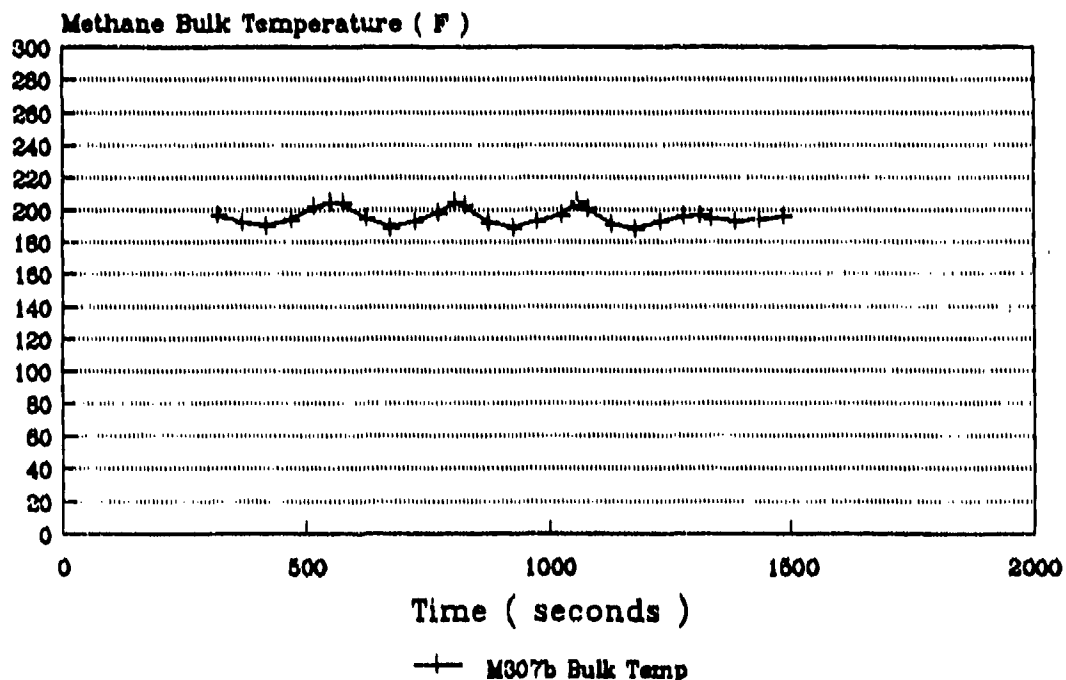


Figure 16. Methane Bulk Temperature vs Time for Test M307b
Operating Conditions: $T_{wall} = 638^{\circ}\text{F}$, Mass Flow = 1.23 lbs/min

Wall Temperature vs Time Test M307b

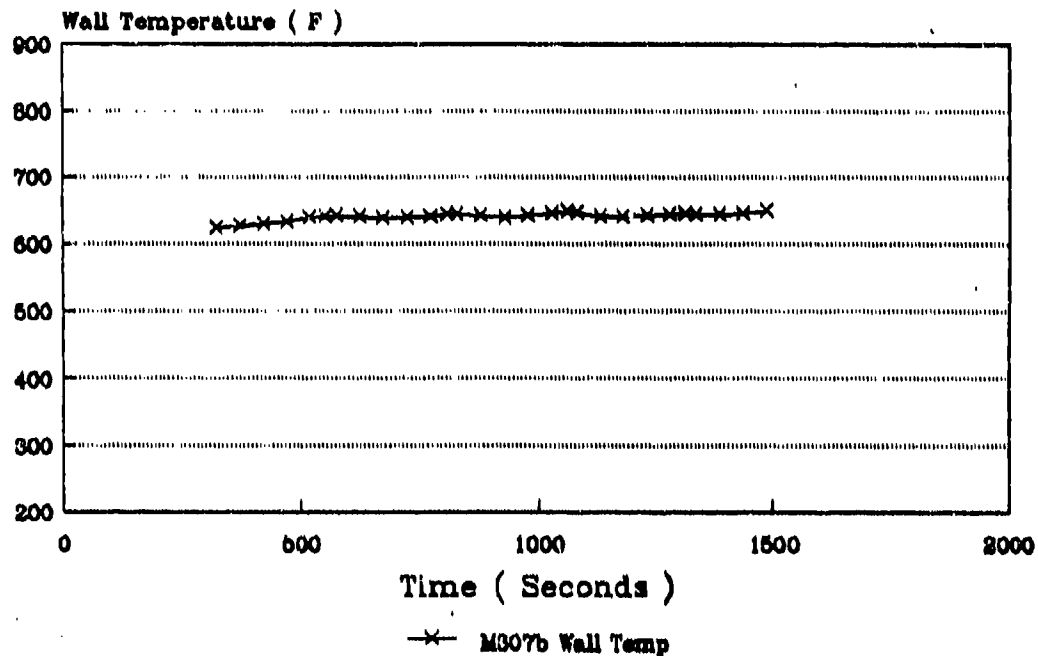


Figure 17. Cooling Channel Wall Temperature vs Time for Test M307b
Operating Conditions: $T_{\text{wall}} = 638^{\circ}\text{F}$, Mass Flow = 1.23 lbs/min

3.2, Dynamic Tests (cont.)

H₂S. Figures 18 and 19 are EDS spectra of "as received" NASA-Z copper and the cooling channel surface of the specimen used in Test M304, respectively. A comparison of the two spectra clearly shows the presence of sulfur on the surface of the M304 test specimen. All the test specimen for tests M301 through M304 had similar EDS spectra.

SEM analysis of the specimen from Tests M301 through M304 showed the presence of only minor amounts of Cu₂S corrosion products, except for the specimen used in Test M302 which had moderate amounts of Cu₂S present. It should be noted that this test specimen was actually subjected to four separate sets of test conditions, including the very harsh conditions of high wall temperatures and low mass flow rates of Tests M302c, d. These harsh conditions are undoubtedly responsible for the significantly greater amounts of Cu₂S relative to the other specimen. Figures 20-24 are SEM photomicrographs of the cooling channels surfaces that clearly shows the presence of the sulfur corrosion. A close comparison of the SEM photomicrographs for all four specimen clearly indicates that the severity of the sulfur corrosion process increases with increasing wall temperature and decreasing mass flow rate. This is exactly what should be expected on the basis of sound chemical principles.

Subsequent to development of a successful refurbishment technique which is discussed in detail later, the test specimen from Tests M301 and M302 were treated with the sodium cyanide (NaCN) refurbishment solution in order to remove the Cu₂S deposits and expose the underlying copper surface for re-examination by SEM and EDS. Figure 25 shows SEM photomicrographs of the cooling channel of M301 test specimen after refurbishment to remove the Cu₂S. Some shallow craters and surface particles are present. It should also be noted that the machine marks are still visible. EDS analysis, Figures 26 and 27, show that the sulfur is gone and that the surface particles are enriched in zirconium and silver, i.e., the alloying elements present in NASA-Z. These results confirm that the minor sulfur corrosion shown in Figure 21 has little effect on the channel surface. On the other hand, removal of the Cu₂S from the M302 test specimen left a surface covered with erratic "black spots." The black spots show up as "light spots" under SEM examination (see Figure 28). These black spots are probably the minor amounts of carbon deposits noted when the test specimen was originally analyzed. In addition, Figure 28 shows a "mud cracking" surface feature which indicates preferential grain boundary attack occurred during sulfur corrosion. These results also confirm that the harsh conditions used in Test M302 do, in fact, lead to more severe corrosion relative to Test M301. Thus, the conclusions drawn from the SEM examinations both prior to and after refurbishment are consistent.

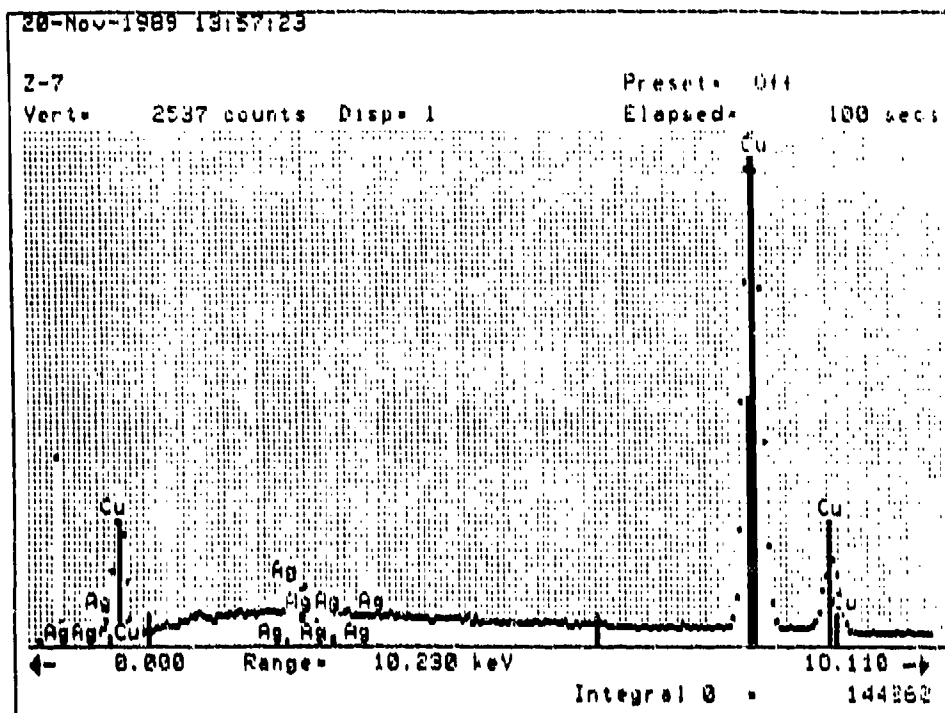


Figure 18. EDS Spectrum of as Received NASA-Z Copper

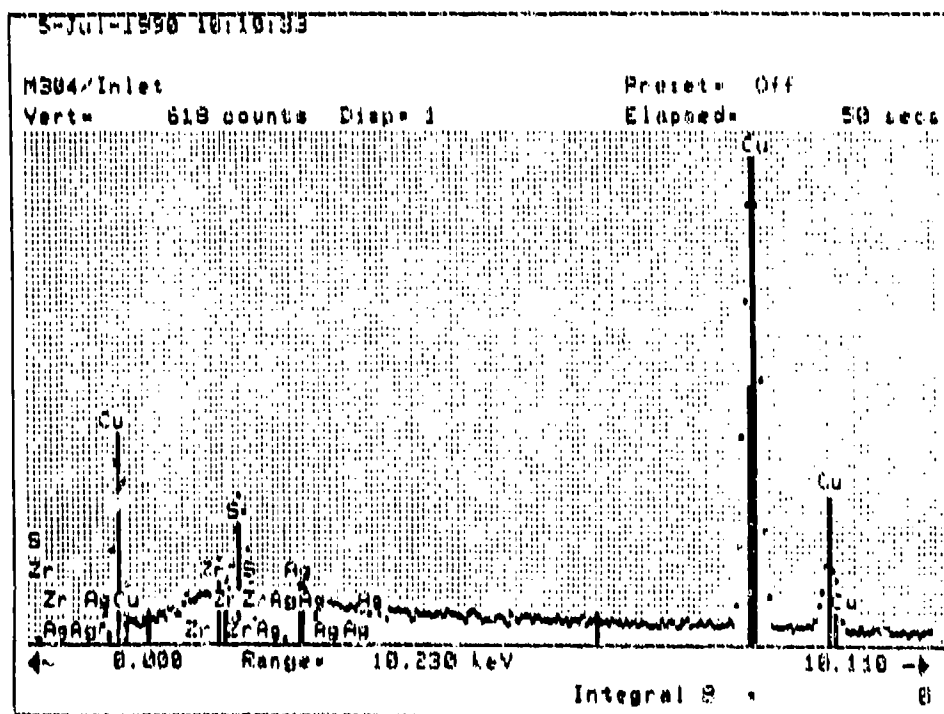


Figure 19. EDS Spectrum of Cooling Channel Surface for Test Specimens Used in Test M304. Note the Presence of Sulfur Which is Absent From the Spectra of as Received NASA-Z Copper

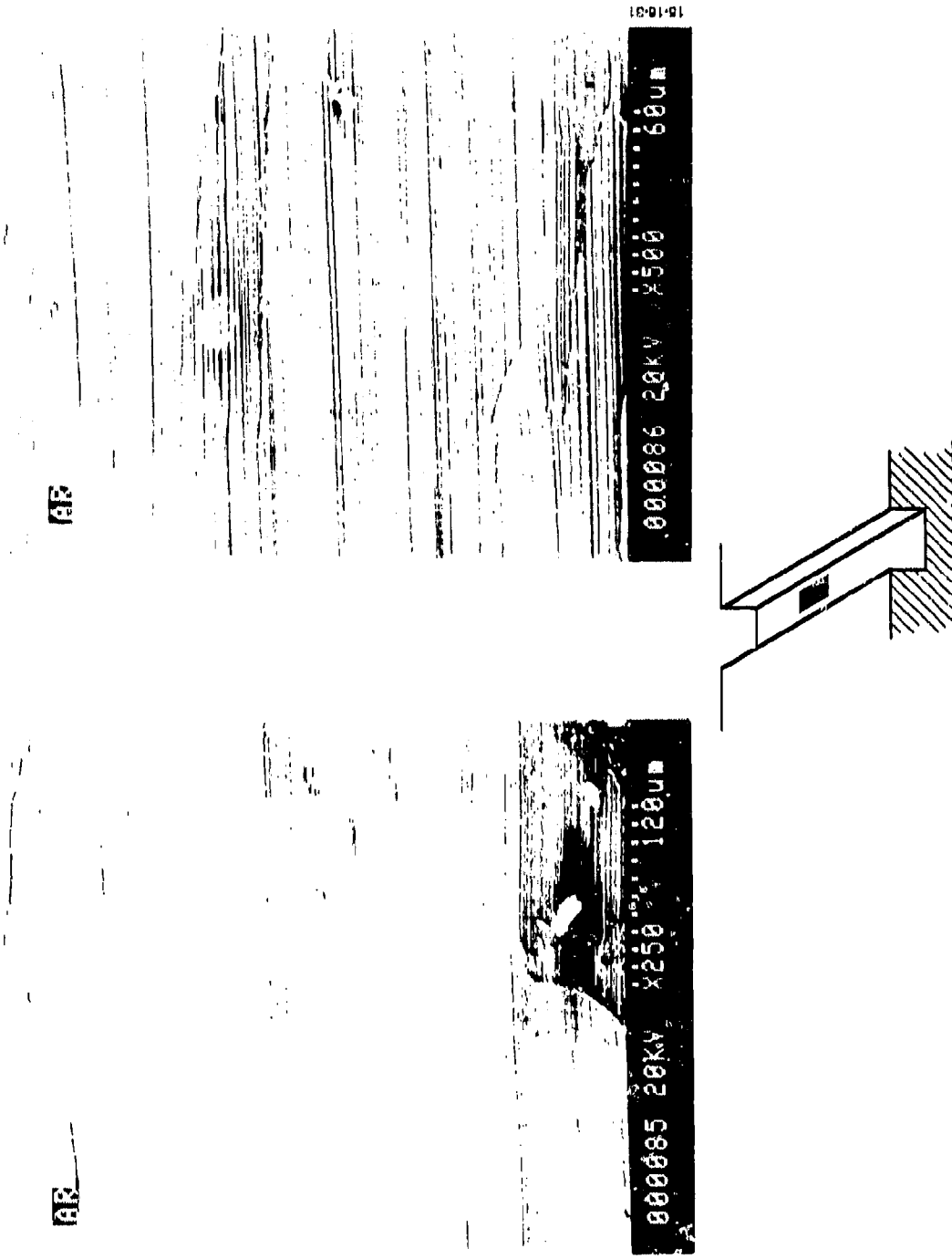


Figure 20. As Received Cooling Channel of NASA-Z Copper Alloy Test Specimen.
Machine Marks Are the Only Distinctive Features

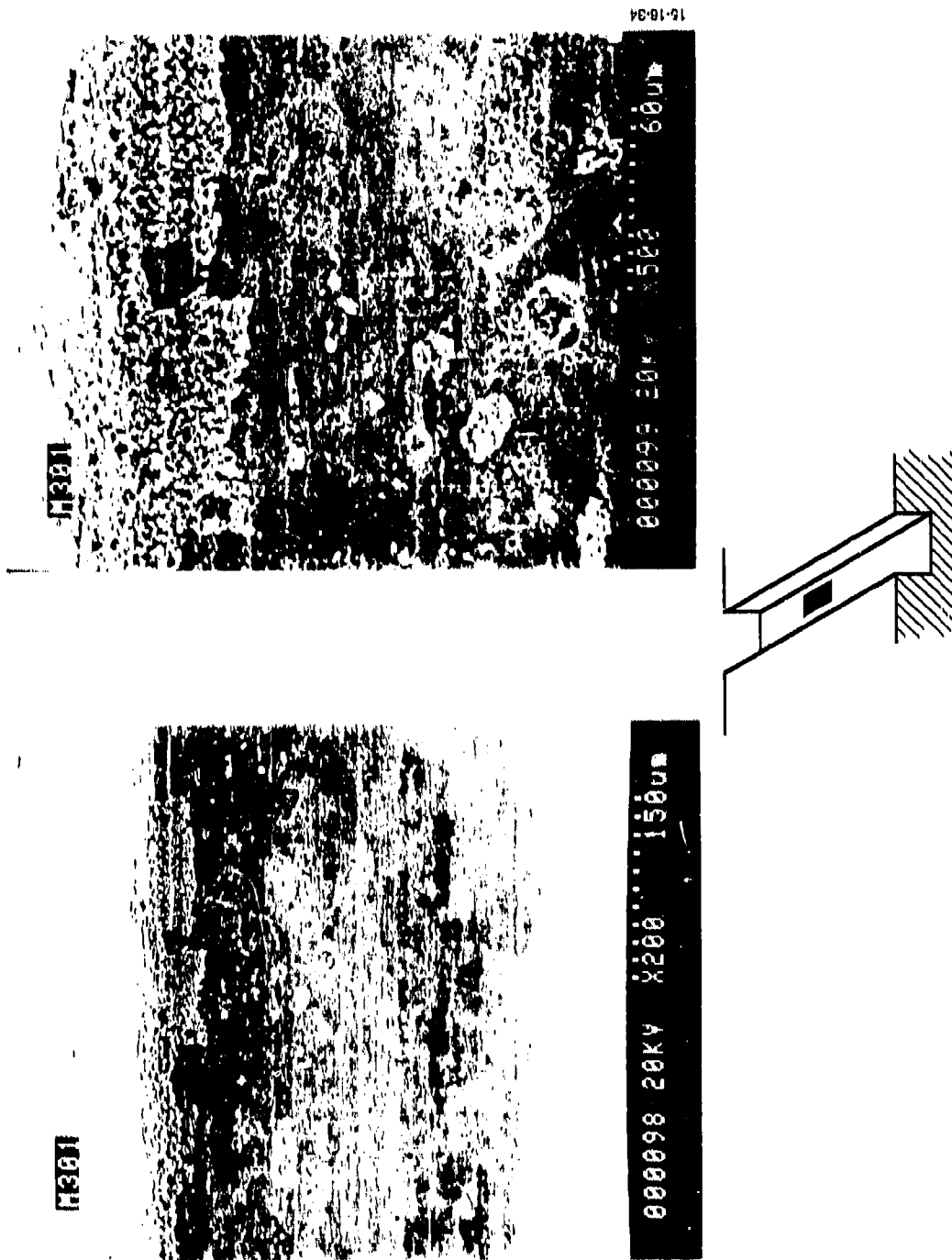


Figure 21. Cooling Channel of Test Specimen After Test M301. Note That Only Small Amounts of Cu_2S Desposits Are Present as Scattered Patches. Machine Markings Are Subdued, But Still Visible. M301 Test Conditions: $T_{\text{Wall}} = 425^\circ\text{F}$, Mass Flow = 0.68 lbs/min

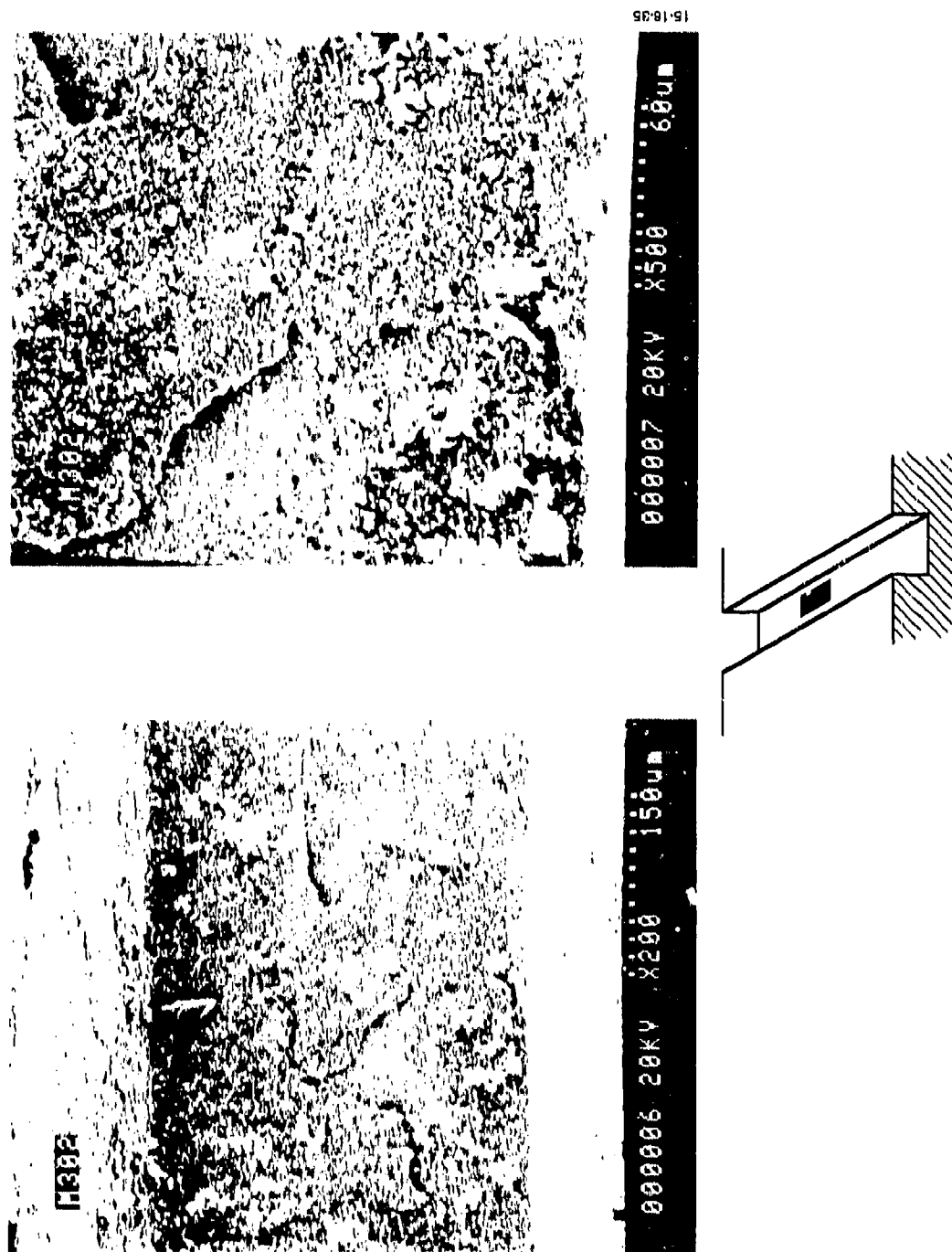


Figure 22. Cooling Channel of Test Specimen After Test M302. Note That Channel Surface Is Almost Completely Covered With a Loosely Bound "Scale" of Cu_2S .
M302d Test Conditions: $T_{\text{Wall}} = 1094^\circ\text{F}$, Mass Flow = 0.41 lbs/min

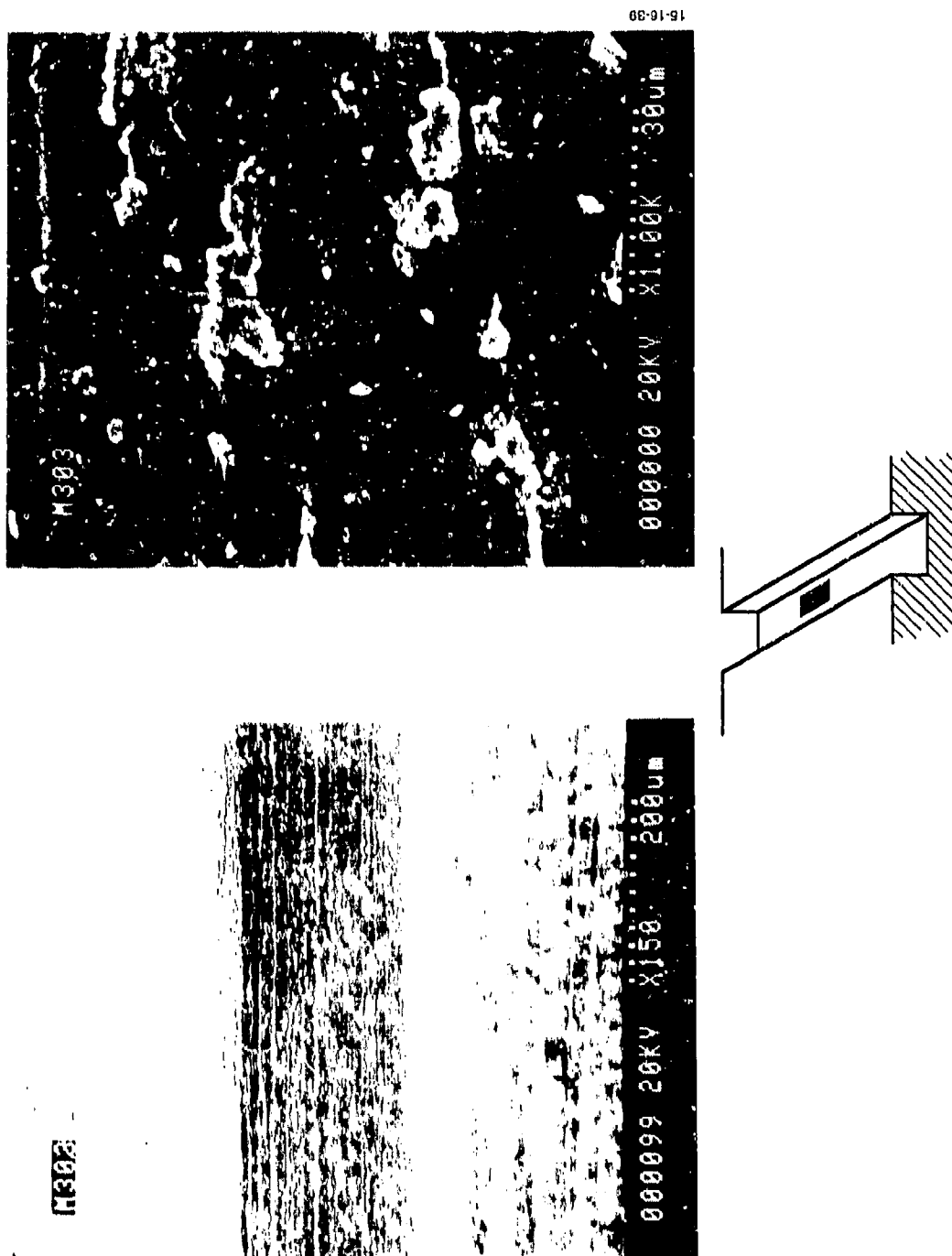


Figure 23. Cooling Channel of Test Specimen After Test M303. Note Very Light Deposits of Cu_2S and That Machine Marks Are Visible. M303 Test Conditions: $T_{\text{Wall}} = 429^\circ\text{F}$, Mass Flow = 1.76 lbs/min

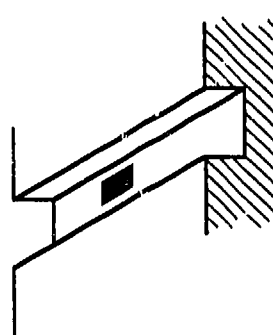
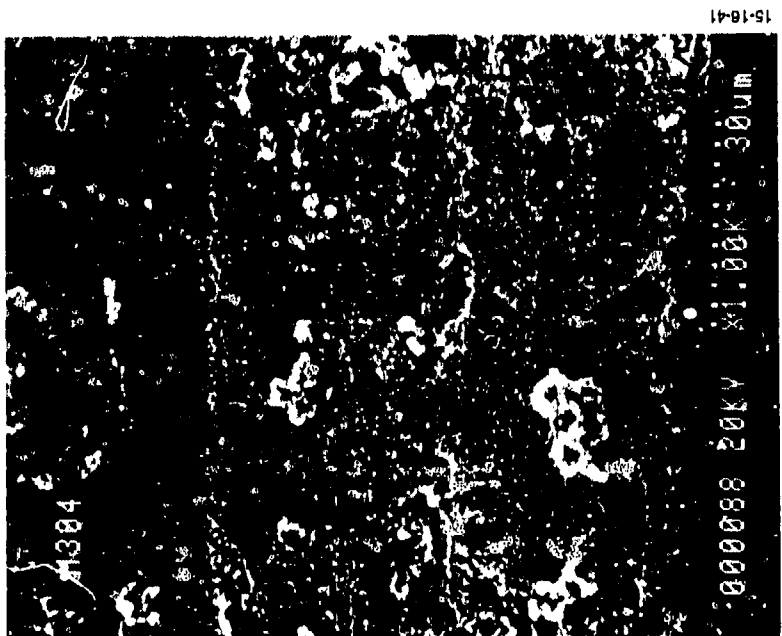
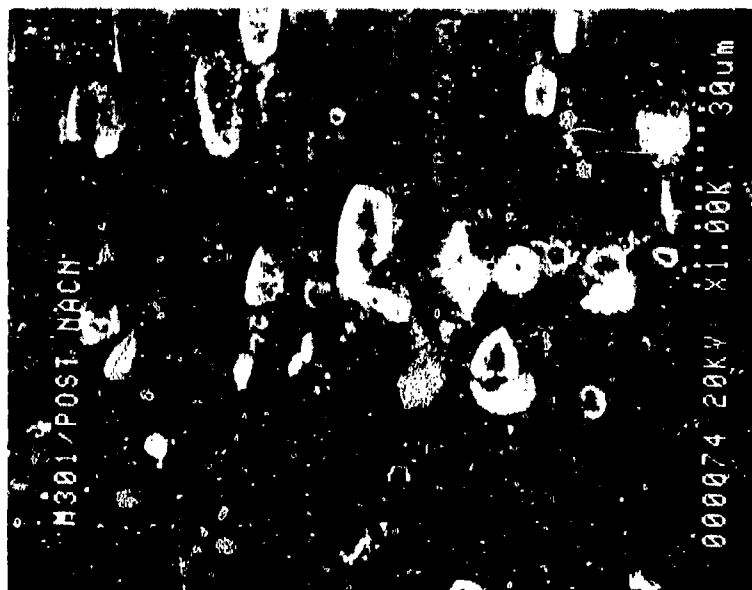


Figure 24. Cooling Channel of Test Specimen After Test M304. Note Scattered Deposits of Cu_2S and That Machine Marks Are Subdued But Still Visible. M304 Test Conditions: $T_{\text{wall}} = 900^\circ\text{F}$, Mass Flow = 0.69 lbs/min

M301/POST NaCN



000073 20KV X150 200um



15-18-40

000074 20KV X100K 30um

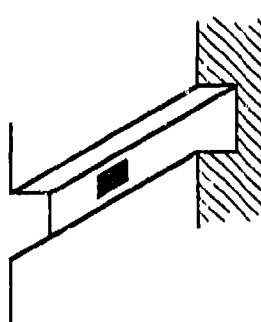


Figure 25. Cooling Channel of M301 Test Specimen After Removal of the Cu_2S Deposits With Aqueous NaCN. Note That Machine Marks Are Clearly Visible Along With Some Shallow Craters and Surface Particles

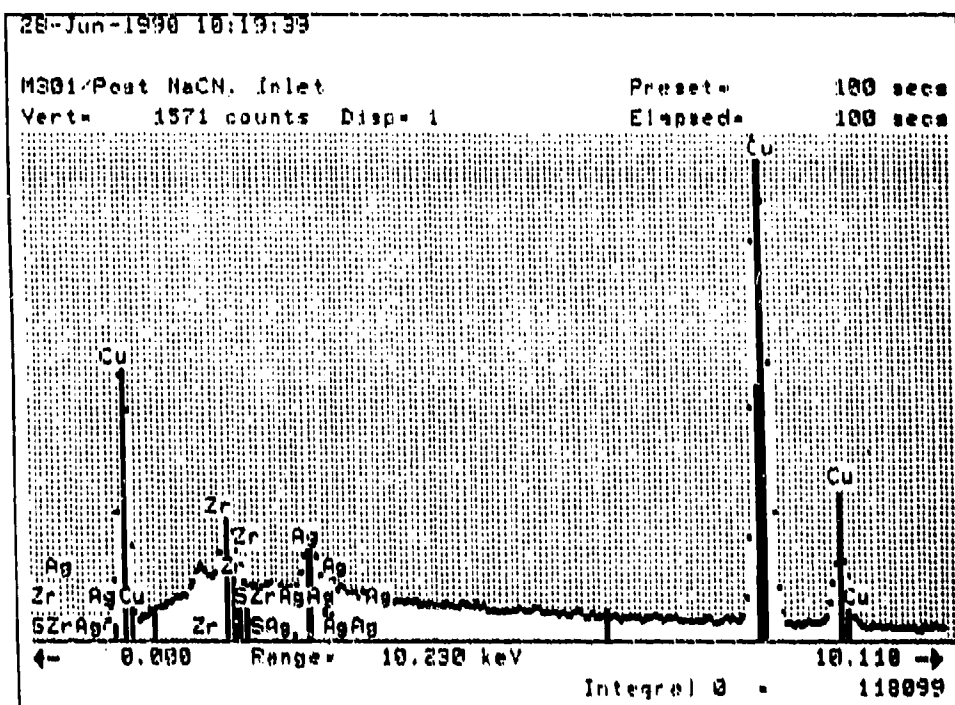


Figure 26. EDS Spectrum of Cooling Channel Surface of M301 Test Specimen After Removal of Sulfur With Aqueous NaCN. Note, No Sulfur is Detectable and Both Zirconium and Silver Show Measurable Responses

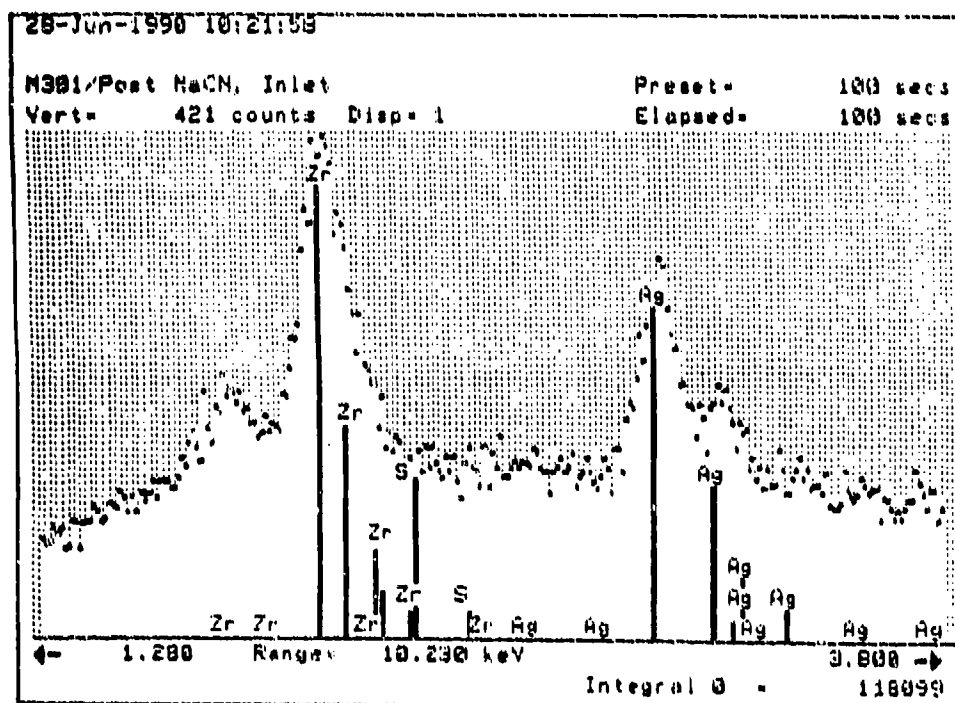


Figure 27. Expanded View of EDS Spectrum Showing Surface Particles are Grains Enriched in Zirconium and Silver and That Sulfur is completely Absent

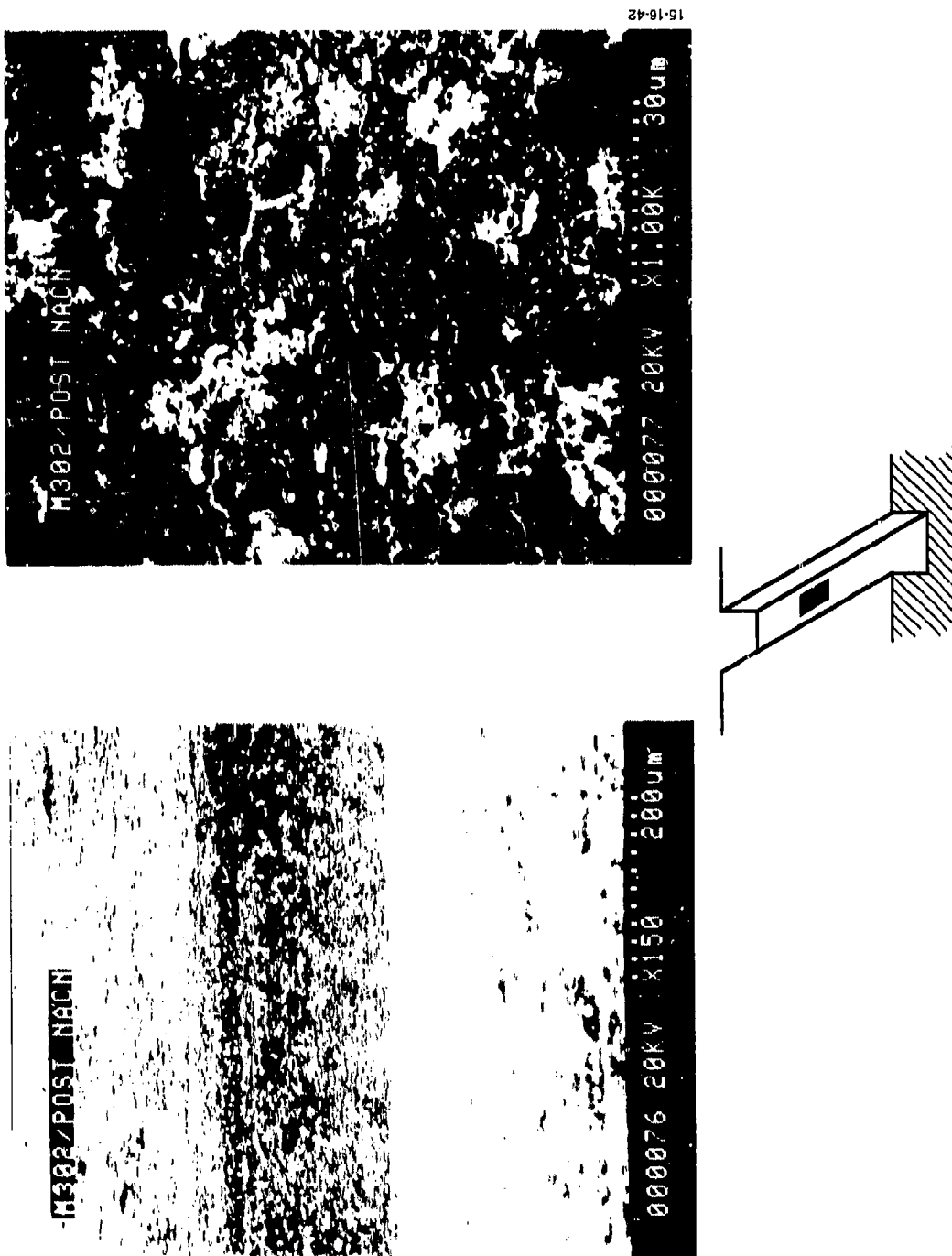


Figure 28. Cooling Channel of M302 Test Specimen After Removal of the Cu_2S Deposits With Aqueous NaCN. Small Patches of Carbon Deposits, Light Spots, and Preferential Grain Boundary Attack is Evident

3.2, Dynamic Tests (cont.)

Finally, it should also be remembered that even though sulfur corrosion was present in the cooling channels, it was never significant enough to show measurable changes in cooling channel performance.

3.2.2 Determination of Acceptable Sulfur Levels

The results discussed in the previous Section, 3.2.1, Expanded Operating Conditions, showed that methane fuel containing 0.5 ppm isobutyl mercaptan does lead to noticeable sulfur corrosion of the cooling channels under a variety of operating conditions. However, in no case was the corrosion severe enough to result in measurable changes in cooling channel performance over the course of the test runs. Thus, this level of sulfur contamination can be tolerated, although no corrosion would be preferable. This section deals with the dynamic test results obtained using methane fuel deliberately contaminated with either H_2S or CH_3SH .

Table 8 summarizes the test results for five experiments with sulfur contaminated methane and one experiment with uncontaminated methane for the sake of comparison. All six experiments were carried out under conditions intended to simulate moderate wall temperatures, i.e., 600-700°F, and moderate to high mass flow rates, i.e., 1.0-2.0 lbs/min. Such operating conditions should be reasonably representative of a real system. In addition, the test specimen from Test M312a (6 ppm CH_3SH) was inspected by optical microscopy, SEM, and EDS. The other test specimen were saved for dynamic test verification of the refurbishment technique.

First of all, the results in Table 8 show that all the tests with added sulfur show an overall degradation in cooling channel performance over the duration of the test. Figures 29-34 are plots of some of the monitored parameters versus time for Test M308 (1 ppm H_2S) that graphically shows performance degradation. A comparison of these plots with the corresponding plots for as received methane, Figures 12-17, clearly emphasize the differences in channel performance brought on by fairly small amounts of added sulfur. For example, a comparison of Figures 12 and 29 shows that the heat transfer efficiency, as measured by the ratio of experimental to predicted Nusselt numbers ($Nu_{(exp)}/Nu_{(pred)}$), is degraded dramatically by the added H_2S and essentially unaffected by as received methane. Similar results are observed for mass flow, methane bulk temperatures, and heat flux. These observations are all consistent with the buildup of a layer of Cu_2S corrosion product on the channel walls that both impedes mass flow through the channel and acts as a thermal insulator. Pressure drop across the channel and channel wall temperature are less sensitive to the Cu_2S buildup than the above parameters.

TABLE 8

DYNAMIC TEST RESULTS WITH METHANE DELIBERATELY CONTAMINATED WITH H₂S or CH₃SH

Test No.	Test Duration (sec)	Sulfur Contamination	Average Wall Temperature (F)	Heat Flux (BTU/in. ² -sec)	Mass Flow Rate (lbs/min)	Pressure Drop Across Channel (psia)	$\frac{Nu_{(exp)}}{Nu_{(pred)}}$	Overall Channel Performance During Test
M308	1407	1 ppm H ₂ S	631	37.8 - 23.0	1.20 - 0.86	2450 - 2550	1.04 - 0.69	Degraded
M309	1452	3 ppm H ₂ S	703	41.0 - 27.3	1.35 - 0.74	2600 - 2740	0.98 - 0.78	Degraded
M310	1250	3 ppm CH ₃ SH	645	38.5 - 31.8	1.40 - 1.18	2430 - 2480	0.90 - 0.75	Degraded
M311	1400	10 ppm CH ₃ SH	769	39.0 - 24.6	0.98 - 0.50	2400 - 2680	1.06 - 0.82	Degraded
M312a	1004	6 ppm CH ₃ SH	631	46.2 - 39.4	1.70 - 1.40	2400 - 2500	0.96 - 0.89	Degraded
M312b	778	None	641	42.5	1.80	2520	0.81	Steady

Heat Transfer vs Time

Test M308

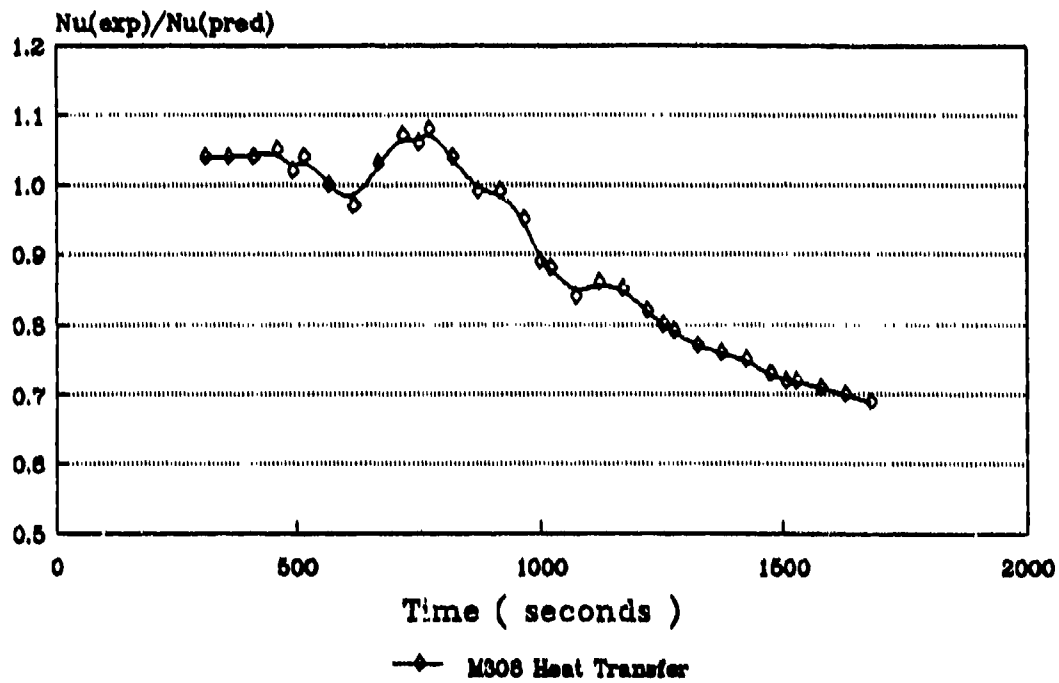


**Figure 29. Heat Transfer Efficiency, $Nu (exp)/Nu (pred)$, vs Time for Test M308
(1 ppm H_2S)
Operating Conditions: $T_{wall} = 631^\circ F$, Mass Flow = 1.20 lbs/min**

Mass Flow vs Time Test M308

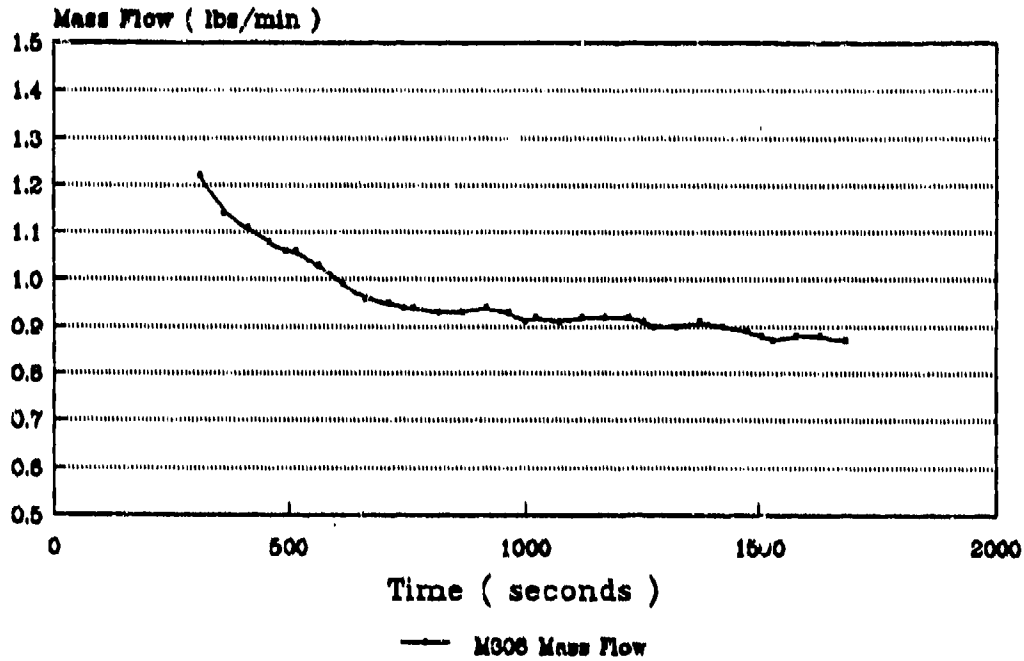
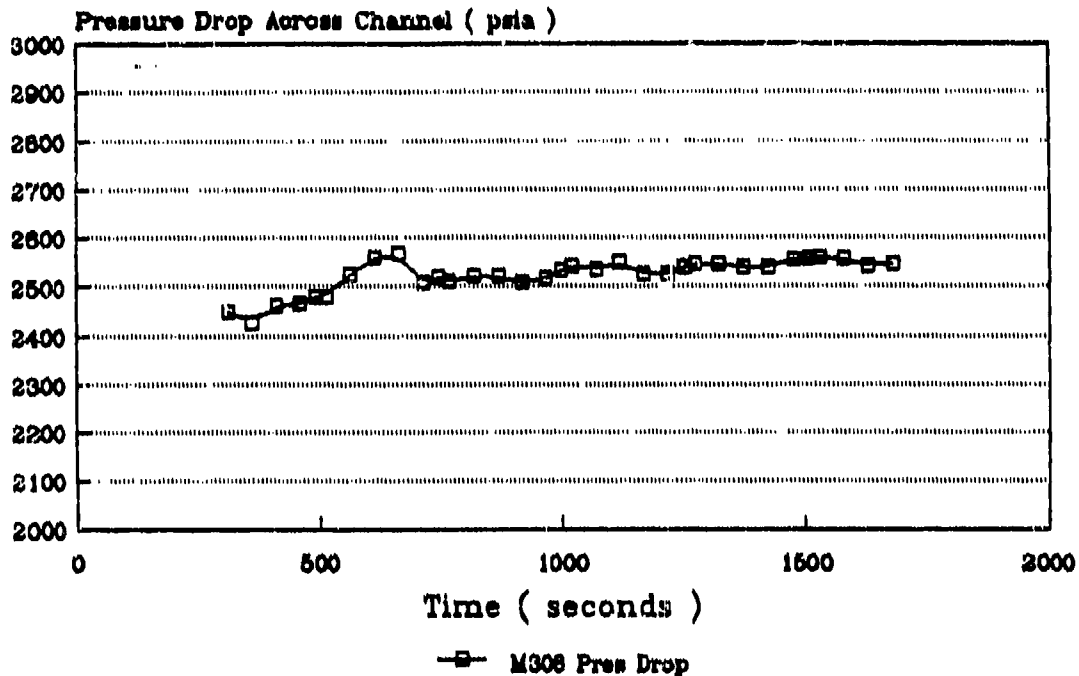


Figure 30. Mass Flow vs Time for Test M308 (1 ppm H₂S)
Operating Conditions: $T_{\text{wall}} = 631^{\circ}\text{F}$, Mass Flow = 1.20 lbs/min

Pressure Drop vs Time Test M308



**Figure 31. Pressure Drop Across the Cooling Channel vs Time for Test M308
(1 ppm H₂S)
Operating Conditions: T_{wall} = 631°F, Mass Flow = 1.20 lbs/rnin**

Heat Flux vs Time Test M308

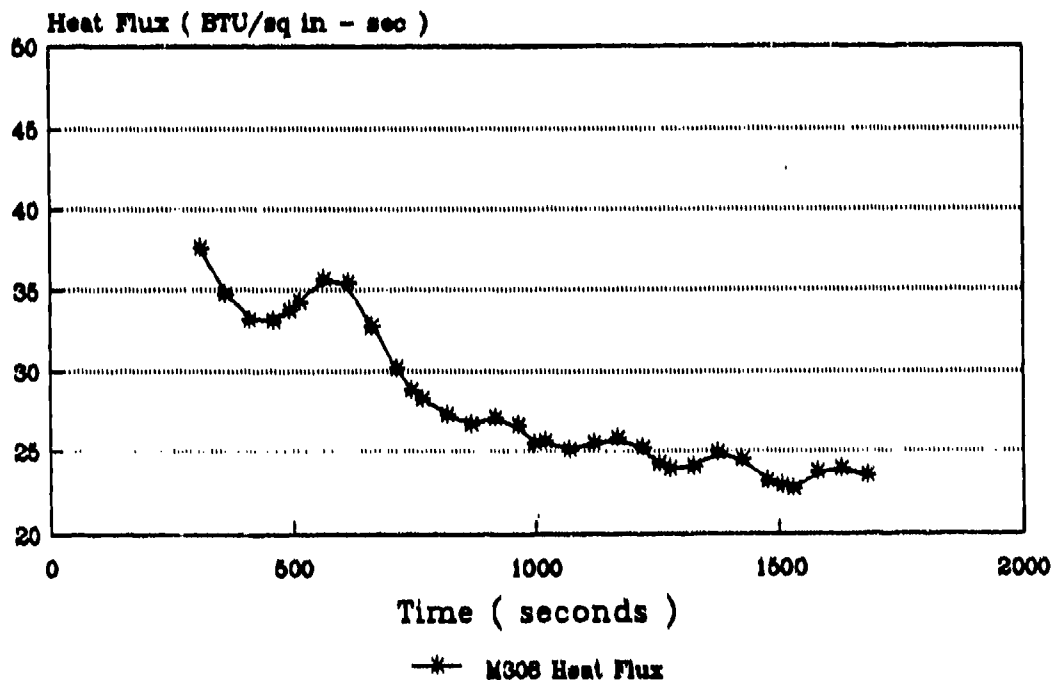


Figure 32. Heat Flux vs Time for Test M308 (1 ppm H₂S)
Operating Conditions: T_{wall} = 631°F, Mass Flow = 1.20 lbs/min

Bulk Temperature vs Time Test M308

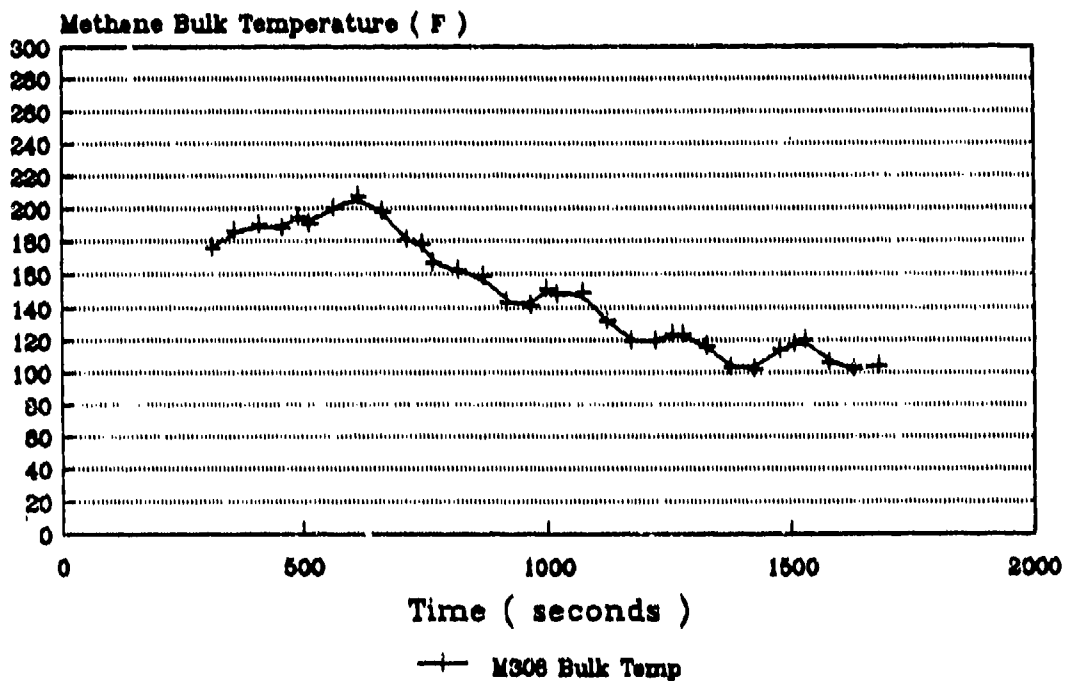


Figure 33. Methane Bulk Temperature vs Time for Test M308 (1 ppm H₂S)
Operating Conditions: T_{wall} = 631°F, Mass Flow = 1.20 lbs/min

Wall Temperature vs Time Test M308

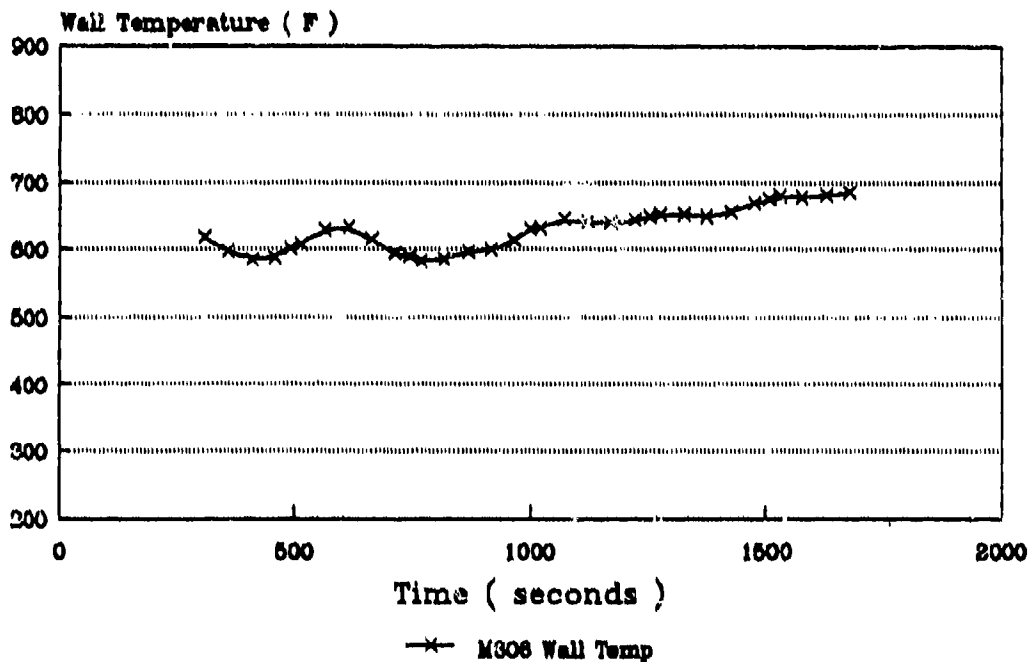


Figure 34. Cooling Channel Wall Temperature vs Time for Test M308 (1ppm H₂S)
Operating Conditions: $T_{wall} = 631^{\circ}\text{F}$, Mass Flow = 1.20 lbs/min

3.2, Dynamic Tests (cont.)

Nevertheless, both of these parameters show a clear upward trend with time for methane containing 1 ppm H_2S , while as received methane shows little or no change. An upward trend in pressure drop and wall temperature is the expected response if the channel walls are building up an insulating layer of Cu_2S . Thus, all the monitored parameters are consistent with the formation of a Cu_2S corrosion product layer on the cooling channel walls.

The test specimen from Test M312a (6 ppm CH_3SH) showed the channel walls to be completely covered with a fibrous or "wool-like" gray-black deposit when viewed under a binocular microscope. SEM photomicrographs shown in Figure 35 illustrate the appearance of these deposits and Figure 36 is a close-up view and its corresponding EDS spectrum that confirms the presence of sulfur. These photographs clearly show that the channel is still largely open, but the walls have been severely roughened by the formation of the Cu_2S deposits. This appearance is completely consistent with the monitored test parameters shown in Figures 29-34.

The results to this point show that very low levels of sulfur contamination, i.e., 0.5 ppm isobutyl mercaptan which is roughly equivalent to 0.1 ppm H_2S , do corrode copper cooling channels under a variety of operating conditions, but the resulting corrosion is not severe enough to cause a measurable effect on cooling channel performance. However, when the as received methane is deliberately contaminated with either H_2S or CH_3SH to levels ranging from 1 ppm to 10 ppm, the resulting increase in corrosion is now severe enough to degrade cooling channel performance. Furthermore, a close examination of the performance parameters for the tests with added H_2S and CH_3SH suggests that H_2S is more aggressive than CH_3SH . This observation is in agreement with the expected order of reactivity shown previously in equation (1). Figure 37 is a plot comparing the decrease in mass flowrate with time for tests M308 (1 ppm H_2S), M309 (3 ppm H_2S), M310 (3 ppm CH_3SH), and M311 (10 ppm CH_3SH) as best fit straight lines. The slope of these lines is a reasonable measure of the average rate of decrease in mass flow rate. Table 9 shows these values along with normalized relative rates. A comparison of the relative rates in Table 9 shows that 1 ppm H_2S is essentially equivalent to 3 ppm CH_3SH and that 3 ppm H_2S is essentially equivalent to 10 ppm CH_3SH . Both of these comparisons suggest that H_2S is roughly three times more aggressive than CH_3SH under our test conditions.

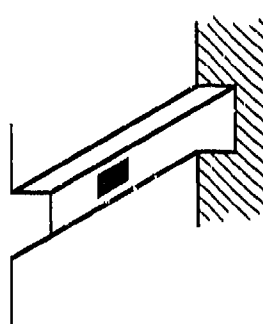
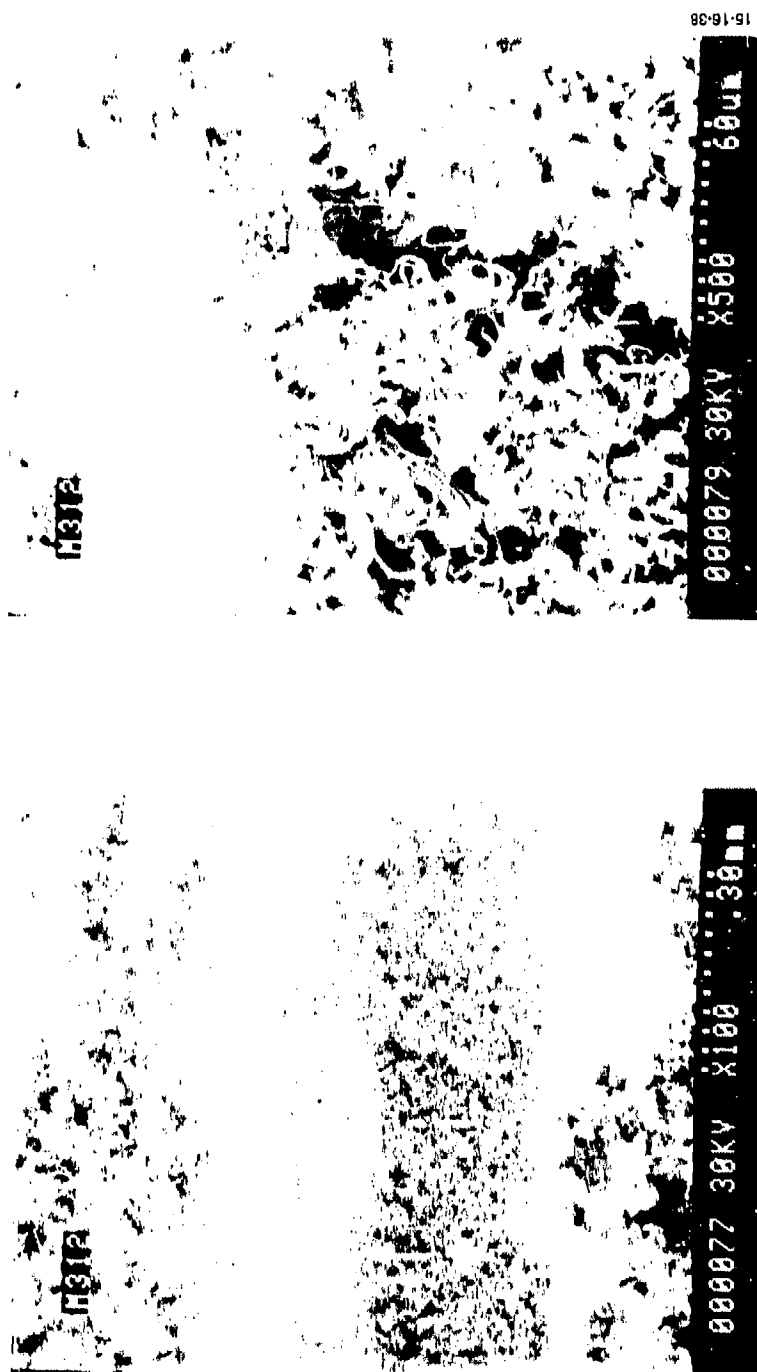


Figure 35. Cooling Channel of Test M312a Test Specimen After Exposure to 6 ppm CH_3SH at $T_{\text{Wall}} = 631^\circ\text{F}$ and Mass Flow ≈ 1.70 lbs/min. Note, A Fibrous Form of Cu_2S Covers All the Channel Walls

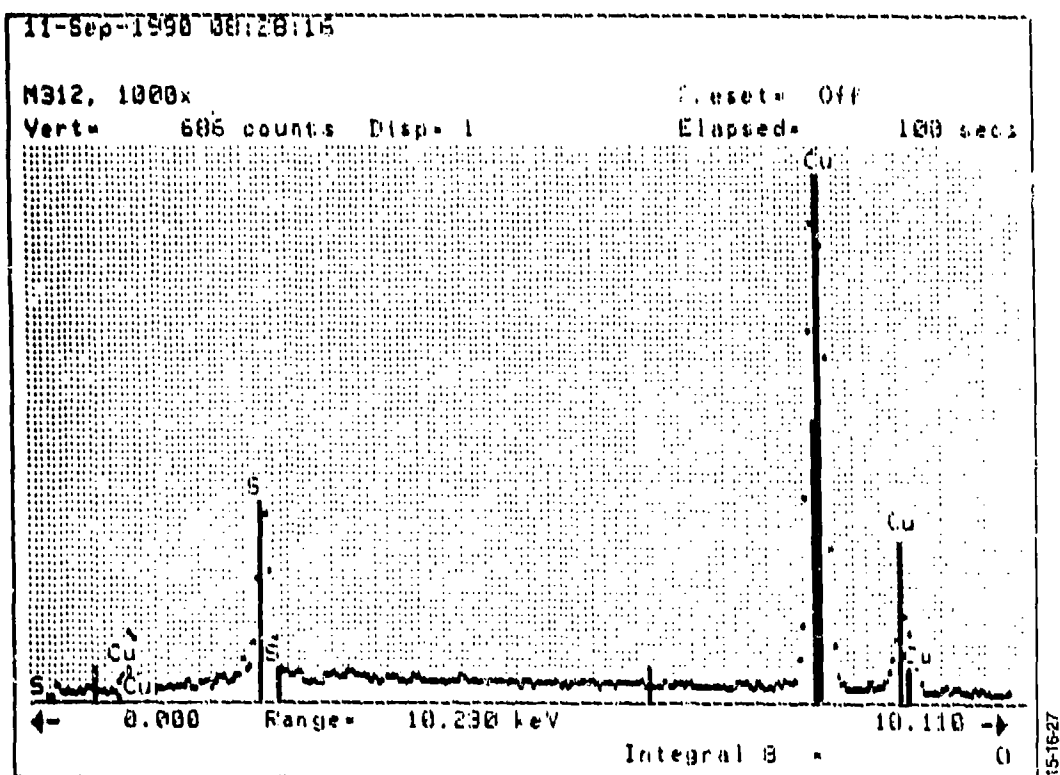


Figure 36. Close-up of the Fibrous Form of Cu_2S on the Test M312a Test Specimen Walls and an EDS Spectrum Showing the Presence of Sulfur

Mass Flow vs Time

Sulfur Contaminated Methane

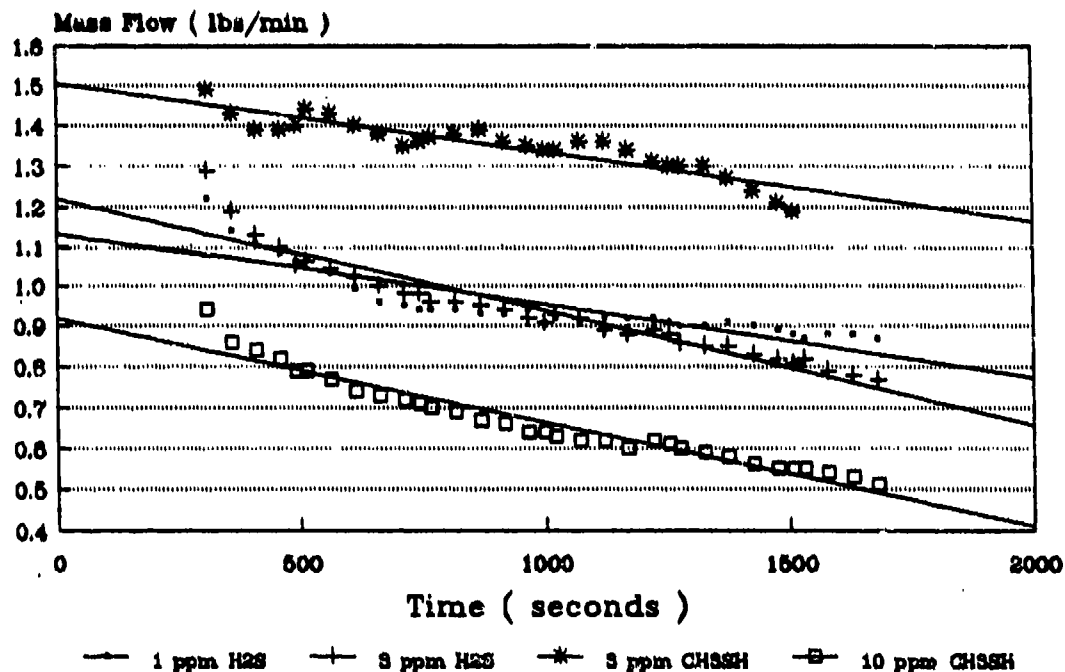


Figure 37. Comparison of the Average Rate of Decrease in Mass Flow Rate for the Tests With Sulfur Contaminated Methane

3.2, Dynamic Tests (cont.)

TABLE 9

**RELATIVE REACTIVITY OF H₂S AND CH₃SH
TOWARD COPPER COOLING CHANNELS**

Test	Average Rate of Decrease in Mass Flow Rate [(lbs/min)/sec]	Relative Rates
M308 (1 ppm H ₂ S)	1.7 x 10 ⁻⁴	1.0
M309 (3 ppm H ₂ S)	3.1 x 10 ⁻⁴	1.8
M310 (3 ppm CH ₃ SH)	1.6 x 10 ⁻⁴	0.9
M311 (10 ppm CH ₃ SH)	2.8 x 10 ⁻⁴	1.7

The real value of this data is to emphasize that any specification for sulfur content in methane that is capable of protecting a reusable copper alloy booster from excessive sulfur corrosion must differentiate between the potential sulfur contaminants as well as set limits for total sulfur. It should also be noted that it makes no sense to set specifications that are beyond the capability of available analytical techniques. With both of these points in mind and in consideration of all the dynamic test results to date, the following table (Table 10) is a proposed sulfur specification for propellant grade methane that should protect reusable copper alloy boosters from excessive sulfur corrosion. This specification sets tight controls on H₂S and mercaptans, the two most aggressive sulfur contaminants, and does not allow the total sulfur content to exceed 0.5 ppm, a level that we know can be tolerated if it's completely a mercaptan, i.e., isobutyl mercaptan. So the recommended spec has a built in margin of safety. Finally, FPD capillary gas chromatographic analysis for sulfur is capable of meeting these low detection requirements if pushed. For example, Core Laboratory routinely measures H₂S, CH₃SH, and all low MW mercaptans, sulfides, and disulfides with a detection limit of 0.1 ppm.

TABLE 10

**PROPOSED SULFUR SPECIFICATION FOR
PROPELLANT GRADE METHANE**

<u>Sulfur Contaminant</u>	<u>Proposed Specification</u>
H ₂ S	0.1 ppm (max)
Mercaptans	0.2 ppm (max)
Total Sulfur	0.5 ppm (max)

3.2, Dynamic Tests (cont.)

It is important to note that the current requirements for bulk liquid methane (LCH₄) propellant imposed by the Department of Defense (PDSFTT-2) does not guarantee that a reusable copper alloy booster will be protected from excessive corrosion (see Table 11). In fact, PDSFTT-2 allows total sulfur to be as high as 1 ppm. If the sulfur were all in the form of H₂S, corrosion would be severe and cooling channel performance would be seriously degraded. Thus, PDSFTT-2 cannot be used to control LCH₄ quality for this end-use.

TABLE 11

**DEPARTMENT OF DEFENSE REQUIREMENTS (PDSFTT-2)
FOR LIQUID METHANE**

CH ₄	=	99.93% (by volume)
Ethane	=	500 ppm (max)
Propane and Higher Hydrocarbons	=	30 ppm (max)
O ₂	=	1 ppm (max)
CO ₂	=	50 ppm (max)
H ₂ O	=	1 ppm (max)
N ₂	=	20 ppm (max)
Total Sulfur	=	1 ppm (max)

3.2.3 High Purity Bulk Liquid Methane Survey

Gaseous methane in standard pressure cylinders was used for the Task 1A experimental work. However, methane in this form would not be used in fully operational launch vehicles. Such a launch vehicle would require LCH₄ in bulk form. Thus, a survey was carried out to obtain important information regarding availability, price sensitivity, and analytical and quality assurance methods for bulk LCH₄.

The survey was conducted by telephone interview of petroleum product suppliers, e.g., Phillips 66, Shell, Chevron, etc., gas suppliers, e.g., Air Products, Liquid Carbonics, and Matheson, etc., and professional institutes and associations in the petroleum and natural gas industries. In addition, independent analytical laboratories were contacted regarding

3.2, Dynamic Tests (cont.)

their capability to assay liquid or gaseous methane. A list of all the organizations solicited for information is given below. In most cases, more than one individual and/or location was interviewed for each organization.

Petroleum Product Suppliers

Phillips 66	Standard Oil
Union Oil of California	Exxon
Chevron USA	Shell Oil
Ashland Oil	

Gas Suppliers

Air Products	Airco Specialty Gases
Liquid Carbonics	Scott Specialty Gases
Matheson Gas Products	Quadren Cryogenic Processing
Union Carbide Corp., Linde Division	

Professional Institutes and Associations

National Institute for Petroleum and Energy Research
American Petroleum Institute
Natural Gas Supply Association
Institute of Gas Technology

Independent Analytical Laboratories

Galbraith Laboratory	Southern Petroleum Laboratory
Huffman Laboratories	Anatec Laboratories
Core Laboratories	American Council of Independent Laboratories

This survey assumes, for the moment, that bulk high purity LCH₄ is material that conforms to the specifications imposed by the Department of Defense PDSFTT-2 which is shown in Table 11. This is necessary since PDSFTT-2 is the current industry recognized standard for bulk high purity LCH₄ and all comments obtained from the above sources were directed

3.2, Dynamic Tests (cont.)

at the PDSFTT-2 requirements. It is recognized that the 1 ppm total sulfur allowable in PDSFTT-2 is too high and that the specification requires further tightening.

Before discussing the results of the survey in detail, it is important to differentiate clearly between Liquid Natural Gas, LNG, and high purity LCH₄. Both fuels are primarily methane. LNG is a world wide item of commerce commonly used for heating. A typical specification for LNG is shown below in Table 12. A comparison of Table 11 with Table 12 clearly shows that commercially available LNG does not meet the requirements of PDSFTT-2 for high purity LCH₄.

TABLE 12

TYPICAL SPECIFICATION FOR LIQUID NATURAL GAS

CH ₄	=	90-94% (by volume)
Ethane	=	2-5% (by volume)
Propane and Higher Hydrocarbons	=	0.5-4% (by volume)
CO ₂	=	1-3% (by volume)
N ₂	=	1-2% (by volume)
Odorant Sulfur and H ₂ S ^a	=	5-10 ppm

^aLNG is deliberately odorized with mercaptans, aliphatic sulfides, or cyclic sulfur compounds prior to distribution to provide a distinctive odor which alerts customers to possible leaks.

The technology to produce high purity LCH₄ in bulk form that meets or exceeds the requirements of PDSFTT-2 is well in-hand according to most interviewed sources. However, the only major market for bulk LCH₄ of this high purity appears to be aerospace launch vehicles. This market is small in comparison to others not requiring that level of purity. For example, Air Products estimates the requirements for LNG and/or LCH₄ in the year 2000 to be approximately 50,000 tons/stream day with aerospace accounting for only 45 tons/stream day, less than 0.1% of the total, while high-speed civil transport and ground transportation systems account for all the rest. Tons/stream day refers to production capacity over 24 hrs under continuous operation. This information was part of a presentation given by Air Products on Liquid Methane at a meeting held at Marshall Space Flight Center on November 17-18, 1987. A

3.2, Dynamic Tests (cont.)

graph from this presentation giving the estimated propellant requirements through FY 2007 is shown in Figure 38. Clearly, the aerospace market will remain a very small part of the overall market well into the foreseeable future. For this reason, potential major producers, such as Air Products, are focusing their efforts on meeting the needs of the larger market segment and have no immediate plans to produce bulk LCH₄ specifically meeting the requirements of PDSFTT-2 even though they have the technology. Thus, at present, there are no major producers of bulk high purity LCH₄ and economic consideration is the driver, not lack of technology.

If a potential supplier should wish to go into the production of bulk high purity LCH₄, the most likely basic raw material or feedstock will be natural gas. Therefore, the cost of producing LCH₄ will be sensitive to natural gas availability, quality, and price.

Regarding availability, the producer has two choices, (1) readily available pipeline gas, or (2) use of producer-owned or leased natural gas fields. Pipeline natural gas is really a mixture of gases originating from several different fields. The gases are partially purified at the wellheads to meet pipeline standards and are then tied into intra- and/or interstate pipelines for transport to distribution centers all around the country. The quality of pipeline natural gas is relatively consistent and the price is a function of field price, (wellhead price), pipeline (transportation) costs, and distribution costs, (municipal and regional utility companies). For example, your cost will be lower if you tap the pipeline and avoid the utility companies. In addition, field prices rise and fall in step with crude oil prices to some degree and fluctuate with the seasons on a yearly basis, e.g., the field price of pipeline quality natural gas might be as low as \$1.20/1000 cu ft during the summer and as high as \$2.20/1000 cu ft during the winter. Larger consumers frequently go to cryogenic storage tanks to avoid this seasonal fluctuation. Table 13 shows the average field and city gate prices over a seven year period. City gate prices are the delivered price to distribution centers. As can be seen, the field prices declined from 1983 through 1987 and then trended upward at a slow rate. This pattern roughly parallels crude oil prices over the same time period. Phillip Budzic of the Natural Gas Supply Association believes the field prices will ultimately stabilize at \$2.25 to 2.75 per 1000 cu ft sometime during the next ten years once the over-supply situation existing in the country normalizes with respect to demand. The Table also shows that the average pipeline costs run about \$1.25 per 1000 cu ft and are fairly constant from year to year. Distribution costs, which are not shown in Table 13, can vary considerably from one distribution center to the next. However, the distribution costs usually run 40 to 80% higher than the pipeline costs. Thus, major consumers normally tap the pipeline directly and avoid the distribution costs.

FY 1989 - FY 2007

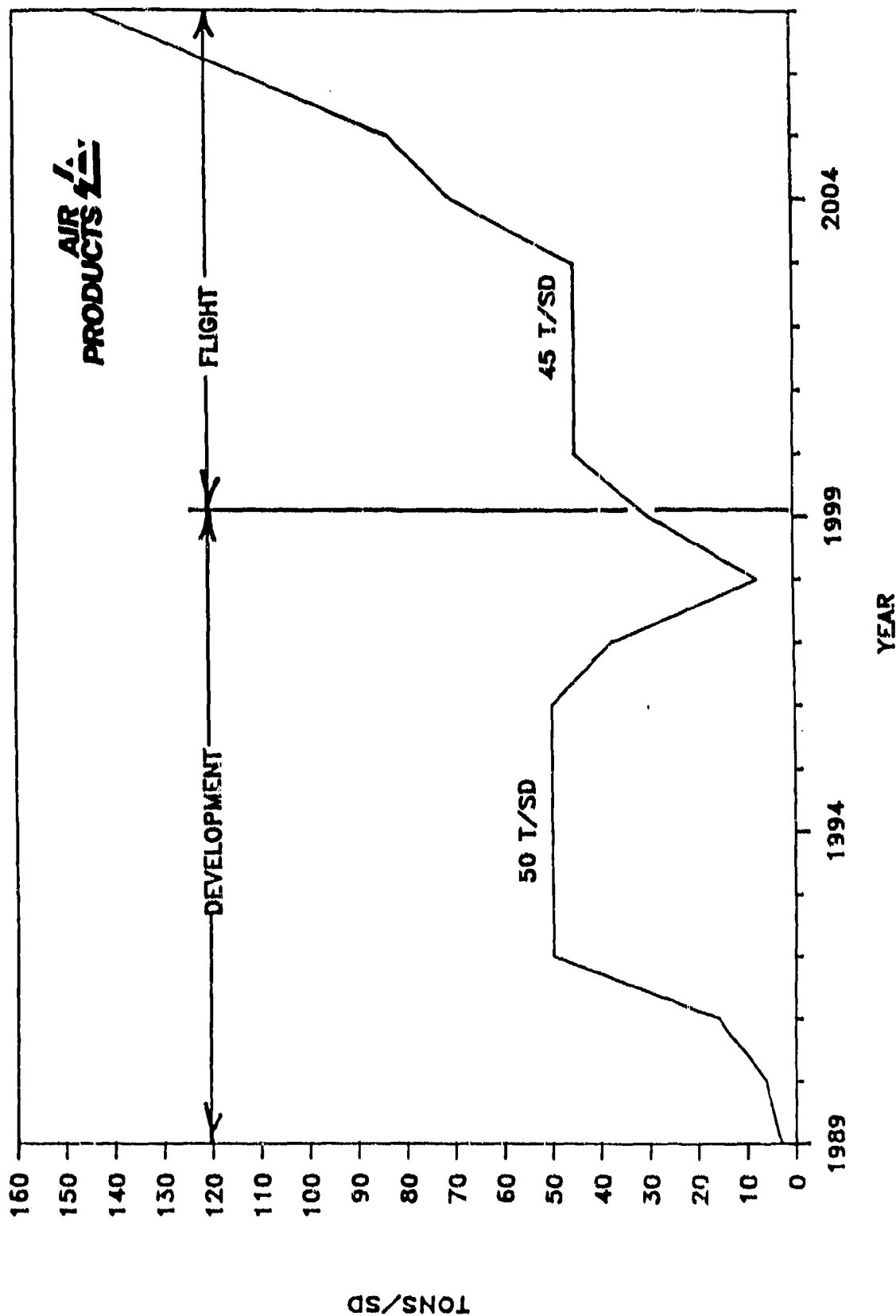


Figure 38. Estimated Requirements for High Purity Liquid Methane Propellant (Tons/Stream Day)

3.2, Dynamic Tests (cont.)

TABLE 13

AVERAGE FIELD AND CITY GATE PRICES FOR NATURAL GAS

	Average Costs Per 1000 Cubic Feet						
	1983	1984	1985	1986	1987	1988	1989
Field	\$2.59	\$2.66	\$2.51	\$1.94	\$1.67	\$1.69	\$1.70
City Gate	—	3.95	3.75	3.22	2.87	2.93	2.95
Difference ^a	—	1.29	1.24	1.28	1.20	1.24	1.25

^aThe difference between the city gate and field costs are essentially the average pipeline or transportation costs.

The cost of producing high purity bulk LCH₄ directly from field gas rather than pipeline gas will be sensitive to the quality of field gas used. The quality of natural gas at the well head varies considerably from field to field. Table 14 shows the composition of various natural gas fields. Clearly, the difficulty and, therefore, the cost of producing bulk LCH₄ to meet PDSFTT-2 would be greater for natural gas from Olds Field, Alberta, Canada or Terrell County, Texas as compared to natural gas from Rio Arriba County, New Mexico. Thus, the viability of using field gas feedstock directly versus pipeline natural gas feedstock is largely a matter of quality and, of course, cost differential. From a technical point of view, the best choice is to use "sweet" field gas feedstock, i.e., sulfur-free, and minimize the purification problem regarding sulfur content.

In regards to actual suppliers or potential future suppliers of bulk high purity LCH₄, the following is a summary of the survey results. These results represent a rather thorough investigation based on inquiry of the sources listed in this section.

Air Products, one of the largest producers of LNG in bulk, is very interested in the overall future market for bulk LCH₄. However, as stated before, it views the aerospace market as small and relatively unattractive in comparison to the transportation market, i.e., trains in particular. Nevertheless, they have done the engineering design work necessary to convert all or part of a liquid hydrogen, LH₂, plant located in New Orleans to the production of high purity bulk LCH₄. The conversion from LH₂ production to LCH₄ production would require about two

3.2, Dynamic Tests (cont.)

months and would only be made if and when the conversion becomes economically attractive. It should also be noted that the capacity of this plant would be 5-6 tons/stream day (SD) which does not meet projected requirements beyond 1992 (see Figure 38). Nevertheless, Air Products is a potential supplier for small quantities of LCH₄ in the near future and a possible source of higher volumes in the more distant future.

TABLE 14

COMPOSITION OF VARIOUS NATURAL GAS FIELDS

Components, Mole %	Rio Arriba County, N. Mex.	Terrel County, Texas	Stanton County, Kansas	San Juan County, N. Mex.	Olds Field, Alberta, Canada	Cliffside Field, Amarillo, Texas
Methane	96.91	45.64	67.56	77.28	52.34	65.8
Ethane	1.33	0.21	6.23	11.18	0.41	3.8
Propane	0.19	0	3.18	5.83	0.14	1.7
Butanes	0.05	0	1.42	2.34	0.16	0.8
Pentanes, Heavier	0.02	0	0.40	1.18	0.41	0.5
Carbon Dioxide	0.82	53.93	0.07	0.80	8.22	0
Hydrogen Sulfide	0	0.01	0	0	35.79	0
Nitrogen	0.68	0.21	21.14	1.39	2.53	25.6
Helium	0	0	0	0	0	0
(Total Sulfur) ^a	(0)	(0.27)	(0)	(0)	(984)	(0)

^aTotal sulfur is expressed as mg/m³.

Air Products has developed a forecast for the cost of bulk high purity LCH₄ which is based on the estimated requirements shown in Figure 38, and assumes the construction of additional facilities or the modification of existing facilities to meet these requirements. The cost forecast shown in Figure 39 was part of the MSFC presentation given in November 1987. The reliability of this forecast may well have changed since 1987, but the general trend is probably valid. Relatively low usage levels, i.e., ≥50 tons/SD, should see the price drop below \$1.00 per gallon. In any case this was Air Products assessment of the economies should they ever enter the LCH₄ market for aerospace.

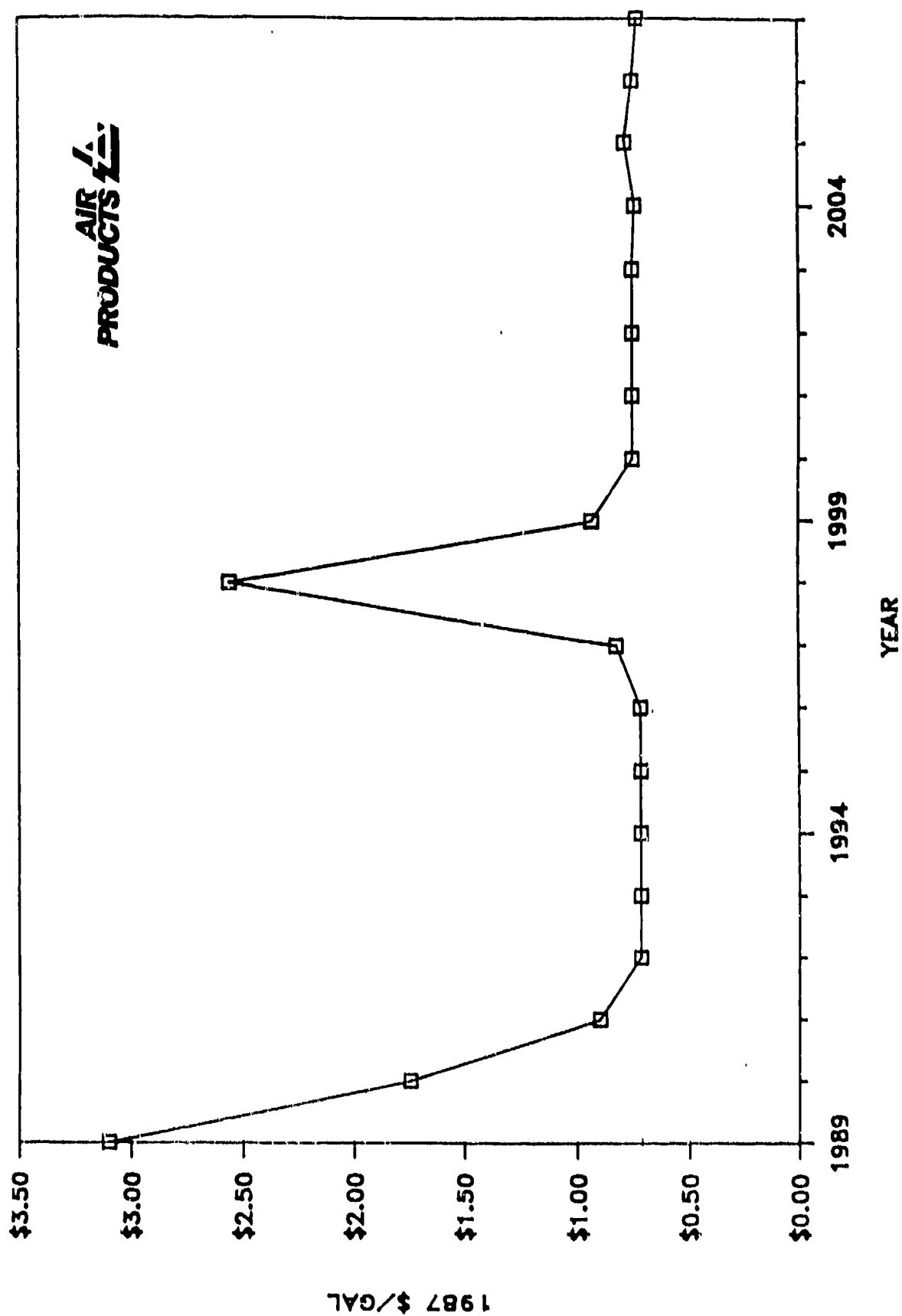


Figure 39. Forecasted Cost of Bulk High Purity Liquid Methane

3.2, Dynamic Tests (cont.)

Liquid Carbonics has a plant in Geismar, Louisiana which obtains high purity bulk LCH_4 in very small quantities as a by-product from another process. Its capacity for LCH_4 is only 700 gals/day when the other process is running and the exact purity is not known, i.e., LC does not assay for all the compounds shown in PDSFTT-2, but the methane content is in excess of 99.9%. It has supplied Aerojet, Rocketdyne, and Kelly AFB with bulk LCH_4 in the past and is still capable of supplying small quantities now. The LCH_4 supplied to Kelly AFB in 1987 sold for \$2.95/gallon. However, Liquid Carbonics should not be considered a viable long-term supplier as they do not appear to be interested in building a dedicated facility for the production of bulk high purity LCH_4 and the present capacity is very low.

The only producer of high purity bulk LCH_4 that meets PDSFTT-2 requirements that was identified during this survey is Quadren Cryogenic Processing, Ltd. Quadren is a small company with a single production facility located near Robbins, California which is about 40 miles north of Sacramento. High purity bulk LCH_4 is their only product. The plant was built in 1986 and employs a new, patented process which uses a concept called Non-Adiabatic Distillation. Using this process, they produce bulk LCH_4 that actually exceeds the requirements of PDSFTT-2, i.e., they offer LCH_4 with purities in excess of 99.999%. The process is interesting in that it operates at relatively low pressures, i.e., about 300 psia as compared to 1500 psia. Since they operate below the critical pressure of ethane and other hydrocarbons, separation of these impurities is easier. Table 15 shows the assay results of two recent shipments of Quadren LCH_4 as compared to the requirements of PDSFTT-2. The data given in Table 15 clearly shows that the bulk LCH_4 offered by Quadren Cryogenic Processing not only meets PDSFTT-2, but also meets the proposed sulfur specification shown in Table 10.

Quadren did not establish its facility specifically to meet the needs of aerospace. Their mainline business is supplying ultra-high purity methane to specialty gas companies. In addition, they supply LCH_4 to major oil companies for an unknown end-use and to the diamond film industry. Thus, there is a small but very real market for bulk purity LCH_4 outside of the aerospace market. It should be noted that Quadren also sells small quantities to Aerojet and Rocketdyne as well. Their current pricing is about \$2.25/gallon for what amounts to relatively small quantities. Quadren further stated that should the demand increase well beyond present usage levels, they can see the price dropping to around \$1.00/gallon or less. However, no specific forecasts were provided. Nevertheless, Quadren's current pricing and their general comment on larger volume pricing is certainly consistent with the Air Products estimates.

3.2, Dynamic Tests (cont.)

TABLE 15

**ASSAY RESULTS OF QUADREN CRYOGENIC PROCESSING LIQUID
METHANE AS COMPARED WITH PDSFTT-2 REQUIREMENTS**

Department of Defense Requirements (PDSFTT-2)		10,000 Gallon Shipment	7,500 Gallon Shipment
Methane	≥ 99.93% (by vol)	99.993	99.994
Ethane	= 500 ppm (max)	30	40
Propane, Higher Hydrocarbons	= 30 ppm (max)	<1	<1
O ₂	= 1 ppm (max)	<1	<1
CO ₂	= 50 ppm (max)	<1	<1
H ₂ O	= 1 ppm (max)	<1	<1
Total Inerts ^a	= 100 ppm (max)	42	21
Total Sulfur	= 1 ppm (max)	ND ^b	ND ^b

^aNitrogen and other inert gases such as argon and helium etc.

^bNone detected. Gas chromatography with flame photometric detection was used.
The limit of detection is 0.1 ppm.

Finally, the Quadren facility is a full scale, modular, working prototype designed to continuously produce LCH₄. At the present time they are running at about 20% of full capacity in order to meet demand. Full rated capacity is about 78 tons/day. They have excess storage capacity for 110 to 120 tons. Thus, Quadren is a viable supplier of high purity bulk LCH₄ that actually exceeds all the requirements of PDSFTT-2 and meets the much tougher sulfur requirements proposed in Table 10 and they have the capacity to meet the projected aerospace demand out to the year 2004 if the forecasts in Figure 38 are accurate.

In summary, there is, at present, only one source for bulk high purity LCH₄, Quadren Cryogenic Processing. If the aerospace demand increases as projected in Figure 38, the capacity of the single production facility now in place at Quadren will be exceeded in the first decade of the next century. Thus, additional sources will have to be established by that time. Air Products, a major LNG producer, has the capability, but may never have the economic incentive, as even the projected increase in aerospace demand does not make this segment a significant part of the overall market for liquified methane products. Thus, Air Products is a potential future

3.2, Dynamic Tests (cont.)

source, but there are no guarantees. Expansion of Quadren's operations is more likely as the aerospace market is much more attractive to a company of their size. However, there still are no guarantees. For these reasons, NASA would be well advised to consider the option of building their own on-site production facility using licensed technology.

4.0 TASK 2A — CHANNEL REFURBISHMENT

4.1 TEST METHODS

This section describes the test apparatus, test specimen, test procedures, analytical methods, and experimental approach used of the static and dynamic testing carried out in Task 2A.

4.1.1 Static Test Methods

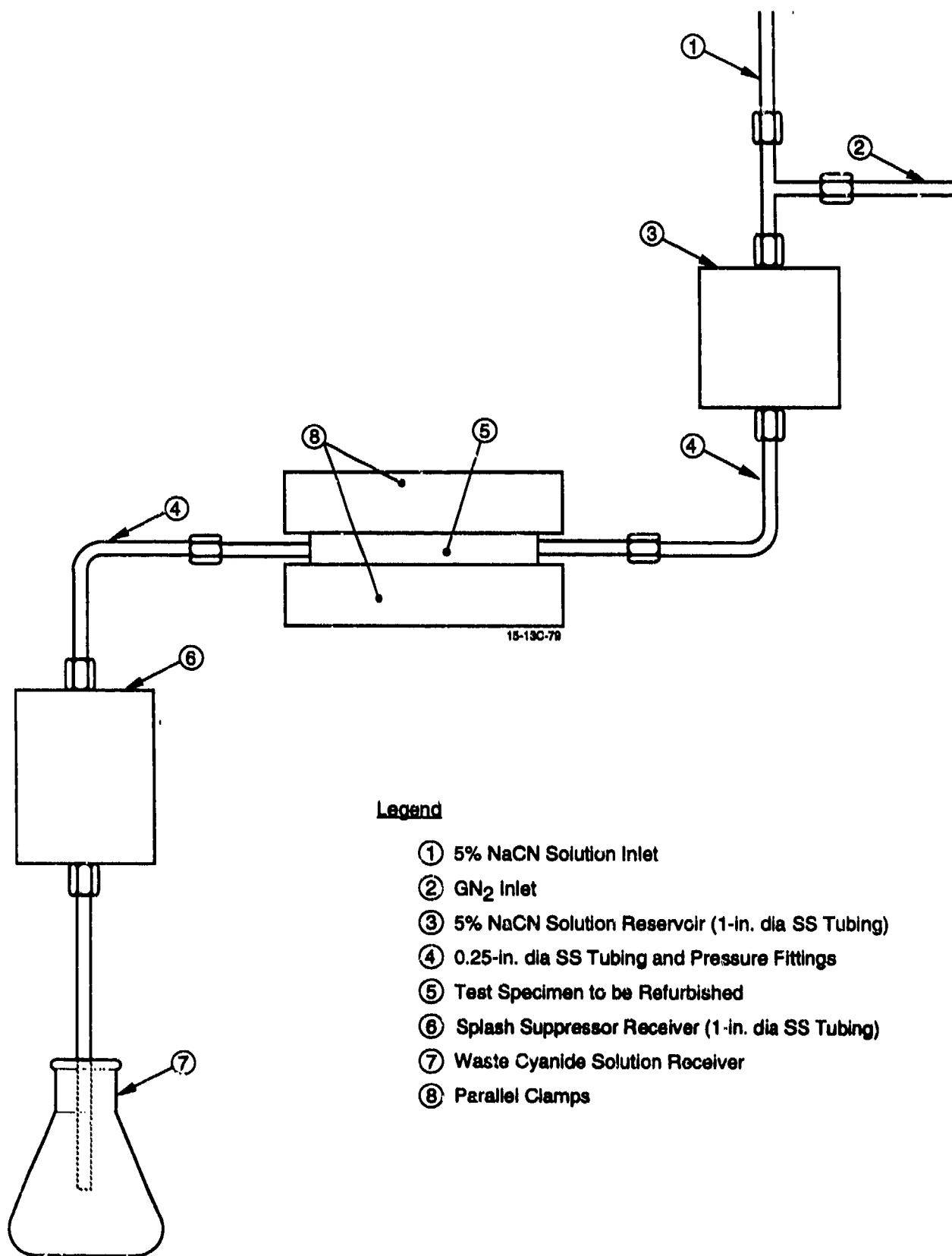
The static testing phase of Task 2A was used to identify candidate refurbishment methods suitable for a more detailed evaluation using dynamic test specimen and the Aerojet Carbothermal Test Facility.

NASA-Z copper coupons, 1-in. diameter and 0.030-in. thick, were electropolished and half of them were then corroded by treatment with methane containing 2000 ppm H₂S in an Aminco Bomb at 650 F and 2500 psig for 30 minutes. Corroded coupons along with an electropolished controls were treated with the candidate refurbishment solutions under controlled conditions. Weight changes, SEM, and EDS were used to evaluate the effectiveness of the refurbishment solutions.

4.1.2 Dynamic Test Methods

The dynamic testing phase of Task 2A was used to demonstrate efficacy of the refurbishment method(s) identified by static testing and more clearly define their application. All test apparatus, test specimen, test procedures, and analytical methods were the same as described in Section 3.1, with the exception of the refurbishment technique which is described below.

Four dynamic test specimens were tested with low sulfur as received methane to establish their performance parameters as baseline controls. The same test specimen were then tested with methane deliberately contaminated with known amounts of H₂S or CH₃SH in order to corrode the cooling channels and degrade their performance. The corroded test specimen were then refurbished by pressure feeding the refurbishment solution through the cooling channels under controlled conditions. Figure 40 shows a drawing of these Static Gas Pressure Refurbishment Apparatus used to complete this task. The NaCN refurbishment procedure simply involved pressure feeding with a 50 psig GN₂, 5% (w/w) NaCN solution through the corroded channels for 4-6 minutes. The excess NaCN solution was removed by rinsing the channels with



Legend

- ① 5% NaCN Solution Inlet
- ② GN₂ Inlet
- ③ 5% NaCN Solution Reservoir (1-in. dia SS Tubing)
- ④ 0.25-in. dia SS Tubing and Pressure Fittings
- ⑤ Test Specimen to be Refurbished
- ⑥ Splash Suppressor Receiver (1-in. dia SS Tubing)
- ⑦ Waste Cyanide Solution Receiver
- ⑧ Parallel Clamps

Figure 40. Static Gas Pressure Refurbishment Apparatus

4.1, Test Methods (cont.)

copious amounts of deionized water, i.e., 5-7 times the volume of 5% (w/w) NaCN used. The channels were then rinsed with isopropyl alcohol, blown dry with GN_2 , and finally dried overnight in a vacuum oven at 160 F. The refurbishment test specimen were then re-tested with low sulfur, as received methane under conditions as identical as possible to the original baseline control operating conditions. Performance parameters and post-dynamic testing metallographic analysis (optical microscopy, SEM, and EDS) were used to evaluate the efficacy of the refurbishment technique and to determine the effect on cooling channel performance of the overall sulfur corrosion/refurbishment process.

4.2 STATIC TESTS

If the cooling channels of a copper alloy booster engine are inadvertently exposed to a fuel containing excessive sulfur contamination, i.e., 0.50 ppm or higher, severe corrosion of the channel walls will occur. Relatively low levels of sulfur are capable of degrading overall cooling channel performance to the extent that the booster is no longer suitable for use. Thus, a refurbishment technique capable of removing the Cu_2S corrosion product from the cooling channel surfaces without damaging the underlying copper is highly desirable. This phase of Task 2A was designed to identify candidate refurbishments for a more detailed evaluation.

Thirty-six (36) NASA-Z copper coupons (1-in. dia and 0.030-in. thick) were cleaned with acetone to remove organic residues and then electropolished to provide a smooth surface. Eighteen (18) of these electropolished coupons were then placed in an Aminco Bomb and treated with methane containing 2000 ppm H_2S at 650 F and 2500 psig for 30 minutes. In this manner, 18 sulfur corroded NASA-Z coupons and 18 uncorroded NASA-Z controls were prepared for the static testing program. Table 16 shows the weight data for all 36 coupons.

Prior to initiating the screening study, a sulfur corroded coupon was submitted for X-Ray Diffraction analysis to confirm that the corrosion product was exclusively Cu_2S . The diffraction pattern was characteristic of Cu_2S completely free of cupric sulfide (CuS) as expected. This is important because CuS is generally more resistant to chemical attack than Cu_2S .

Seven general refurbishment methods were selected for initial screening. A brief description of the seven methods follows.

TABLE 16

PREPARATION OF NASA-Z COUPONS FOR STATIC TESTING

NASA-Z Controls		Sulfur Corroded NASA-Z Coupons			
Coupon No.	Weight After Electropolishing (grams)	Coupon No.	Weight After Electropolishing (grams)	Weight After Sulfur Corrosion (grams)	Calculated Cu ₂ S Weight (grams)
ZA2	2.0457	ZA1	2.0471	2.0495	0.0119
ZA3	2.0292	ZA4	2.0255	2.0276	0.0104
ZA7	2.0448	ZA5	2.0622	2.0632	0.0050
ZA9	2.0424	ZA6	2.0620	2.0638	0.0089
ZA10	2.0494	ZA8	2.0592	2.0606	0.0070
ZA11	2.0274	ZA12	2.0444	2.0463	0.0094
ZA15	2.0230	ZA13	2.0315	2.0340	0.0124
ZA18	2.0425	ZA14	2.0272	2.0285	0.0065
ZA20	2.0338	ZA16	2.0537	2.0562	0.0124
ZA21	3.0515	ZA17	2.0529	2.0553	0.0119
ZA22	2.0657	ZA19	2.0439	2.0458	0.0094
ZA23	2.0787	ZA24	2.0346	2.0366	0.0099
ZA25	2.0028	ZA27	2.0615	2.0638	0.0114
ZA26	2.0678	ZA30	2.0594	2.0618	0.0119
ZA28	2.0003	ZA32	2.0369	2.0396	0.0134
ZA29	2.0583	ZA33	2.0515	2.0535	0.0099
ZA31	1.9936	ZA34	2.0265	2.0290	0.0124
ZA35	2.0265	ZA36	2.0489	2.0512	0.0114

4.2, Static Tests (cont.)

4.2.1 "Fire Off" Solution

"Fire Off" solution is a mixture of sulfuric acid, nitric acid, and water which is commonly used to remove heavy oxide layers on copper and copper alloys prior to electroplating. A nominal working solution is shown below.

H₂SO₄ - 25% (w/w)

HNO₃ - 40% (w/w)

H₂O - 35% (w/w)

"Fire Off" solution is normally used at room temperature. Since it contains nitric acid, it was expected to be corrosive to copper and its alloys.

4.2.2 Bright Dip Solution

Bright Dip solution is a mixture of sulfuric acid, nitric acid, and water that contains a small amount of hydrochloric acid. It is commonly used to improve surface luster on copper and copper alloys just prior to electroplating. A typical treatment involves a very brief, 5-10 seconds, dip in the working solution at room temperature. Presumably a brief exposure is used since the solution should be highly corrosive to copper and its alloys. A nominal working solution is shown below.

H₂SO₄ - 60% (w/w)

HNO₃ - 20% (w/w)

H₂O - 15% (w/w)

HCl - 5% (w/w)

4.2.3 Sulfuric Acid Pickle

Sulfuric Acid Pickle is simply a mixture of sulfuric acid and water which is used to remove surface oxides from copper and copper alloys prior to electroplating. It is typically used between room temperature and 180°F with contact times up to 20 minutes. Since Sulfuric Acid Pickle contains no oxidizing acids, i.e., HNO₃ or HNO₃/HCl it is not expected to be corrosive to copper and copper alloys. A nominal working solution is shown below.

4.2, Static Tests (cont.)

H_2SO_4 - 40% (w/w)

H_2O - 60% (w/w)

4.2.4 Ferric Chloride Etch Solution

Ferric Chloride Etch solution is simply a saturated aqueous solution of ferric chloride. This solution is acidic and highly corrosive to most metals, e.g., it readily attacks stainless steel at 130°F. It is included in this screening series primarily to provide an oxidation-reduction approach that does not involve nitric acid. A nominal working solution is shown below.

FeCl_3 - 40-45% (w/w)

H_2O - 55-60% (w/w)

4.2.5 Inorganic and Organic Amines

The acidic solutions shown above, with the possible exception of Sulfuric Acid Pickle, should all be fairly corrosive to copper and copper alloys. Non-acidic or basic solutions should be generally less corrosive, and therefore attractive, if effective methods can be found. The effectiveness of these materials will be dependent on their ability to dissolve Cu_2S and form stable water soluble copper complexes. Such water soluble copper complexes are well known.

4.2.6 Ethylenediamine Tetraacetic Acid (EDTA)

Ethylenediamine tetraacetic acid, a weak organic acid, is a powerful complexing agent for most transition elements, including copper. EDTA complexes of copper are water soluble. Thus, an aqueous solution of EDTA alone or with the aid of an appropriate co-reagent may be capable of solubilizing Cu_2S without serious attack on copper.

4.2.7 Sodium Cyanide (NaCN) Solution

Sodium Cyanide solution readily dissolves Cu_2S by forming the stable copper cyanide complex. Unfortunately, the solution also attacks copper and copper alloys for the same reason. However, if the Cu_2S solubility rate is high relative to the copper corrosion rate, practical process may be possible.

4.2, Static Tests (cont.)

The seven candidate methods were screened under a variety of conditions using uncorroded and sulfur corroded strips of NASA-Z. The screening tests were simply intended to select candidate methods for more detailed evaluation. The results are summarized in Table 17.

TABLE 17

SCREENING TESTS FOR CANDIDATE REFURBISHMENT METHODS

Refurbishment Method	Temperature (F)	Time (min)	Cu ₂ S Layer Removed	Bare Copper Attacked
1. "Fire Off" Solution	72	2	Yes	Vigorously
2. Bright Dip Solution	72	5	No	Vigorously
3. Sulfuric Acid Pickle	72	5	No	No
4. Sulfuric Acid Pickle	176	5	No	No
5. Ferric Chloride Etch	72	3	Yes	Vigorously
6. 10% (w/w) Hydrazine	Inorganic and Organic Amines	120	No	No
7. 10% (w/w) NH ₄ OH		15	No	No
8. Bipyridine Solution		120	No	Slightly
9. 10% (w/w) EDTA		1080	No	Slightly
10. 10% (w/w) EDTA		180	No	Slightly
11. 3% (w/w) NaCN		2	Yes	No

The results in Table 17 show that aqueous sodium cyanide (NaCN) is the only candidate method worthy of a more detailed evaluation. All other candidate methods were either ineffective in removing Cu₂S or vigorously corrosive toward bare NASA-Z copper.

Table 18 shows the results of a more detailed investigation of the effects of aqueous NaCN on both sulfur corroded and uncorroded NASA-Z copper. The results in Table 18 show that all the concentrations investigated, except 0.1% (w/w) NaCN, were effective in removing Cu₂S. The 0.1% (w/w) NaCN solution was too slow and the final weight change was less than the calculated amount of Cu₂S present. All the other solutions required only 4 minutes or less to remove the Cu₂S and the final weight changes exceeded the calculated amount of Cu₂S. It is tempting to account for extra weight loss by simple dissolution of the bare copper once the Cu₂S is removed, since all the NASA-Z controls show that the bare copper is attacked

TABLE 18

DETAILED EVALUATION OF THE AQUEOUS NaCN REFURBISHMENT METHOD

Solution	Solution pH	Coupons Used	Cu ₂ S Removal Time (sec) ^a	Total Exposure Time (min)	Coupon Weight (grams)		Weight Loss (grams)	Calculated ^b Cu ₂ S Weight (grams)
					Before	After		
1. 0.1% (w/w) NaCN	10.8	ZA24 (Cu ₂ S) ZA11 (Bare Cu)	1140 —	19 10	2.0366 2.0274	2.0274 2.0257	0.0092 0.0017	0.0099 —
2. 1.0% (w/w) NaCN	11.4	ZA27 (Cu ₂ S) ZA9 (Bare Cu)	246 —	5 10	2.0638 2.0424	2.0479 2.0377	0.0159 0.0047	0.0114 —
3. 3.0% (w/w) NaCN	11.6	ZA13 (Cu ₂ S) ZA20 (Bare Cu)	90 —	5 10	2.0340 2.0338	2.0188 2.0316	0.0152 0.0022	0.0124 —
4. 3% (w/w) NaCN with added caustic to increase pH	12.1	ZA6 (Cu ₂ S) ZA35 (Bare Cu)	65 —	5 10	2.0638 2.0265	2.0515 2.0244	0.0123 0.0021	0.0089 —
5. 10% (w/w) NaCN	11.8	ZA14 (Cu ₂ S) ZA22 (Bare Cu)	30 —	5 10	2.0285 2.0657	2.0163 2.0641	0.0122 0.0016	0.0065 —
6. 5% (w/w) NaCN	11.7	ZA1 (Cu ₂ S) ZA28 (Bare Cu)	70 —	1.5 1.5	2.0495 2.0003	2.0329 1.9998	0.0166 0.0005	0.0119 —

^a As determined by visual observation^b Based on measured weight grain resulting from sulfur corrosion and the X-ray diffraction analysis of the corroded coupons that shows that the corrosion product is stoichiometrically pure Cu₂S.

4.2, Static Tests (cont.)

at a slow but real rate. However, a close inspection of the data also shows that the bare copper dissolution rate is far too slow to explain the extra weight loss over the time frame of the experiments. Experiment 6 is the best example of this point. In this experiment coupons ZA1 (Cu_2S) and ZA28 (Bare Cu) were exposed to 5% (w/w) NaCN for slightly longer than the time required for the gray Cu_2S coating to visually disappear from ZA1. Both coupons were then removed, rinsed with deionized water, dried, and weighed. The weight loss data shows that ZA1 lost 0.0047 gms over the 0.0119 gms of Cu_2S calculated to be present. This represents a weight loss of 139.5% of the calculated value. The weight loss data for ZA28 shows a loss of only 0.0005 gms during this same time period, almost an order of magnitude less than the extra weight lost by ZA1. Thus, it appears that the NaCN refurbishment treatment removes bare uncorroded copper in addition to the Cu_2S via a mechanism that goes beyond simple Cu metal dissolution.

Figures 41 and 42 are EDS spectra of the surface of test coupon ZA1 before and after the NaCN refurbishment treatment. Figure 41 clearly shows a very large response for sulfur before refurbishment and Figure 42 shows that the sulfur is totally gone after refurbishment. Thus, the refurbishment process is both fast and efficient.

Figures 43, 44, and 45 are SEM photomicrographs showing a freshly electropolished test coupon, a test coupon after sulfur corrosion/NaCN refurbishment, and an electropolished test coupon after exposure to 5% (w/w) NaCN, respectively. Comparing the three figures shows that the sulfur corrosion/NaCN refurbishment process converts a smooth featureless copper surface (Figure 43) into a highly pitted and roughened surface (Figure 44). Furthermore, treatment of an electropolished coupon also roughens the surface (Figure 45), but the effect is minor in comparison to the sulfur corrosion/NaCN refurbishment effect. The surface appearance shown in Figure 44 suggests that the sulfur corrosive preferentially attacks the grain boundaries. If this is true, it is possible that some surface grains are completely undermined and isolated by the corrosion process and that subsequent removal of the Cu_2S corrosion product with NaCN solution causes the loss of these uncorroded grains as well. This mechanism accounts for the extra weight loss noted in Table 18 and the pitted surface. The proposed mechanism is shown in Figure 46.

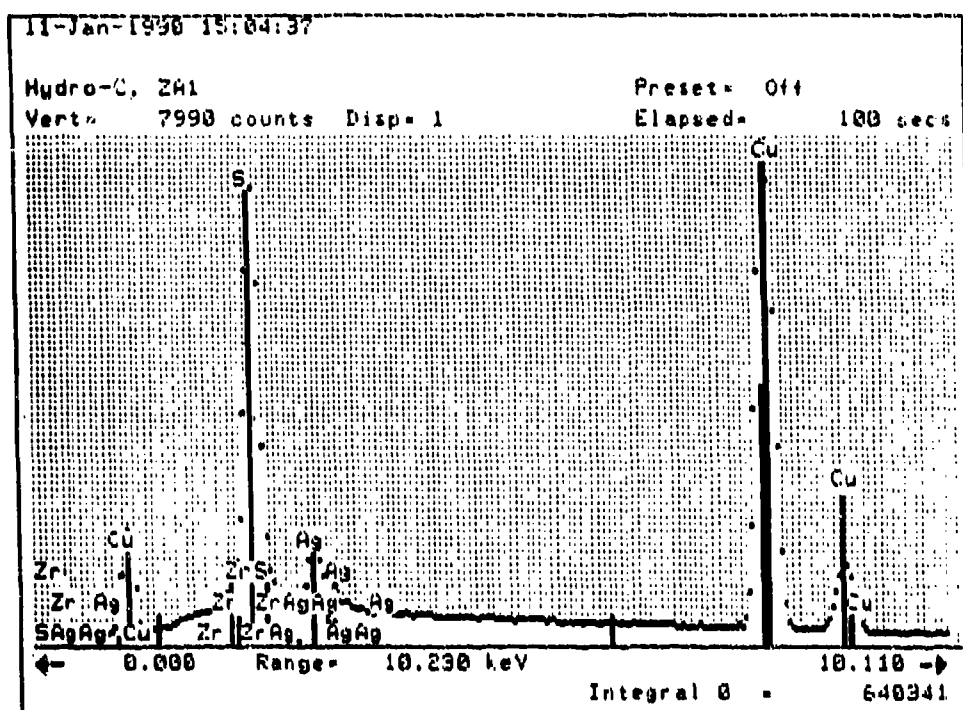


Figure 41. EDS Spectrum of Test Coupon ZA1 Before NaCN Refurbishment.
Note, Large Response for Sulfur

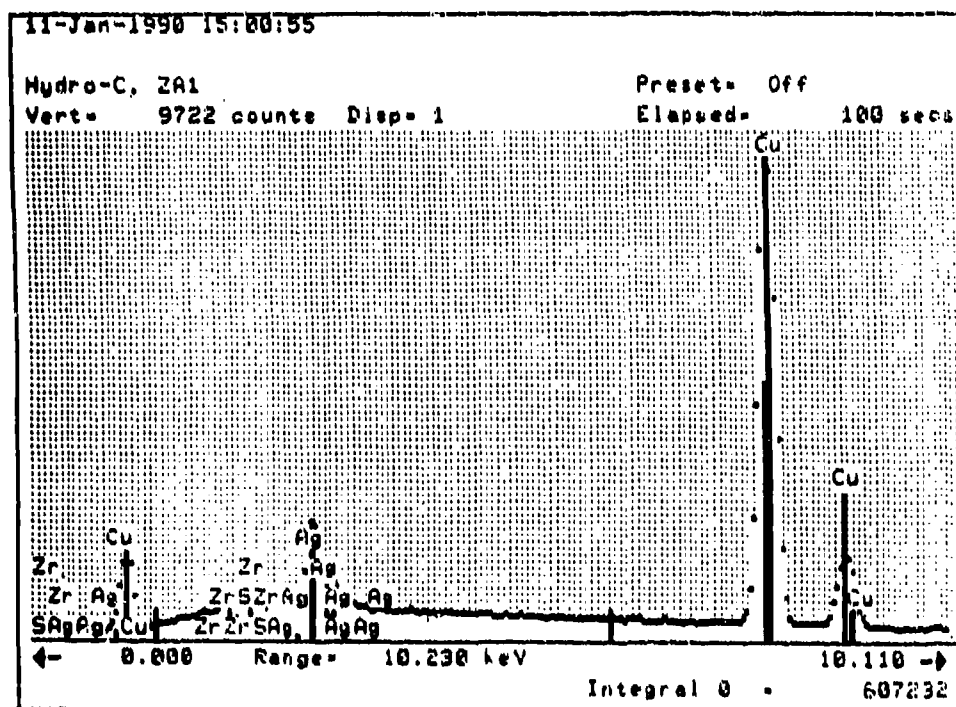
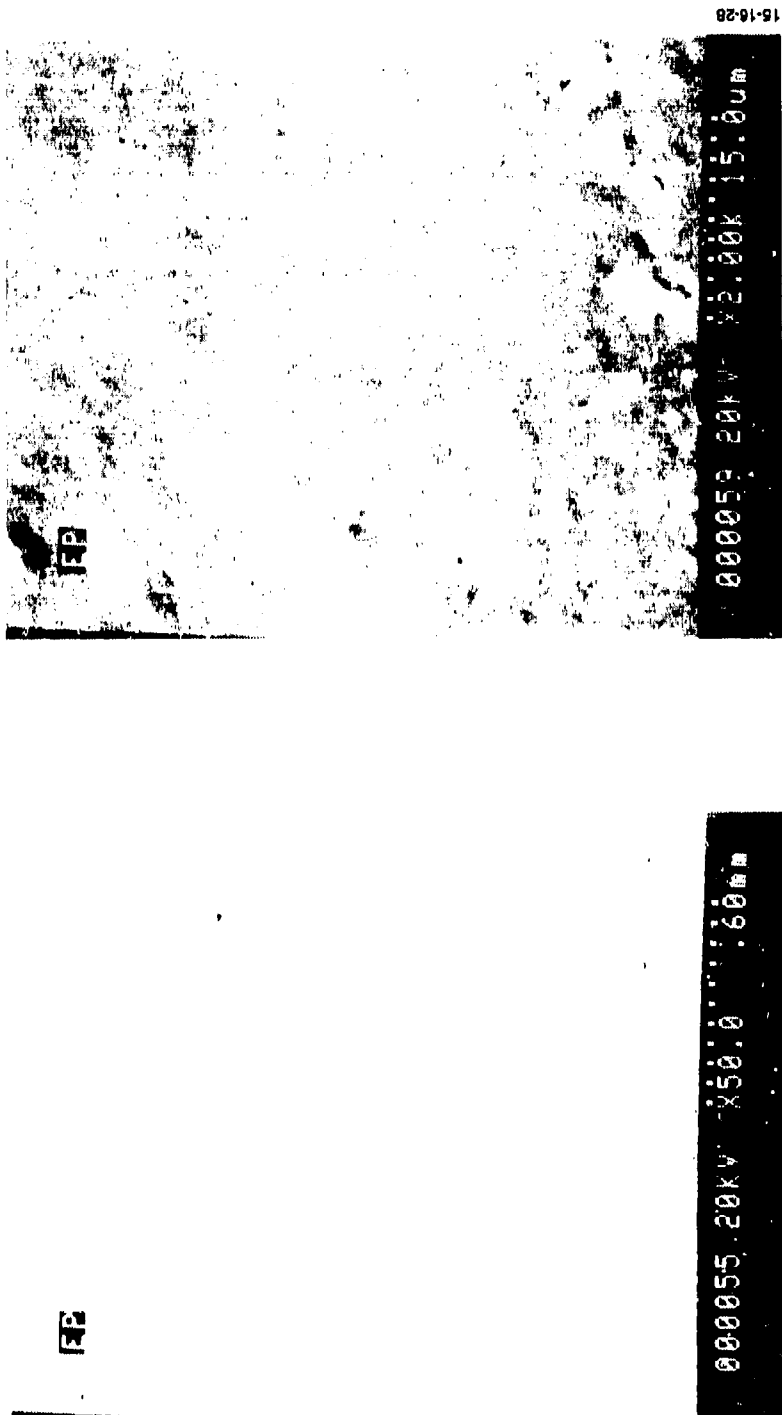


Figure 42. EDS Spectrum of Test Coupon ZA1 After NaCN Refurbishment.
Note, the Sulfur has Been Completely Removed



**Figure 43. SEM Photomicrograph of a Freshly Electropolished NASA-Z Copper Coupon
Note, the Smooth and Nearly Featureless Surface**

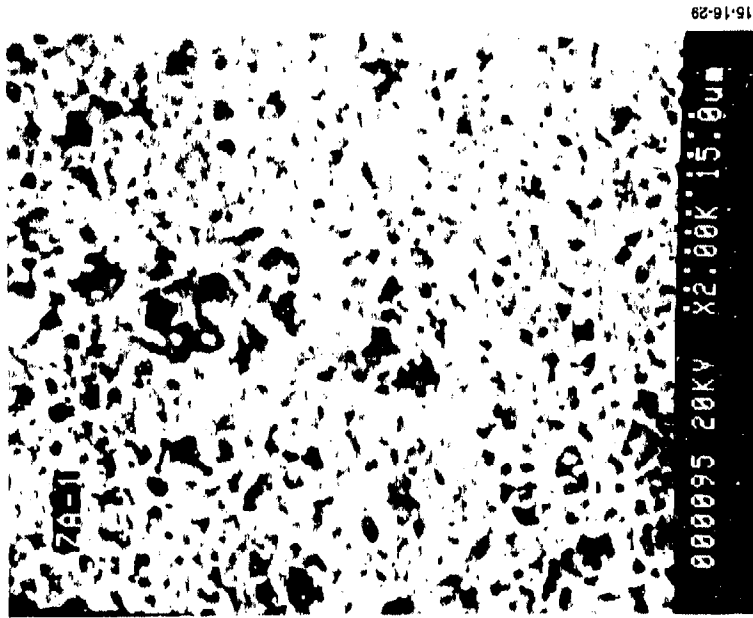
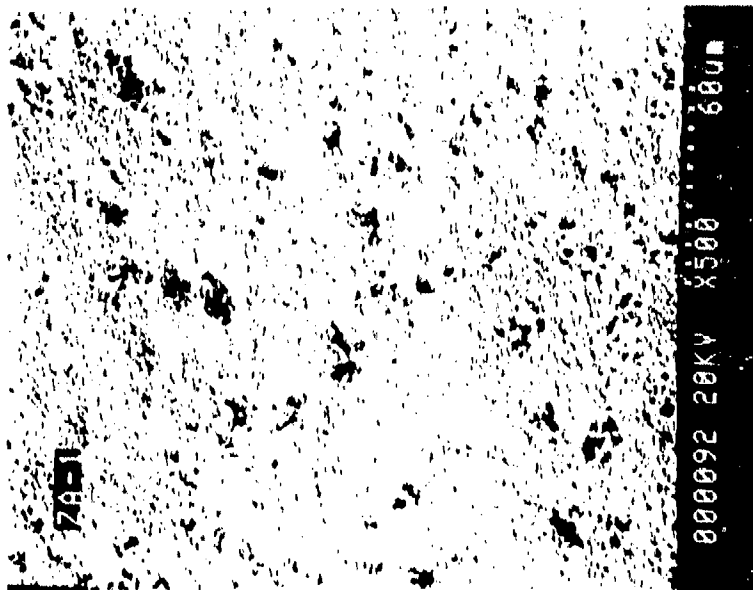


Figure 44. SEM Photomicrograph of Test Coupon ZA1 After Sulfur Corrosion and NaCN Refurbishment. Note, the Extensive Pitting and Overall Roughness of the Surface Compared to the Electropolished Surface Shown in Figure 43

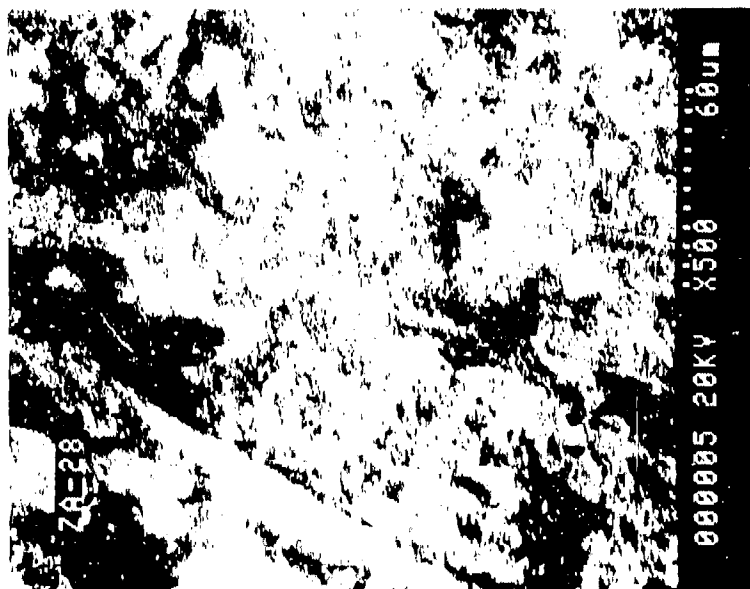


Figure 45. SEM Photomicrograph of Test Coupon ZA28 After Exposure to 5% (w/w) NaCN. Note, A Slight Amount of Pitting is Visual, but the Effect is Less Dramatic Than That Shown in Figure 44

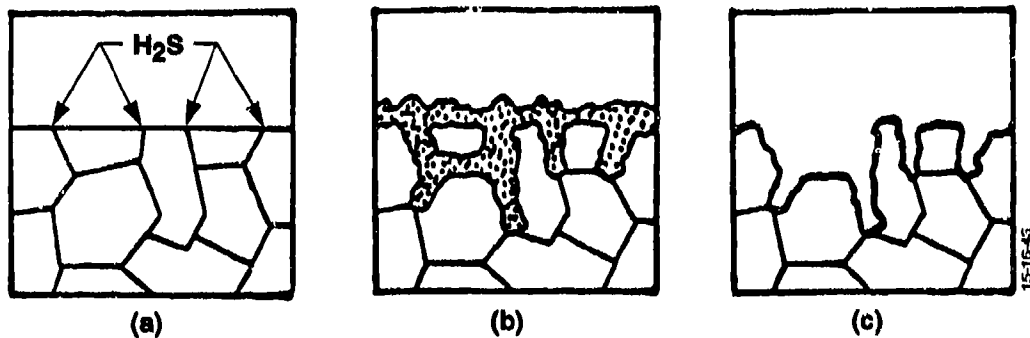


Figure 46. Pictorial Representation of Overall Sulfur Corrosion and Cuprous Sulfide Removal Process

- (a) Preferential Grain Boundary Attack By H_2S on Cu Alloy**
- (b) Resulting Cu_2S Corrosion Product, Has Penetrated the Grain Boundaries, Completely Undermining and Isolating Some Surface Grains**
- (c) Removal of the Cu_2S With Aqueous NaCN Also Leads to the Loss of the Isolated Grains, Leaving a Rough, Highly Pitted Surface**

4.2, Static Tests (cont.)

In any case, the important conclusion from this work is that aqueous NaCN quickly and efficiently removes the Cu_2S corrosion product and is therefore a suitable refurbishment technique for sulfur-corroded, copper-alloy cooling channels. However, the overall sulfur corrosion/NaCN refurbishment process leaves a highly roughened surface which may alter cooling channel performance. The dynamic testing discussed in the next section was carried out for the express purpose of defining the overall effect of the sulfur corrosion/NaCN refurbishment process on cooling channel performance under realistic booster engine conditions.

4.3 DYNAMIC TESTS

In the previous section aqueous NaCN was identified as a refurbishment solution capable of quickly and efficiently removing Cu_2S corrosion from NASA-Z. The resulting clean copper surface is highly roughened as a result of the overall sulfur corrosion/NaCN refurbishment process. The dynamic testing described in this section was carried out to specifically demonstrate the efficacy of the refurbishment technique under realistic booster engine conditions and to define the effect of the sulfur corrosion/NaCN refurbishment process on cooling channel performance.

Four dynamic test specimen, i.e., ZA3, ZA13, ZA18, and ZA23, were carried through the four step program outlined below. When the four step program was complete the test specimen underwent metallographic analysis.

- Step 1 - Control tests with as received methane to establish baseline performance parameters for the as received test specimen.
- Step 2 - Tests with sulfur contaminated methane to create badly corroded cooling channels and establish performance parameters for these conditions.
- Step 3 - Refurbishment of the test specimen with 5% (w/w) NaCN to demonstrate efficacy of the technique.
- Step 4 - Re-testing with as received methane under Step 1 conditions to establish the effect of sulfur corrosion/NaCN refurbishment on cooling channel performance.

4.3, Dynamic Tests (cont.)

Table 19 summarizes the dynamic test results for the four step programs. Tests M305, M306, M307a, and M307b are the results for Step 1, the control tests. Figures 12-17 are plots of the monitored performance parameters versus time for Test M307b, specimen ZA3. A review of those plots shows steady cooling channel performance. Tests M308, M309, M310, and M311 are the results of Step 2, sulfur corrosion tests. Figures 29-34 are plots of the monitored parameters versus time for Test M308, Specimen ZA3 run with 1 ppm H_2S . A review of those plots shows that the cooling channel performance is seriously degraded as a result of sulfur corrosion. Tests M313, M314, M315, and M316 are the results of Step 4 after successfully completing Step 3 with the sulfur corroded specimen. Figures 47-52 are the corresponding performance plots for Test M316, Specimen ZA3 after sulfur corrosion/NaCN refurbishment. Examination of those plots shows that steady cooling channel performance is restored by the refurbishment technique. Thus, this simple refurbishment procedure, based on the facile dissolution of Cu_2S by aqueous NaCN, does represent an effective method for cleaning the cooling channels of a copper alloy booster engine inadvertently corroded by contact with sulfur contaminated fuel.

The second goal of this test program was to determine the effect of the overall sulfur corrosion/NaCN refurbishment process on cooling channel performance. To do this, one needs to compare the results for specimen ZA3, ZA13, and ZA18, and ZA23 before sulfur corrosion and after sulfur corrosion/NaCN refurbishment. Figures 53-60 are mass flow and heat transfer comparison plots for the four specimen. These plots clearly show that the mass flow rate through the cooling channels, under comparable inlet temperature, wall temperature, and pressure drop conditions, is substantially decreased for all the specimen as a result of the sulfur corrosion/NaCN refurbishment process. In like manner, heat transfer for all the specimen is substantially improved. These observations are consistent with highly roughened cooling channel surfaces resulting from the sulfur corrosion/NaCN refurbishment process as predicted by the static test results in Section 4.2. The decrease in mass flow ranges from a low of 7% for specimen ZA18 (3 ppm CH_3SH) to a high of 48% for specimen ZA3 (1 ppm H_2S), while the increase in heat transfer performance ranges from 21% for specimen ZA18 (3 ppm CH_3SH) to 31% for specimen ZA3 (1 ppm H_2S). Thus, a copper alloy booster engine inadvertently corroded by sulfur contaminated fuel and then refurbished with NaCN solution is very likely to have cooling channel performance significantly different from initial baseline performance.

TABLE 19

SUMMARY OF DYNAMIC TEST DATA FOR THE SULFUR CORROSION/NaCN REFURBISHMENT STUDY

Test No.	Specimen No.	Additives	Test Duration (sec)	Average Wall Temperature (F)	Average Mass Flow (lbs/min)	Average Pressure Drop Across Channel (psia)	Average Methane Bulk Temperature (F)	Average Heat Flux (Btu/in. ² -s)	Average Heat Transfer Efficiency $(Nu_{(exp)}/Nu_{(pred)})$
M305	ZA23	None	1329	647	1.06	2349	184	28.1	0.78
M306	ZA18	None	1567	676	0.93	2536	191	31.5	0.90
M307a	ZA13	None	1352	667	1.15	2323	185	34.6	0.87
M307b	ZA3	None	1324	638	1.23	2471	193	37.5	0.91
M308	ZA3	1 ppm H ₂ S	1407	631	1.03a	2500b	148a	30.4a	0.87a
M509	ZA13	3 ppm H ₂ S	1452	703	1.05a	2670b	135a	34.2a	0.88a
M310	ZA18	3 ppm CH ₃ SH	1250	645	1.29a	2453b	170a	35.2a	0.83a
M311	ZA23	10 ppm CH ₃ SH	1400	769	0.74a	2540b	175a	31.8a	0.94a
M313	ZA23	None	1423	671	0.92	2640	152	32.9	1.03
M314	ZA18	None	1445	635	0.87	2490	176	31.9	1.09
M315	ZA13	None	1357	628	0.80	2550	181	30.2	1.12
M316	ZA3	None	1379	636	0.83	2550	148	32.3	1.19

a Initial values decrease over the duration of the test.

b Initial values increase over the duration of the test.

Heat Transfer vs Time

Test M316

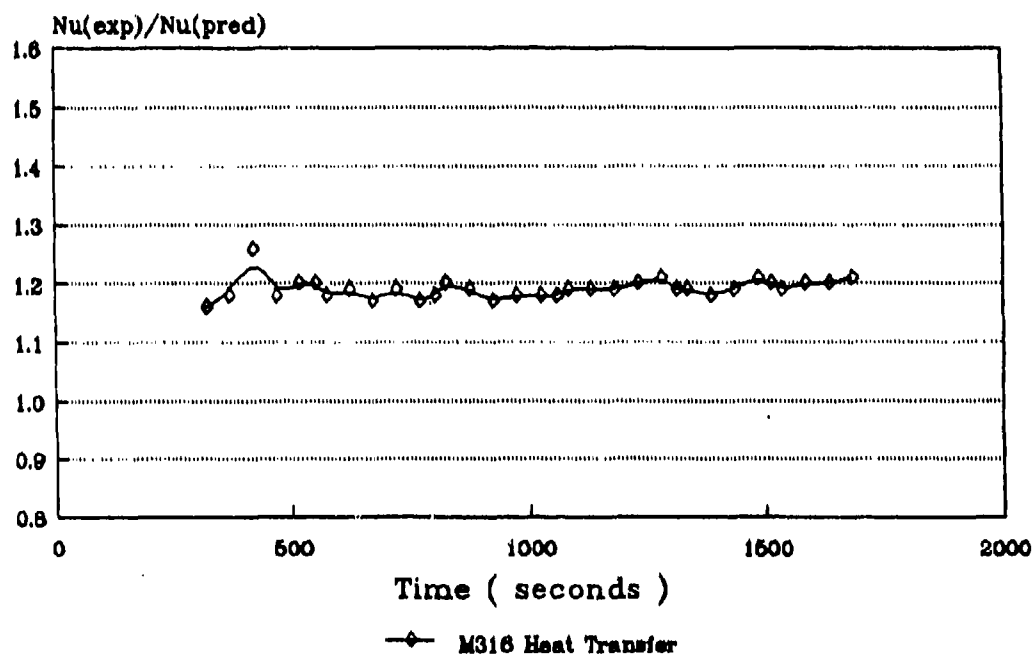


Figure 47. Heat Transfer Efficiency, $Nu(exp)/Nu(pred)$, vs Time for Test M316. Test Specimen ZA3 After Sulfur Corrosion/NaCN Refurbishment

Mass Flow vs Time

Test M316

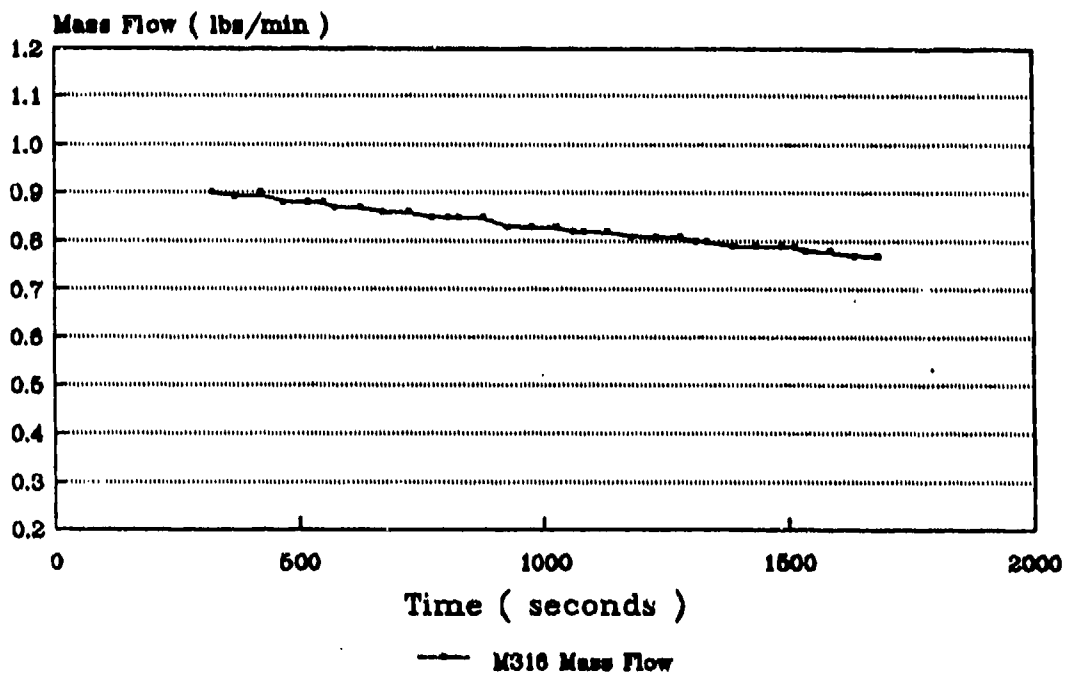
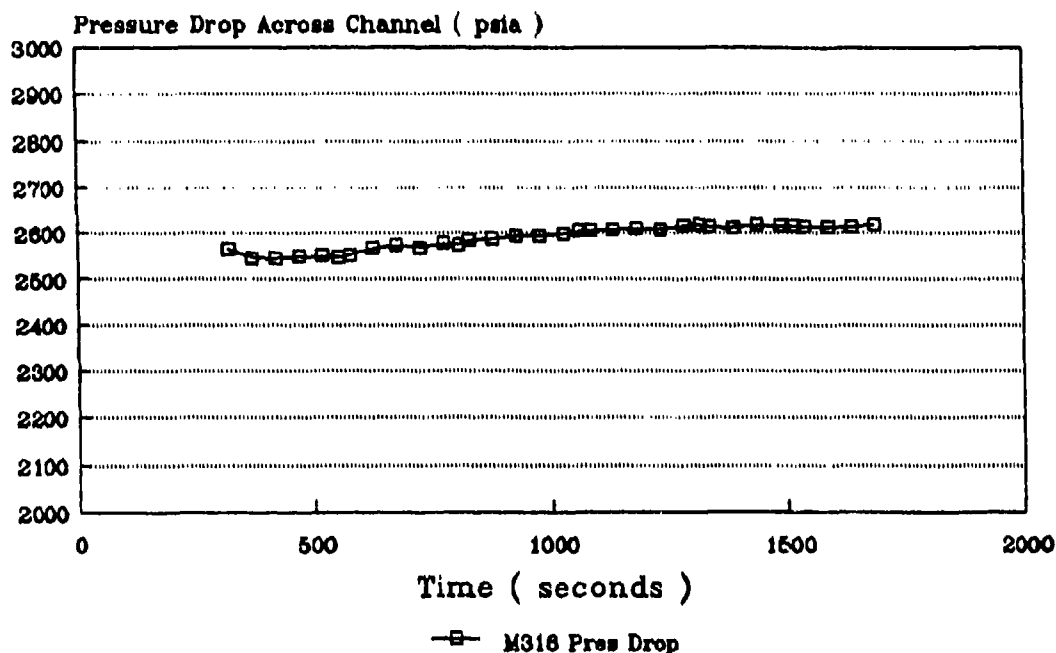


Figure 48. Mass Flow vs Time for Test M316. Test Specimen ZA3 After Sulfur Corrosion/NaCN Refurbishment

Pressure Drop vs Time

Test M316



**Figure 49. Pressure Drop Across the Cooling Channel vs Time for Test M316.
Test Specimen ZA3 After Sulfur Corrosion/NaCN Refurbishment**

Heat Flux vs Time

Test M316

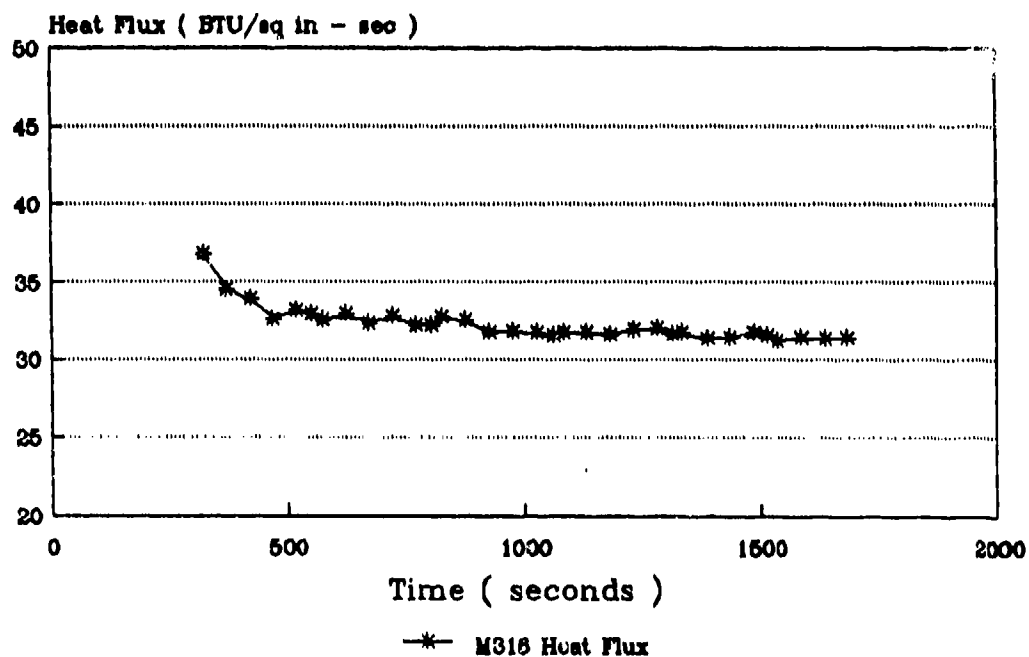


Figure 50. Heat Flux vs Time for Test M316. Test Specimen ZA3 After Sulfur Corrosion/NaCN Refurbishment

Bulk Temperature vs Time

Test M316

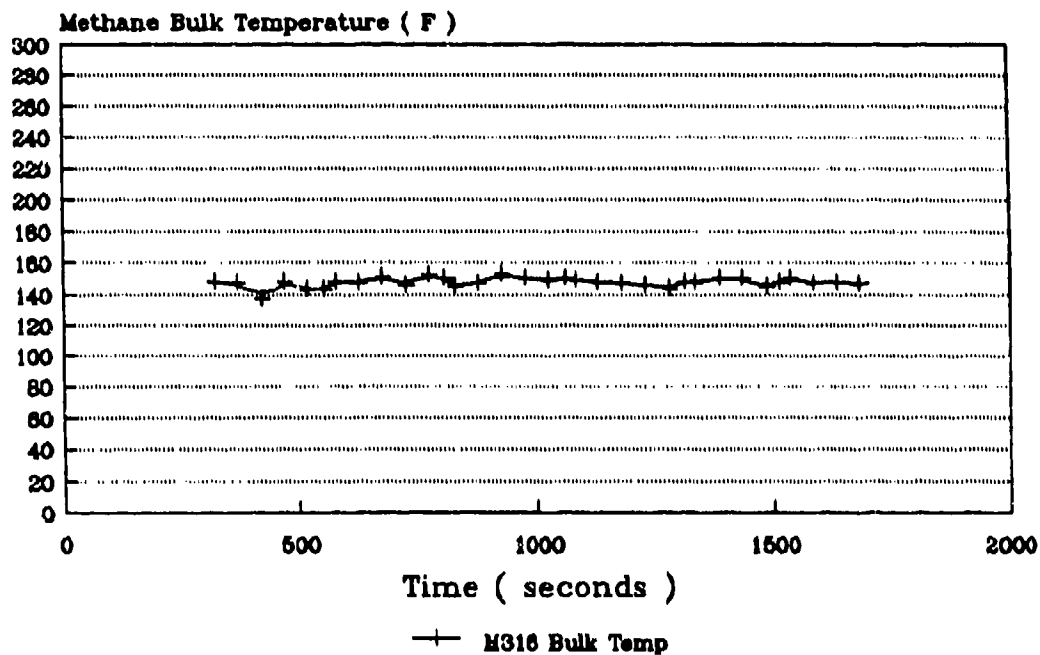


Figure 51. Methane Bulk Temperature vs Time for Test M316. Test Specimen ZA3 After Sulfur Corrosion/NaCN Refurbishment

Wall Temperature vs Time

Test M316

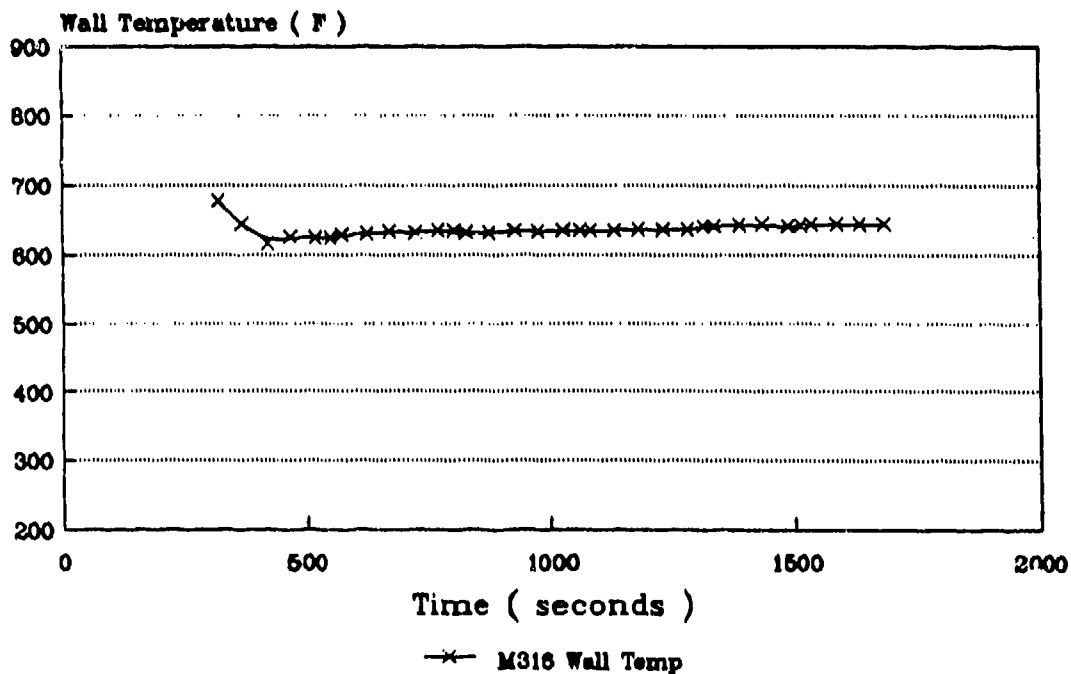


Figure 52. Cooling Channel Wall Temperature vs Time for Test M316. Test Specimen ZA3 After Sulfur Corrosion/NaCN Refurbishment

Specimen ZA3 Performance

Mass Flow

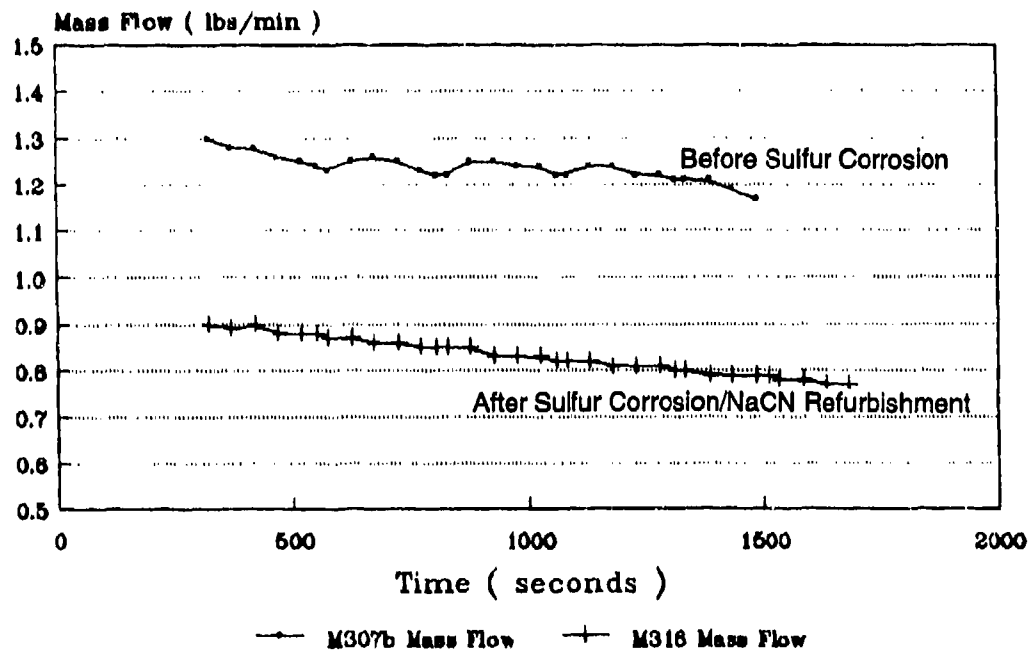


Figure 53. Mass Flow Performance for Specimen ZA3 Before Sulfur Corrosion (M307b) and After Sulfur Corrosion/NaCN Refurbishment (M316).

Specimen ZA3 Performance

Heat Transfer

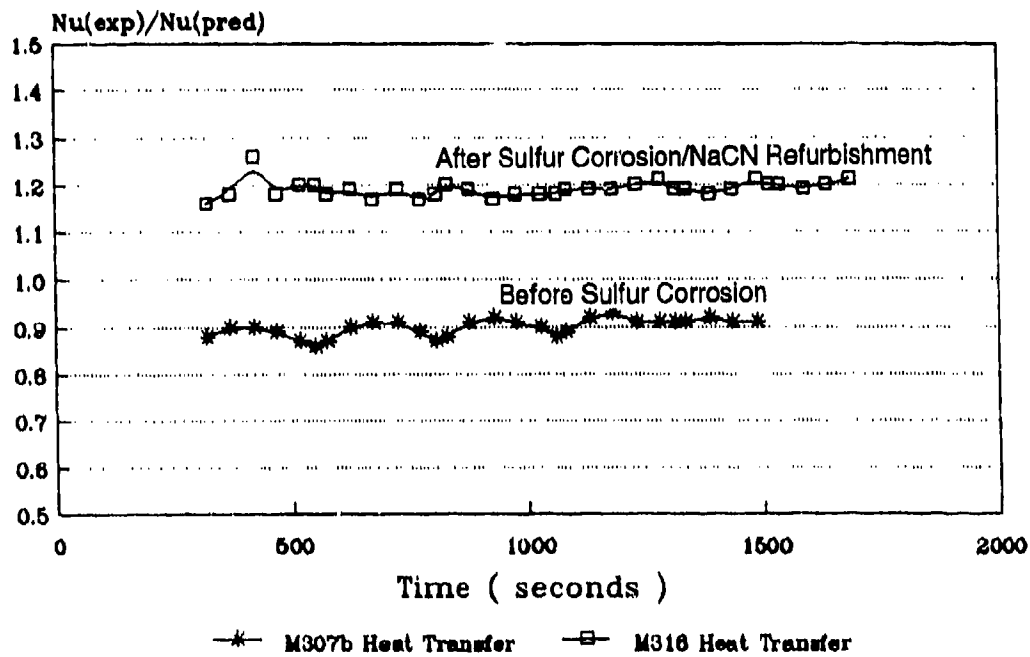


Figure 54. Heat Transfer Performance of Specimen ZA3 Before Sulfur Corrosion (M307b) and After Sulfur Corrosion/NaCN Refurbishment (M316)

Specimen ZA13 Performance

Mass Flow

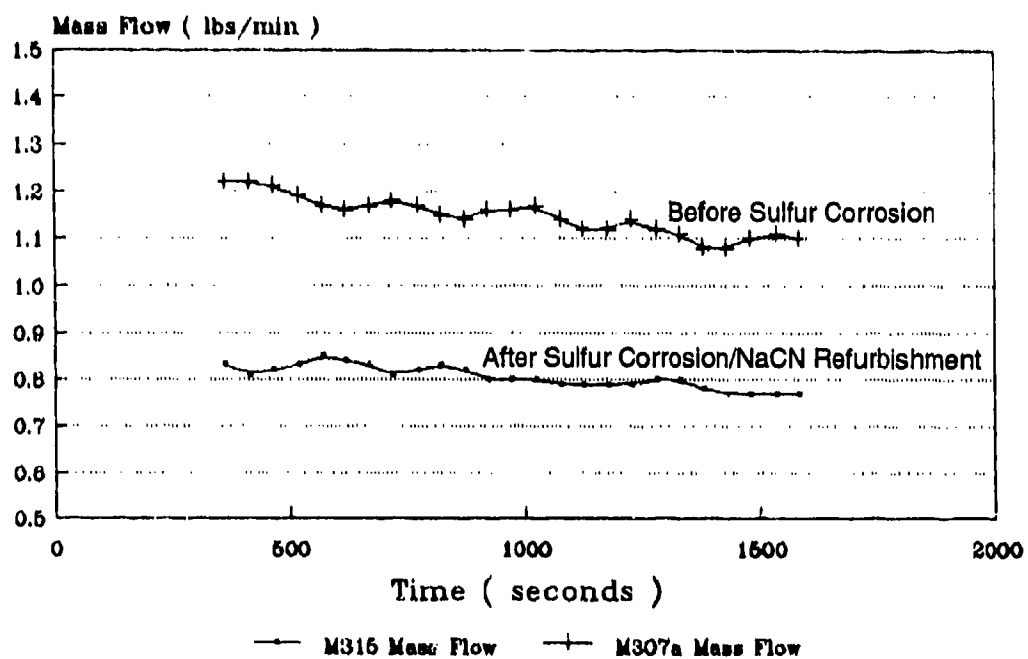


Figure 55. Mass Flow Performance for Specimen ZA13 Before Sulfur Corrosion (M307a) and After Sulfur Corrosion/NaCN Refurbishment (M315)

Specimen ZA13 Performance

Heat Transfer

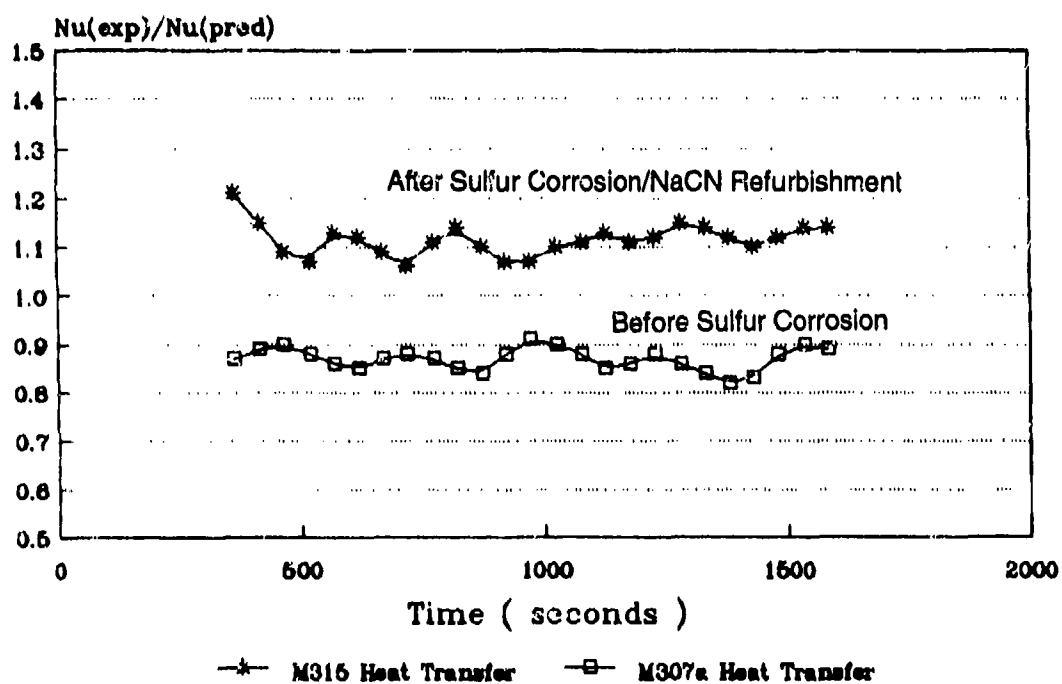


Figure 56. Heat Transfer Performance for Specimen ZA13 Before Sulfur Corrosion (M307a) and After Sulfur Corrosion/NaCN Refurbishment (M315)

Specimen ZA18 Performance

Mass Flow

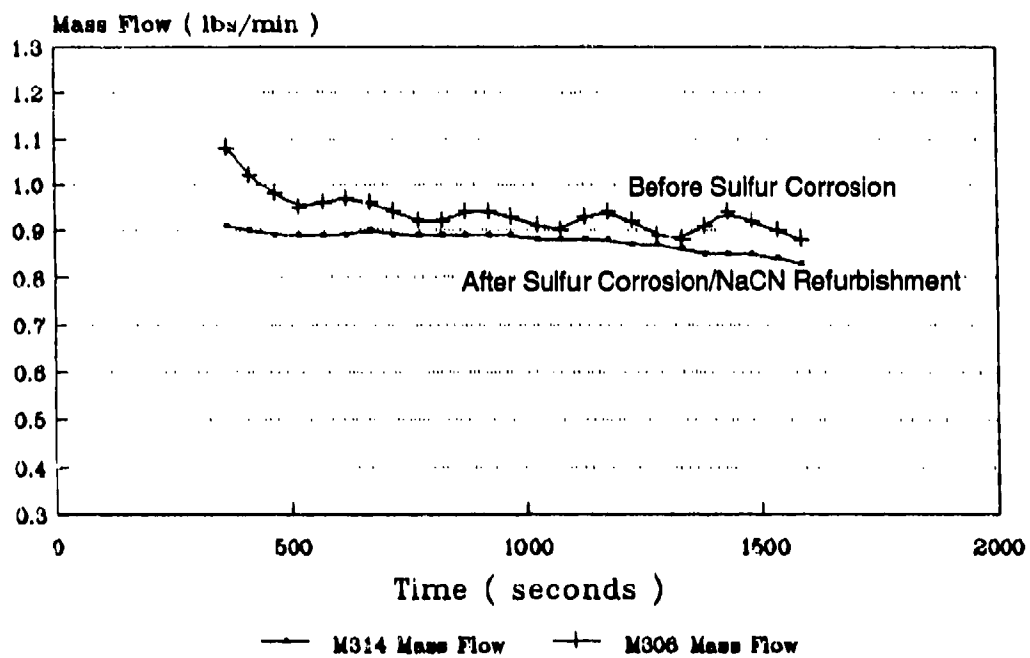


Figure 57. Mass Flow Performance for Specimen ZA18 Before Sulfur Corrosion (M306) and After Sulfur Corrosion/NaCN Refurbishment (M314)

Specimen ZA18 Performance

Heat Transfer

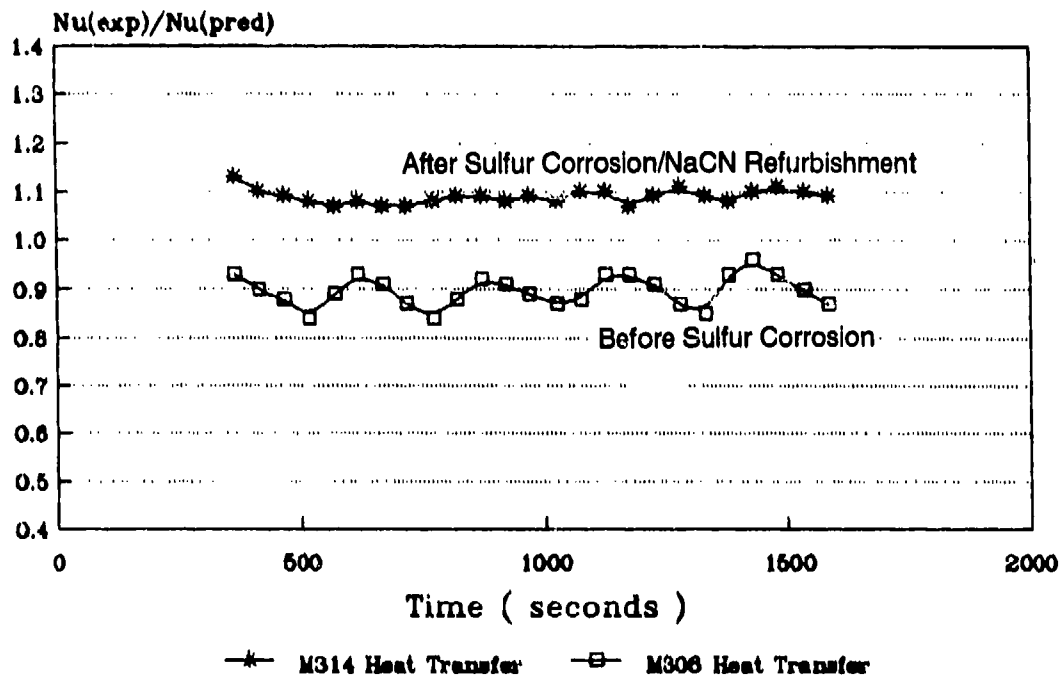


Figure 58. Heat Transfer Performance for Specimen ZA18 Before Sulfur Corrosion (M306) and After Sulfur Corrosion/NaCN Refurbishment (M314)

Specimen ZA23 Performance

Mass Flow

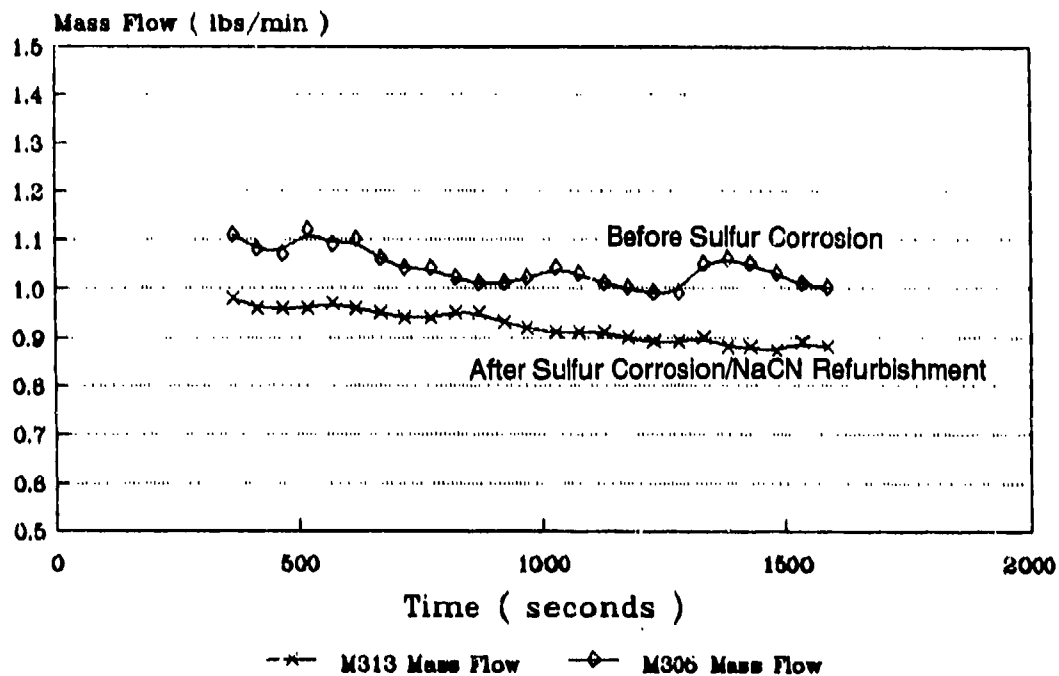


Figure 59. Mass Flow Performance for Specimen ZA23 Before Sulfur Corrosion (M305) and After Sulfur Corrosion/NaCN Refurbishment (M313)

Specimen ZA23 Performance

Heat Transfer

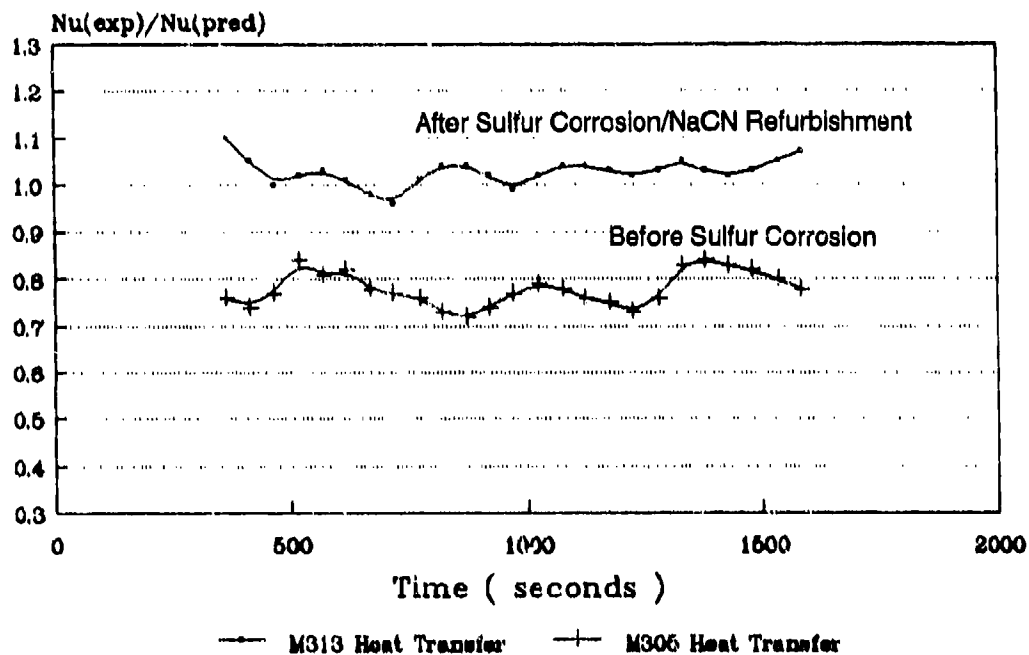
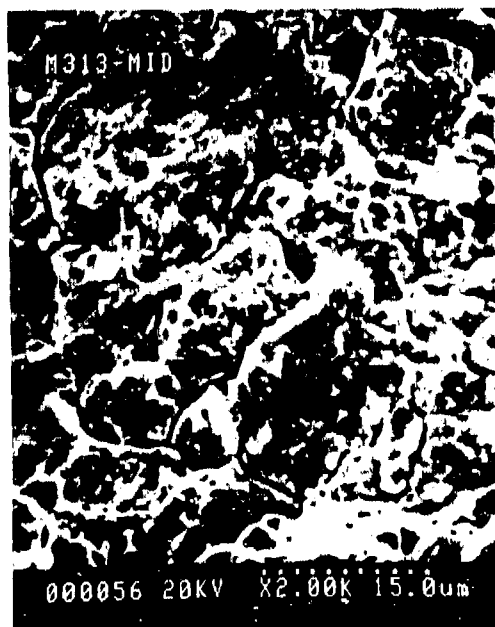


Figure 60. Heat Transfer Performance for Specimen ZA23 Before Sulfur Corrosion (M305) and After Sulfur Corrosion/NaCN Refurbishment (M313)

4.3, Dynamic Tests (cont.)

When the dynamic testing was complete, test specimen ZA3, ZA13, ZA18, and ZA23 were opened and inspected. Visual examination by binocular microscope showed no indication of coking, only minor staining near the channel outlets was observed. However, all cooling channel surfaces were heavily etched and pitted as expected. In addition, the channel walls also contained minor to moderate amounts of a copper-colored "wool-like" feature. This interesting feature was apparently well attached to the wall surfaces since they could not be removed by directing a strong jet of compressed air into the channels.

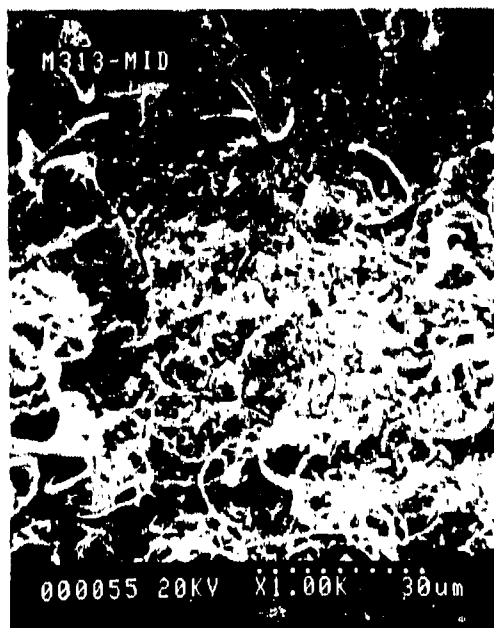
Figure 61 is a collection of SEM photomicrographs that show the common channel surface features. Pitting (Figure 61b) and "mud cracking", i.e., well defined grain boundaries (Figure 61a,c), were the most common features. Both of these features support the mechanism of preferential grain boundary attack by the sulfur corrosion as shown pictorially in Figure 46. The "copper wool" feature is shown in Figure 61c,d where it appears to be growing out of the side wall. This feature was far less common than the other features, but it was present in all four test specimen. Figure 62 is a collection of SEM photomicrographs of the "copper wool" that clearly shows the complex nature of its structure. Finally, Figure 63 is an EDS spectrum of the "copper wool" taken from the close-up in Figure 62d. Note, that only the elements present in NASA-Z are detected. Thus, this interesting feature is truly "copper wool." The origin of this highly unusual feature is unknown, however it should be noted that it bares a remarkable resemblance to the fibrous form of Cu_2S shown in Figure 35. Thus, one possible explanation is that the "copper wool" is derived from the fibrous form of Cu_2S . This could only be possible if the fibrous form of Cu_2S actually contains a copper alloy core because aqueous NaCN would completely remove the feature if it were pure Cu_2S . Fibrous Cu_2S with a copper alloy core might occur in the following manner. NASA-Z is not a completely homogeneous alloy, i.e., there are intermetallic stringers within the alloy itself. The stringers have a higher zirconium content than the surrounding matrix and may corrode at a different rate than the matrix. If this rate is slower than that of the surrounding matrix, the matrix can corrode preferentially leaving the stringers intact. This can lead to fibrous Cu_2S structures with a copper alloy core. As the matrix grains and grain boundaries are corroded, the fibrous Cu_2S will appear to emerge from the surface by being "pushed" by the volume increase as the copper reacts to form Cu_2S . When the Cu_2S is removed by the NaCN treatment, the "copper wool" remains behind. Whether this speculative mechanistic hypothesis is correct or not, it is certainly clear that this feature as well as the other surface features do represent a very significant increase in surface roughness that easily explains the observed increase in heat transfer performance and attendant loss in mass flow that results from the overall sulfur corrosion/NaCN refurbishment process.



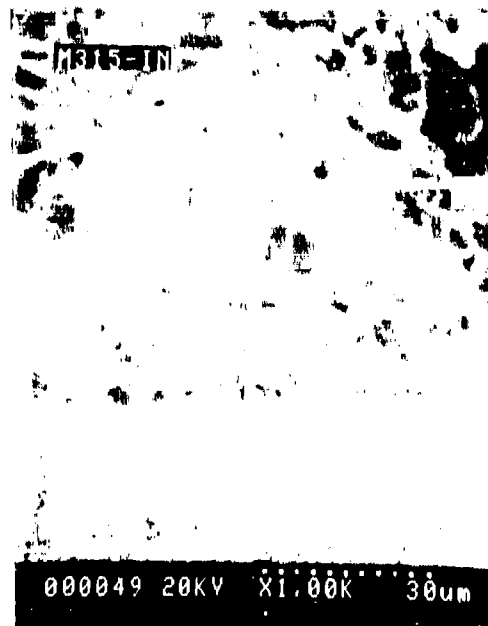
(a)



(b)



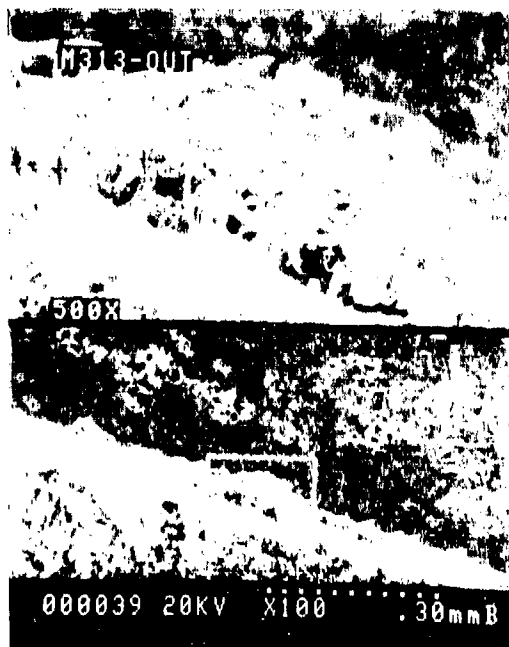
(c)



(d)

Figure 61. Cooling Channel Surface Features Resulting From the Overall Sulfur Corrosion/NaCN Refurbishment Process

- (a) Well Defined Grain Boundaries and Pitting (Very Common)
- (b) Pitting (Very Common)
- (c) "Copper Wool" (Moderately Common)
- (d) Close-up of "Copper Wool". Note Similarity to Fibrous Form of Cu_2S Shown in Figure 35



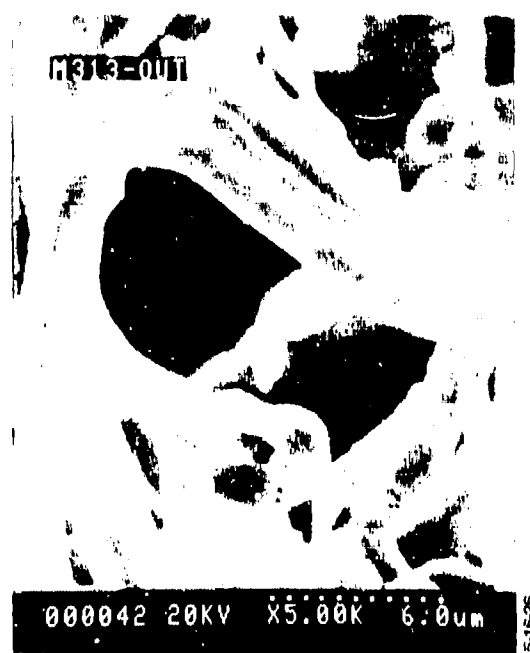
(a)



(b)



(c)



(d)

Figure 62. SEM Photomicrographs of "Copper Wool"

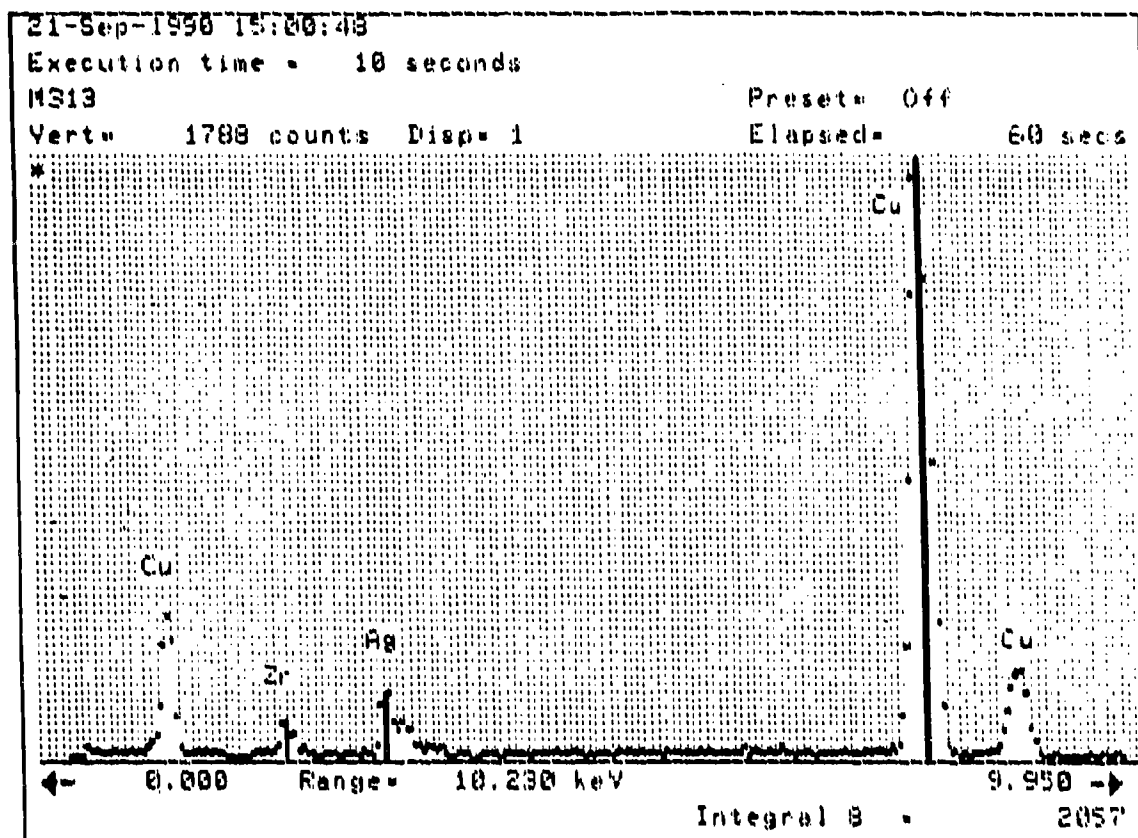


Figure 63. EDS Spectrum of "Copper Wool" From Close-Up in Figure 62d

5.0 CONCLUSIONS

The important conclusions to be drawn from this work are as follows:

- Coking is not a problem for methane fuel and copper alloy cooling channels. However, very harsh conditions, i.e., high wall temperature combined with low mass flow rates, should be avoided.
- Very low levels of sulfur are corrosive to copper under typical cooling channel operating conditions. The following specification is recommended as being capable of protecting a long-life or reusable copper booster engine from sulfur corrosion.

H ₂ S	≤	0.1 ppm (max)
Mercaptans	≤	0.2 ppm (max)
Total Sulfur	≤	0.5 ppm (max)

- High purity LCH₄ in bulk form is not generally available. This is not due to a lack of technology, but to a lack of demand. Aerospace requirements are insignificant compared to other end-uses not requiring high purity. However, there is one small supplier that meets or exceeds the purity requirements shown above. The capacity of this supplier can meet the projected Aerospace demand into the year 2004.
- 5% (w/w) NaCN quickly and efficiently refurbishes sulfur-corroded copper-alloy cooling channels by dissolving the Cu₂S corrosion product.
- The copper surface resulting from the overall sulfur corrosion/NaCN refurbishment process is highly roughened. This surface roughening is extensive enough to cause changes in cooling channel performance. The performance changes are improved heat transfer brought on by reduced mass flow when compared with the performance of the same test specimen under the same test conditions prior to being corroded.

APPENDIX A
DYNAMIC TEST LABORATORY PROCEDURES

**AEROSOL TECHSYSTEMS COMPANY
TEST OPERATIONS**

PAGE	1 of 4
PREPARED BY	W.E. Sobieralski 22 Sep 88
APPROVED	<i>[Signature]</i>
APPROVED	N.A.
REFERENCE	

ATP-TDO	A-CARBOT-1000
ACTIVITY	CHEM BAY 5
TEST NO.	
UNIT S/N	

CARBOTHERMAL
METHANE
TEST

INITIAL		OPERATION
T.D.	WSP	
		Index and ATP-TDO Change Letters and Revision Dates Verified.
		1.0 Record specimen number _____, specimen size _____, fuel used _____.
		2.0 Zero and calibrate transducers, thermocouples and M.M.
		3.0 Ensure that the CH ₄ system is connected to test plumbing and check that the RP-1 system is disconnected.
		4.0 CLOSE all hand and remote valves.
		5.0 Verify 6000 psig in methane cylinders.
		6.0 Set methane regulator outlet to _____ psig.
		7.0 Verify GN ₂ supply valve for remote valves is OPEN.
		8.0 Ensure sample bottle is attached to system.
		9.0 Hook vacuum pump to HV-16. OPEN HV-16 and HV-15 and pull vacuum on sample bottle.
		10.0 CLOSE HV-16 and disconnect vacuum pump.
		11.0 OPEN HV-10 and RV-4.
		12.0 Set GN ₂ supply regulator to _____ psig.
		13.0 OPEN RV-3 and verify flowmeter working.
		14.0 CLOSE RV-3 and RV-4.
		15.0 Torque channel support bolts 2, 4, 6 and 8 to 140 in-lbs. Torque edge support bolts to 60 in-lbs.

INITIAL		OPERATION
T.D.	INSP.	
		16.0 OPEN RV-3 and pressurize system to 2000 psig and leak check system.
		17.0 CLOSE RV-3.
		18.0 OPEN CH ₄ supply valve and RV-2. Pressurize the system to 4000 psig. Leak check.
		19.0 Once leak check is accomplished, vent pressure through HV-17.
		20.0 Torque channel support bolts 2, 4, 6 and 8 to 80 in-lbs.
		21.0 OPEN HV-17.
		22.0 OPEN RV-4.
		23.0 OPEN RV-3 and adjust GN ₂ supply regulator to desired flow rate.
		24.0 OPEN main LN ₂ valve (at tank), secondary LN ₂ valve and bypass LN ₂ valve.
		25.0 OPEN cooling water valve HV-19.
		26.0 Give 10 minute warning.
		27.0 OPEN HV-18 GN ₂ purge to waste drum and HV-20 GN ₂ . Purge to test block.
		28.0 Put cover on box.
		29.0 Turn GN ₂ purges on to electrical boxes.
		30.0 Turn overhead blowers ON.
		31.0 Verify heater control box plugged in.
		32.0 Begin data.
		33.0 Turn 440 main breaker ON.
		34.0 Turn heater main switch ON.
		35.0 OPEN HV-11, HV-12, HV-13 and HV-14.
		36.0 CLOSE HV-10 and RV-4.

INITIAL		OPERATION
T.D.	INSP.	
		37.0 Turn control panel heater switch ON and begin adjusting temperature with potentiometer to desired temperature.
		38.0 OPEN methane valve valve at cylinder regulator.
		39.0 Give 5 minute warning
		40.0 CLOSE RV-3 and immediately OPEN RV-2.
		41.0 Use HV-17 to adjust back pressure to 1000 psig and watch for any abnormalities (if filters begin to clog - OPEN RV-4).
		42.0 Run methane for approximately _____ seconds.
		43.0 OPEN RV-5 and take sample of methane at _____ seconds into test.
		44.0 When test duration is completed CLOSE RV-2 and immediately OPEN RV-3.
		45.0 OPEN HV-17 all the way.
		46.0 Turn heaters OFF and begin cool down.
		47.0 Turn bay heater switch OFF on 440 breaker.
		48.0 Clear bay to authorized personnel only.
		49.0 CLOSE methane valve at regulator ,
		50.0 OPEN HV-32, cooling water to block.
		51.0 CLOSE LN ₂ bypass valve and secondary LN ₂ valve.
		52.0 CLOSE sample bottle valve.
		53.0 Re-restrict the bay to all personnel.
		54.0 CLOSE main LN ₂ valve.
		55.0 When the block reaches 500°F, vent remaining methane through RV-2.
		56.0 End data.
		57.0 When the block reaches 200°F, clear bay to all personnel.
		58.0 Turn blowers and GN ₂ purges OFF.

REPORT DOCUMENTATION PAGE

1. Report No. NASA CR-187104		2. Government Accession No.		3. Recipient's Catalog No.	
4. Title And Subtitle Hydrocarbon-Fuel/Combustion Chamber-Liner Materials Compatibility Final Report				5. Report Date April 1991	
				6. Performing Organization Code	
7. Author(s) G. David Homer Sanders D. Rosenberg				8. Performing Organization Report No.	
				10. Work Unit No.	
9. Performing Organization Name and Address Aerojet Propulsion Division P.O. Box 13222 Sacramento, CA 95813				11. Contract or Grant No. NAS 3-25070	
				13. Type of Report and Period Covered Final Report 10/31/89 - 3/31/91	
12. Sponsoring Agency Name and Address NASA/Lewis Research Center Cleveland, Ohio 44135				14. Sponsoring Agency Code	
15. Supplementary Notes Project Manager, Ms. Elizabeth A. Roncace NASA/LcRC, Cleveland, Ohio					
16. Abstract The results of dynamic tests using methane and NASA-Z copper test specimen under conditions that simulate those expected in the cooling channels of a regeneratively cooled LOX/hydrocarbon booster engine operating at chamber pressures up to 3000 psi are presented. Methane with less than 0.5 ppm sulfur contamination has little or no effect on cooling channel performance. At higher sulfur concentrations, severe corrosion of the NASA-Z copper alloy occurs and the cuprous sulfide, Cu ₂ S, thus formed impedes mass flow rate and heat transfer efficiency. Therefore, it is recommended that the methane specification for this end use set the allowable sulfur content at 0.5 ppm (max). Bulk high purity liquid methane that meets this low sulfur requirement is currently available from only one producer. Pricing, availability, and quality assurance are discussed in detail. Additionally, it was found that dilute sodium cyanide solutions, i.e., 5% (w/w), effectively refurbish sulfur corroded cooling channels in only 2-5 minutes by completely dissolving all the Cu ₂ S. Sulfur corroded/sodium cyanide refurbished channels are highly roughened and the increase surface roughness leads to significant improvements in heat transfer efficiency with an attendant loss in mass flow rate. Both the sulfur corrosion and refurbishment effects are discussed in detail.					
17. Key Words (Suggested by Author(s)) NASA-Z, Methane, Sulfur Corrosion, Material Compatibility, Refurbishment, Heat Transfer Efficiency, Mass Flow Rate			18. Distribution Statement Unlimited		
19. Security Classif. (of this report) Unclassified	20. Security Classif. (of this page) Unclassified		21. No. of pages 115	22. Price	